Transition Boiling Heat Transfer in a Vertical Round Tube

EPRI

Keywords:
Transition Boiling
Reflood
LOCA
LWR Safety

EPRI NP-895
Project 688-1
Interim Report
September 1978

Prepared by
University of Cincinnati
Cincinnati, Ohio

ELECTRIC POWER RESEARCH INSTITUTE

Transition Boiling Heat Transfer in a Vertical Round Tube

NP-895
Research Project 688-1

Interim Report, September 1978

Prepared by

UNIVERSITY OF CINCINNATI
Department of Chemical and Nuclear Engineering
Cincinnati, Ohio 45221

Principal Investigators
J. Weisman
Y. K. Kao
G. Rahrooh

Prepared for

Electric Power Research Institute
3412 Hillview Avenue
Palo Alto, California 94304

EPRI Project Manager
David Cain
Nuclear Power Division

EPRI PERSPECTIVE

PROJECT DESCRIPTION

The transition boiling heat transfer process plays an important role in the post-LOCA, reflood phase of a hypothetical loss-of-coolant accident (LOCA). It is also one of the less understood phenomena that occur during LOCA. From the time emergency core cooling water enters the fuel region until liquid contact with the fuel rods is reestablished, a complex sequence of interacting thermal hydraulic phenomena takes place. The quasi-stable transition boiling process provides necessary continuity between film boiling, where vapor blanketing of the fuel rod is maintained, and rewetting of the fuel rods.

The problem in understanding transition boiling heat transfer has to do with its unstable behavior and general physical complexity. More fundamentally, however, the problem stems from a lack of good experimental data, particularly for the low pressures characteristic of reflood. Given sufficient data, it should be possible to establish greater confidence in empirical correlations for the transition boiling process. In addition, such data accumulation may eventually lead to the development of a physical model and a fundamental understanding of transition boiling heat transfer mechanisms.

This project, part of a continuing study of the transition boiling heat transfer process, was designed to obtain experimental measurements of transition boiling heat transfer coefficients covering a wide range of reflood conditions. This task was greatly facilitated by use of an experimental heat transfer rig capable of establishing and maintaining transition boiling under quasi-steady conditions. This design feature enabled average values for heat transfer coefficients to be taken in a simpler and more direct manner than otherwise might have been possible.

PROJECT OBJECTIVES

The purpose of this project was to perform heat transfer experiments covering a wide range of void fraction, mass flow rate, and pressures. This effort was expected to result in: (1) a comprehensive set of transition boiling heat transfer data that could be used as a reference for further analytical investigations of the transition boiling phenomenon, and (2) possible confirmation of an empirical heat transfer model previously developed from a limited set of data.

CONCLUSIONS AND RECOMMENDATIONS

The project has resulted in an accumulation of data on transition boiling heat transfer under reflood conditions extending well beyond previously available ranges. It is concluded that, for these conditions, the empirical transition boiling heat model developed by Ramu and Weisman is applicable within the uncertainty provided.

As with all experimental investigations, it is possible to look back and point out areas where improvements and/or further refinements might be made. In particular, the following are felt to be significant:

(a) The positioning of test section thermocouples was a troublesome factor in data reduction and interpretation. A uniform "effective" distance from the wall was established from single phase measurements and applied to all test section thermocouples. Despite the fact that thermocouples were spot-welded to the tube wall in the same manner, a better approach would have been to assume that thermocouple-to-wall distances were not necessarily the same.

(b) The interpretation of data did not account for the possible effect of subcooled voidage. Although heat transfer coefficients at higher qualities would be unaffected, the Ramu-Weisman correlation may predict larger heat transfer coefficients than actually occur under low quality conditions.

(c) Data plots provided in the report are fairly standard representations of heat transfer results. However, there is reason to believe that additional parametric information is contained within the data but not brought out by the graphical presentation. For instance, channel quality appears to be an influential parameter in the overall transition boiling heat transfer process. The apparent scatter in heat transfer data might have been appreciably reduced had these parameters been linked to heat transfer values in an appropriate graphical format.

(d) Although existing instrumentation was sufficient to provide the desired experimental data, no provisions were made for backup or consistency checks. It would have been advantageous, for example, to have had some capability for performing mass and energy balance checks across the test section.

(e) Transition boiling tests were carried out under steady-state conditions; however, reflood is essentially a transient phenomenon. Although there is no apparent technical reason why steady-state transition boiling results cannot be used in the transient case, confirmatory experiments should be performed.

The work described by this report is being followed up by additional transition boiling studies under low quality, reverse flow, and transient conditions. A new test section will be installed permitting water flow in the outer annulus and mercury flow inside the central tube. Additional instrumentation will be provided and viewing ports arranged to allow visual study combined with high speed photography.

David G. Cain, Project Manager
Nuclear Power Division

ABSTRACT

Transition boiling heat transfer coefficients have been obtained for water at pressures of 25 to 75 psia and mass velocities from 14,000 to 140,000 lbs/hr ft^2. The water flowed inside a 1/2 in O.D. tube and was heated by hot mercury flowing in an annulus around the tube. Thermocouple pairs placed on the outside of the central tube and outer pipe at several axial elevations allowed the rate of heat transfer to be determined. The data agreed reasonably with the correlation previously proposed. However, the observed heat transfer coefficients show less of a decrease with increasing temperature than was seen in previous tests in which the water flowed in an annulus.

CONTENTS

Blank Page

ILLUSTRATIONS

TABLES

SUMMARY

At a given system pressure, the total heat transferred via the boiling process increases with increasing wall temperature until a maximum or critical heat flux is reached. The heat transferred then decreases as the wall temperature is increased further. The heat transfer continues to decrease until the entire surface is covered by a layer of vapor and stable film boiling exists. The region where heat transfer decreases with increasing wall temperature is called the "transition boiling" region since it marks the transition from nucleate to film boiling.

Understanding of the transition boiling process is important for the understanding of the reflood phase of a hypothetical LOCA. Those portions of the fuel rods just below the froth level will generally be in transition boiling. The quenching process will therefore be strongly influenced by the heat transfer coefficients which pertain during transition boiling.

Most of the available transaction boiling data are obtained at high pressures since obtaining low pressure data is difficult. Without very complex control equipment, electrically-heated tubes cannot be used to obtain steady-state transition boiling data at low pressures. Nearly all of the available data at low pressures have therefore been obtained from transient tests where fluid conditions are imperfectly known.

Steady-state transition boiling data at low pressures can be obtained by using a hot fluid as the heat source. Previous experiments at the University of Cincinnati used this approach with hot mercury as the heat source. Some low-pressure data were obtained at conditions of interest. However, the data where obtained were at a single pressure level, were at

mass flow rates somewhat below those usually encountered during reflood and there was some uncertainty on the radial position of the thermocouples used to measure the mercury temperature. The present tests were undertaken to remedy these deficiencies.

In the present test section, water, which was flowing upward in a tube, was surrounded by an annulus of mercury in downward flow. Pipe wall temperatures were measured by thermocouples on the mercury side of the inner pipe and the insulation side of the pipe. By making these measurements at four different axial positions, the rate at which heat was being transferred over each short subsection could be determined.

Computation of the heat transferred to the water side required that the radial temperature profile in the mercury stream be calculated at each axial level. This could be done fairly readily because the mercury flow was turbulent but the flow was below the critical Peclet number. This meant that the velocity profile was flat but that radial heat transfer due to turbulent eddies was negligible in comparison with heat transfer by conduction. Rod-like flow could thus be assumed and computer solutions for the radial profiles could be obtained for any set of axial wall temperature measurements.

Experiments were conducted at pressures between 25 and 75 psia and water mass velocities from 14,000 to 140,000 lbs/hr.ft^2. Transition boiling heat transfer coefficients were obtained at tube wall temperatures ranging from 50 to 270^{o}F above saturation. These data were generally similar to those obtained in previous tests at the University of Cincinnati. However, the present data showed less of decrease with increasing temperature than seen in the previous tests in which the water flowed in an annulus. The data agreed reasonably with the correlation previously proposed.

1.0 Introduction

1.1 Background

Current research in transition boiling is largely concerned with elucidating the behavior to be expected during the reflood phase of a hypothetical loss of coolant accident. Safeguards analyses indicate that the peak cladding temperature reached at the hot spot during the accident is limited by the cooling obtained from the steam generated in the lower portions of the core. Much of this steam is generated in the quench region where transition boiling occurs. An understanding of transition boiling phenomena is therefore required for accurate modeling of the critical phase of core reflood.

A number of steady state experiments (1-7) examining transition boiling at high pressures (600-3045 psia) have been conducted. At high pressure and flows,post criticalheat flux (CHF),heat transfer coefficients can be fairly high and it is possible to exceed CHF without excessive heater temperatures. At the low pressure and flow typical of reflood conditions, the post CHF heat transfer coefficients are low and steady state tests with water which do not result in excessive heater temperatures are difficult to conduct. As a result, most of the information germaine to reflooding in a PWR has been obtained from transient tests under the FLECHT program.[8]

Interpretation of transient cooling tests are difficult and it is desirable to have steady state data which can confirm these results and which can be used more readily in establishing physically based correlations. Steady state, transition boiling data with water highly subcooled conditions were obtained by Ellion[9] at pressures between 16 and 60 psia and liquid velocities from 1.1 to 5.0 ft/sec. Plummer[10] obtained transition boiling data with liquid nitrogen. Peterson et al[11] obtained transition boiling data at low velocities using a thin (0.005 in diameter) vertical wire. In view of the very large difference in diameters between the test wire and a fuel rod, the applicability of their data to reactor conditions is questionable.

The most directly applicable steady-state transition boiling data is that of Ramu and Weisman [(12)]. They used a scheme, originally suggested by McDonough et al [(4)], whereby the heat was supplied by a liquid metal. In Ramu and Weisman's [(12)] experiment, the heat source was hot mercury flowing within a central tube. Boiling took place in an annulus around the central tube containing the mercury. By measuring mercury temperatures at several axial positions, they were able to determine the heat transferred to the water and the temperature difference between the water and pipe wall. Since the maximum mercury temperature was limited, steady-state data could be obtained without overheating of the heater wall.

The experimental data of Ramu and Weisman [(12)] were limited to system pressures of 25 to 30 psia and mass flow rates from 12,000 to 34,000 lbs/hr ft^2. These flow rates and pressures are the lower end of the reflood range and tests at higher pressures and mass flow rates were desired. Further, the data at values of $(T_w - T_{sat})$ above about 150^oF were appreciably lower than expected.

1.2 Objectives and General Approach of Experiment

In view of the gaps in knowledge in regard to transition boiling heat transfer at low pressures, an experimental program was designed to obtain additional low pressure data under well-defined conditions. The present experiments were intended to extend the range of data obtained by Ramu and Weisman [(12)] and to reexamine the heat transfer rates at high wall superheat. To accomplish these objectives, the present test series was designed to obtain steady-state transition.boiling heat transfer data with water over the following range:

Pressure	10-60 psig
Mass Flow Rate	$1.4 \times 10^4 - 1.4 \times 10^5$ lbs/hr ft^2
Wall Temperature	0^o - 300^oF above saturation

This parameter range overlapped that investigated by Ramu and Weisman[12] but extended the tests to both higher pressures and mass flows than previously examined.

These experiments were conducted using the same test loop as that used by Ramu and Weisman[12]. Hence, hot mercury again provided the heat source and allowed post CHF heat transfer to be examined at steady-state. However, the test section was revised to allow the larger parameter range to be explored and to attempt to eliminate some of the uncertainties in the original experiment.

In the original test section used by Ramu and Weisman[12], mercury was contained within a central steel tube and boiling of water occurred in an annulus formed by a 1 in. glass tube and the 0.54 in OD central tube. Mercury temperatures were measured by thin tantalum-sheathed thermocouples which were placed in the mercury stream at several axial locations. As the thermocouples were flexible, their radial location could not be determined precisely. Since the radial temperature gradient in the mercury is significant, correction factors, based on nonboiling runs with an essentially constant heat flux over the test section, were required to revise the measured temperatures. It was desired that the present tests eliminate this difficulty.

To achieve the higher mass velocities desired, the approach taken in the present tests was to use a new test section in which the water flowed inside a 0.5 in. OD tube. This reduced the water flow area and allowed the higher mass velocities desired. The mercury flowed in an annulus around the central tube. By welding the thermocouples to the inner and outer walls of the test section, the uncertainty in the thermocouple location was eliminated.

The entire test section was fabricated of stainless steel. While this eliminated the ability to observe the boiling phenomena visually, it eliminated the pressure limitations imposed by the glass outer tube in the earlier tests. Use of stainless steel in the test section also eliminated the need for the use of potassium dichromate as a water corrosion inhibitor.

The new test section was somewhat shorter than the original unit. The shorter test section together with the slightly reduced heat transfer area per unit length led to about a 35% decrease in total heat transfer area. It was hoped that this would allow higher critical heat flux to be attained and thus allow transition boiling to be observed at lower qualities than Ramu and Weisman[12] obtained. However, under the modififed conditions of the present tests, little decrease was seen in the qualities at which transition boiling was found.

2.0 Experimental Program

2.1 Experimental Apparatus

2.1.1 The Heat-Transfer Loop

The University of Cincinnati heat transfer loop uses a two fluid system. A detailed description of the construction of this loop has been presented previously(12). The heating fluid (mercury) is heated by a set of resistance heater bands with a total power rating of 30 KW. Hot mercury at a prescribed temperature is introduced to the test section (for test section details see Section 2.3.1) and loses heat to the water coolant. Burnout is impossible since the wall temperature can never exceed the controlled temperature of the mercury.

A flow diagram of the heat transfer loop is shown in Figure 2-1. This apparatus consists of two independent loops: a water loop and a mercury loop. Water is circulated by a centrifugal pump and is metered by either two rotameters (100-1000 cc or 0-3 gpm ranges). It then flows upward in the test section and picks up heat from hot mercury which flows counter-currently in an annulus region of the test section. Water and steam from the test section then passes through a condenser, a regenerative heat exchanger, and finally back to the pump. A diaphragm accumulator served the dual purpose of providing a surge volume and allowing ready control of the system pressure.

Mercury is circulated by a canned-rotor pump. The flow rate of mercury is measured by a flow tube located downstream from the pump. The mercury is heated in the heating section by a set of resistance band heaters with a total power rating of 30 KW. Hot mercury then flows downward in the test section where it releases heat to water. In order to cool the mercury to the allowable pump operating temperature while minimizing the required heat input, the mercury passes through a regenerative heat exchanger before returning to the pump. A spray cooler is also installed after the regenerative heat exchanger for additional temperature control. This device was never used during the course of the current tests.

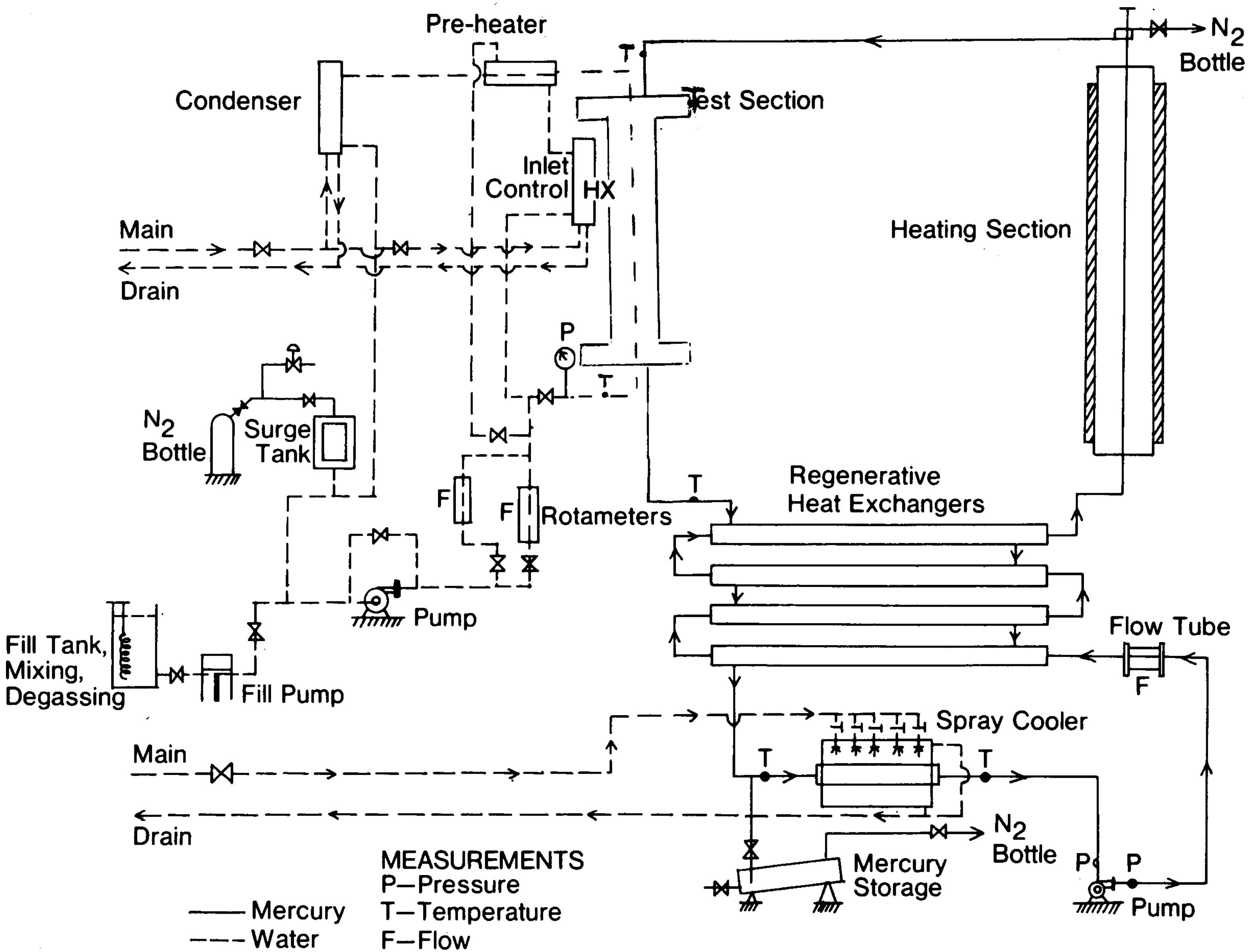

Fig. 2-1 Test Loop Diagram

The previous test section, in which mercury flowed inside a Croloy tube and water in a concentric annulur space between the central tube and the glass tubing, has been replaced. The new 304 stainless steel test section was specifically designed to meet the objectives of the project. Water flows inside the tube surrounded by hot mercury which flows in the annulus. In addition to increasing the water mass velocity, the new design eliminates the unheated glass surface which may have affected the earlier heat transfer test results.

A cross sectional diagram of the new test section is shown in Figure 2-2. The active length of the test section is 20" made up of a 1/2" OD, BWG 18 inner tube and a 1 1/4" Sch. 80 outer pipe. Mercury flows in the annulur region and water inside the central tube. Four pairs of stainless steel sheathed, magnesia insulated, iron-constantan thermocouples were spot welded on the outside of the tube and the pipe at four elevations. There was 5 1/2 inches between each pair. The sheathed thermocouples on the inner tube were brought out of the mercury through a Conax fitting. The test section was fully insulated in order to minimize the heat losses.

2.1.4 Instrumentation - The instrumentation used by Ramu and Weisman[12] was revised in several respects. The most significant revisions were:

a) Replacement of Flow Tube (Measuring mercury flow): The previous flow tube in the mercury stream gave a differential pressure reading of only about 2" of H_2O at operating conditions. This was only about 20% of the full range of the readout meter. A new flow tube that gave a differential pressure reading of about 9" of H_2O was purchased and installed in the mercury loop. A more accurate assessment of mercury flow was therefore possible.

b) Replacement of potentiometer measuring thermocouple output by a dual channel strip chart recorder.

A dual channel strip chart temperature recorder, connected to a pair of rotary two-pole multiposition switches, was used to record the temperature drop from the reference point (inlet mercury temperature) to the welded thermocouples on the

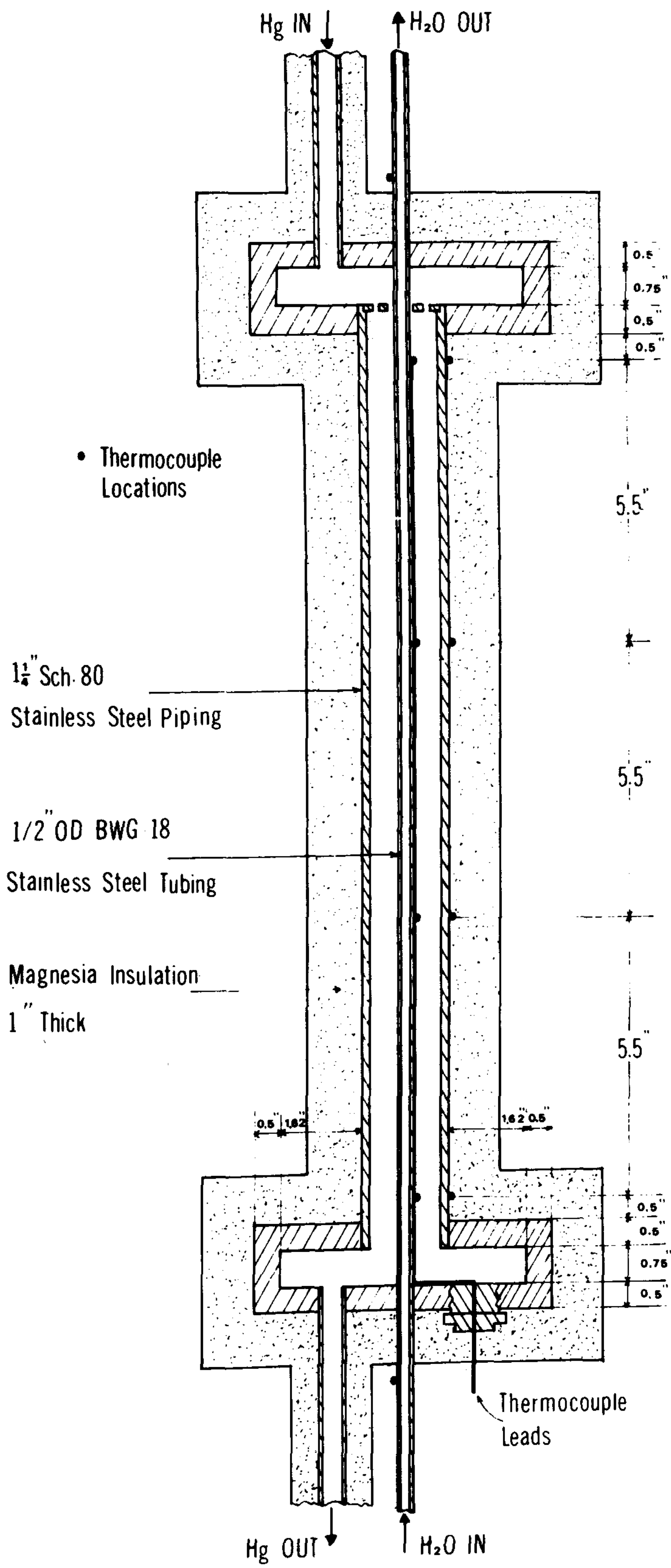

Figure 2-2 Cross sectional view of Test Section

inner tube and outer pipe in the test section (Figure 2-2). This was accomplished by successively bucking the reference thermocouple with the welded thermocouples in the test section. The strip chart recorder allowed the temperature fluctuations on the inner pipe wall to be recorded and an average temperature to be estimated readily. Determination of an average wall temperature with a potentiometer while such fluctuations are occurring is difficult.

c) Installation of Revised and Improved Safety Instrumentation

Cavitation at the inlet to the mercury pump can rapidly lead to pump damage. A differential pressure switch which shuts the pump at low flow was installed across the mercury pump. An over-ride allows normal starting to take place.

The water side safety valves were replaced by higher pressure units. In addition, an additional gas regulating valve was added to control the system overpressure at the higher pressures.

2.2 Test Operation

To prevent any mercury leaks from an unattended loop, the mercury loop was normally drained each day. The apparatus was filled by evacuating the loop and then pressurizing the drain tank. After filling the loop, a nitrogen overpressure was applied to maintain a pressure sufficient to prevent cavitation at the pump inlet. Conduction type level probes provided an indication of Hg level in the surge tank.

The water loop was normally left full of water during a given series of runs. The water system was filled with thoroughly degassed water by a fill pump while venting air at the high points of the system.

The pressure at which the water system operated was set by adjusting the nitrogen supply and relief valves. These maintained a nearly constant pressure above the rubber diaphragm in the surge tank despite changes in surge volumes as the loop temperature and voids varied.

After system pressures were set, water and mercury flow were initiated. The water side temperature was controlled by manipulating the amount of water circulating through the preheater. At high inlet mercury temperatures (above 450°F), a very small amount of cooling water is sent through the condenser. The mercury inlet temperature is controlled by an automatic controller, installed on the control panel, which adjusts the ratio of on/off time for the electric band heaters proportionally to the difference between the temperature to the test section and the set temperature.

During each run, the water flow rate was fixed and the inlet mercury temperature was increased by increments of about 20°F. After each increment, steady state conditions were established prior to data collection. After the data were obtained, the set point temperature was increased again. This procedure was repeated until the inlet mercury temperature reached the highest value which could be reached. This was about 600°F for most runs because of the limitation on power to the heaters.

Since mercury vapor is very toxic, the entire apparatus is within a hood. The hood blower maintains a negative pressure within the hood at all times. A mercury vapor detector is placed within the hood as an additional safety precaution.

When conditions were stable, the following data were recorded:

1. Temperature of mercury at inlet and outlet of the test section.
2. Temperature differences between mercury inlet temperature and thermocouples on the outer walls of the inner tube and outer pipe in the test section (locations of these thermocouples are shown in Figure 2-2).
3. Temperature of water at inlet and outlet of the test section.
4. Water side pressure.
5. Water and mercury flow rates.

Items (1) and (3) were measured with a potentiometer; (2) was measured by a dual-channel strip chart recorder which recorded any two temperature differences simultaneously; (4) was measured by a Bourdon pressure guage just before the test section; and (5) was measured by one of the two rotameters (Rotameter selection depended on the flow rate.)

2.3 Heat Loss and Thermocouple Corrections

In the process of converting the temperature readings to the heat transfer between mercury and water, the heat loss to the surroundings must be considered. This heat loss is proportional to the outer surface temperature of the test section. A series of runs with no water in the test section were conducted to determine this heat loss as a function of surface temperature. The temperature drop from the mercury inlet to the outlet was considered to be caused by the heat loss to surroundings. An equation for the heat losses as a function of average mercury temperature was obtained from Fig. 2.3.

There are two types of thermocouples used in the test section: (1) high quality sheathed thermocouples that were spot welded onto the active part of the test section, and (2) bare thermocouples which were simply clamped onto the pipes and used for measurement of fluid inlet and outlet temperatures. It was found that the couples clamped to the surface indicated temperatures which were below the true temperatures (e.g. thermocouple measuring temperature of exit stream indicated uncorrected temperatures below the known saturation temperature during runs with significant boiling). The lower temperature readings of the clamped thermocouple may in large measure be attributed to the relatively poor contact achievable with a clamp-on device and the thin layer of electrical insulation placed between couple and pipe to prevent pickup of stray voltages. The reading of the water side thermocouples were corrected by the amount necessary to bring the exit couple to the saturation temperature in boiling runs at low exit quality (where no significant steam superheat expected).

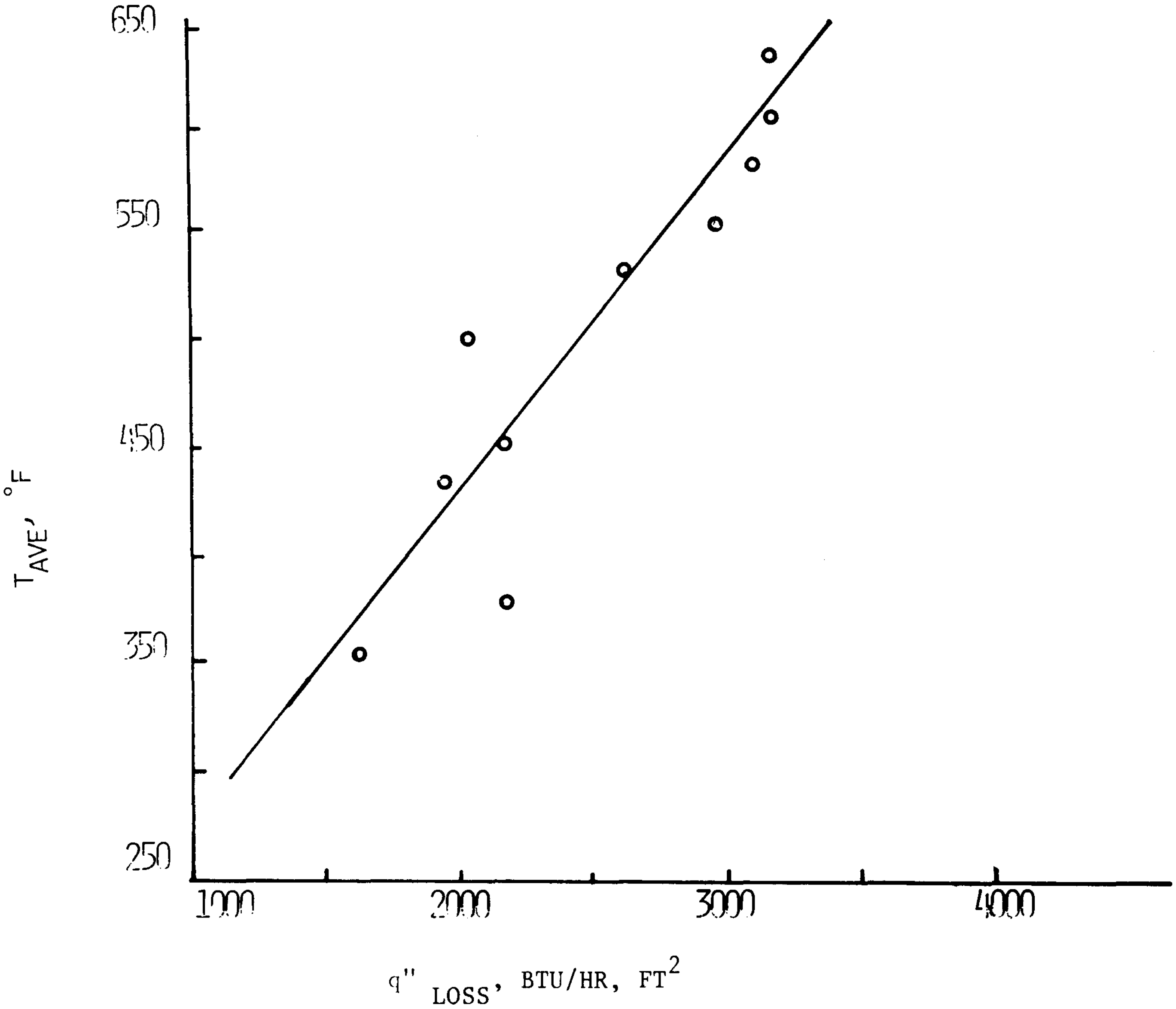

Fig. 2-3 Heat Loss Estimation in the Test Section

The clamped thermocouples used to record mercury inlet and outlet temperatures were corrected using the tack welded thermocouples as the standard. Thus, for the couple reading mercury inlet temperature, a correction curve which brought its reading in line with the uppermost welded thermocouples was devised. The data for this correction was obtained from the run made to determine heat losses without water present. It was assumed that the inlet temperature should equal that of the uppermost couple plus a small increment for the temperature drop due to heat loss between the two positions. The heat loss correction was quite small and introduced little error since the maximum temperature drop across the entire test section during this run was less than 12°F.

2.4 Test Observations

Although visual observations of the boiling phenomena were not possible, the strip chart temperature recorder was a good indicator of different regimes of boiling occurring in the test section. When the water wall temperature was below the saturation temperature of water, there was no oscillation in the recorder signal (no boiling) as shown in Figure 2-4a. After the wall temperature exceeded the saturation temperature of water, small oscillation was noticed in the recorder signal which was an indication of nucleate boiling as shown in Figure 2-4b. Depending on the water flow rate and pressure as the superheat reached the range of 80-130°F, significant oscillation in the recorder tracing was noticed which was an indication of transition boiling. In general, a ± 10°F fluctuation was noticed in the surface temperature for the transition region as shown in Figure 2-4c. For most runs, nonboiling, nucleate, and transition boiling occurred simultaneously in the bottom, the middle, and the top part of the test section respectively.

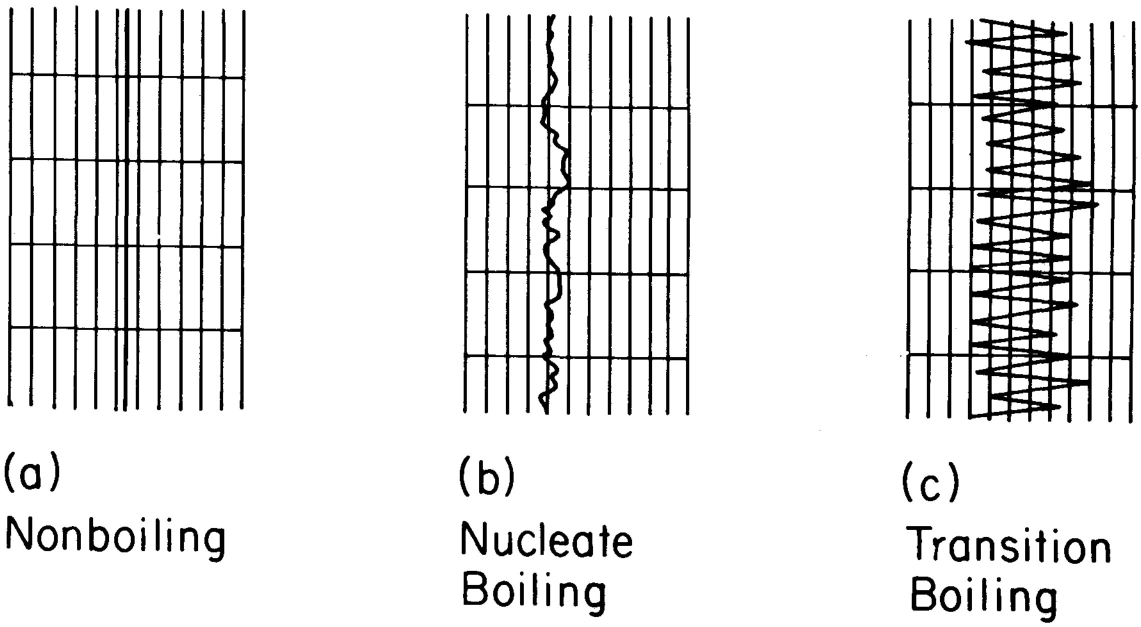

Figure 2-4. Recorder signal for nonboiling, nucleate, and transition boiling.

Because of limited power input available, the transition boiling region at higher flow rates was reached in a somewhat different manner. Normally, the mercury inlet temperature was increased periodically for a constant water flow rate and data were obtained as wall temperature exceeded the saturation. This was not possible for the higher flow rates since the loop cannot attain the high critical heat flux for high water flow rates. Therefore, a high wall temperature was established with low flow conditions and then the flow rate was increased gradually to reach the desired high flow conditions. Transition boiling data were then obtained as mercury inlet temperature was decreased periodically. For intermediate flows, both procedures for data acquisition were used during some runs and no significant difference was observed in the data obtained.

Test data were obtained at mass flow rates ranging from 14,000 to 140,000 lbs/hr ft^2, pressures from approximately 10 to 60 psig and wall temperatures ranging up to 300° above saturation. The specific parameter ranges examined are shown in Table 2-1. The data obtained are tabulated in the Appendix.

Table 2-1 Matrix of Transition Boiling Tests

Mass Flow Rate lbs/hr ft^2	Operating Pressure (psig)		
	~10	~40	~60
14,000	ΔT_{sat} 10-300°F		
28,000	ΔT_{sat} 10-300°F	ΔT_{sat} 10-300°F	ΔT_{sat} 10-270°F
57,000	ΔT_{sat} 10-250°F		
85,000		ΔT_{sat} 10-230°F	ΔT_{sat} 10-190°F
140,000	ΔT_{sat} 10-175°F	ΔT_{sat} 10-150°F	

Note: $\Delta T_{sat} = T_{wall} - T_{sat}$

It should be observed that once boiling begins the rate of boiling heat transfer depends on ΔT_{sat}; the difference between the wall and saturation temperatures. This is true even when the bulk of the liquid is sub-cooled.

3.0 Experimental Results

To express the results of this investigation in simple usable form, the convention of defining a total heat transfer coefficient by

$$h = \frac{q''_w}{\Delta T_{sat}} \tag{3-1}$$

where h = total heat transfer coefficient, BTU/hr.ft^2 °F

q''_w = wall heat flux, BTU/hr.ft^2

ΔT_{sat} = wall temperature minus saturation temperature

= $T_w - T_{sat}$, °F

was followed. Under the condition of the present experiments, the exit steam temperature was generally quite close to saturation (maximum of about 25°F above saturation when ΔT_{sat} above 250°F). Further, heat transfer to steam was low, hence any non-equilibrium effects were quite small and the definition of h by Equation (3-1) is acceptable.

Satisfactory evaluation of h depends on the appropriate determination of q'' and ΔT_{sat}. Since neither of these quantities are directly measured an appropriate calculational scheme is required.

3.1 Calculational Procedures: The wall heat flux q''_w may be determined simply from

$$q''_w = Q/(\Pi D \Delta L) \tag{3-2}$$

where D = outer diameter of tube

Q = total heat released in length ΔL

The quantity, Q, is in turn determined by the change in the average mercury temperature in length (ΔL). That is

$$Q = W C_p \Delta T_{avg} \tag{3-3}$$

W = mercury flow rate, lbs/hr

C_p = specific heat of mercury, Btu/lb

ΔT_{avg} = change in average temperature of mercury

Useful results hinge on the correctness of the estimate of ΔT_{avg}.

Alternatively, the heat flux may be calculated by the estimated mercury temperature gradient at the tube wall. That is

$$q'' = -k\, dT/dr \tag{3-4}$$

where r = radial location.

Here the validity of the results depends on the accuracy of the estimate of dT/ dr.

In the tests, previously reported by Ramu and Weisman[12], changes in the average mercury temperature were based on the readings of the thermocouples located in approximately the center of the mercury stream. In the present tests, the average mercury temperature was based upon temperature measurements of sheathed thermocouples affixed to the inner and outer pipes of the annulus. An enlarged view of this arrangement is shown in Fig. 3-1. It is clear from this figure that

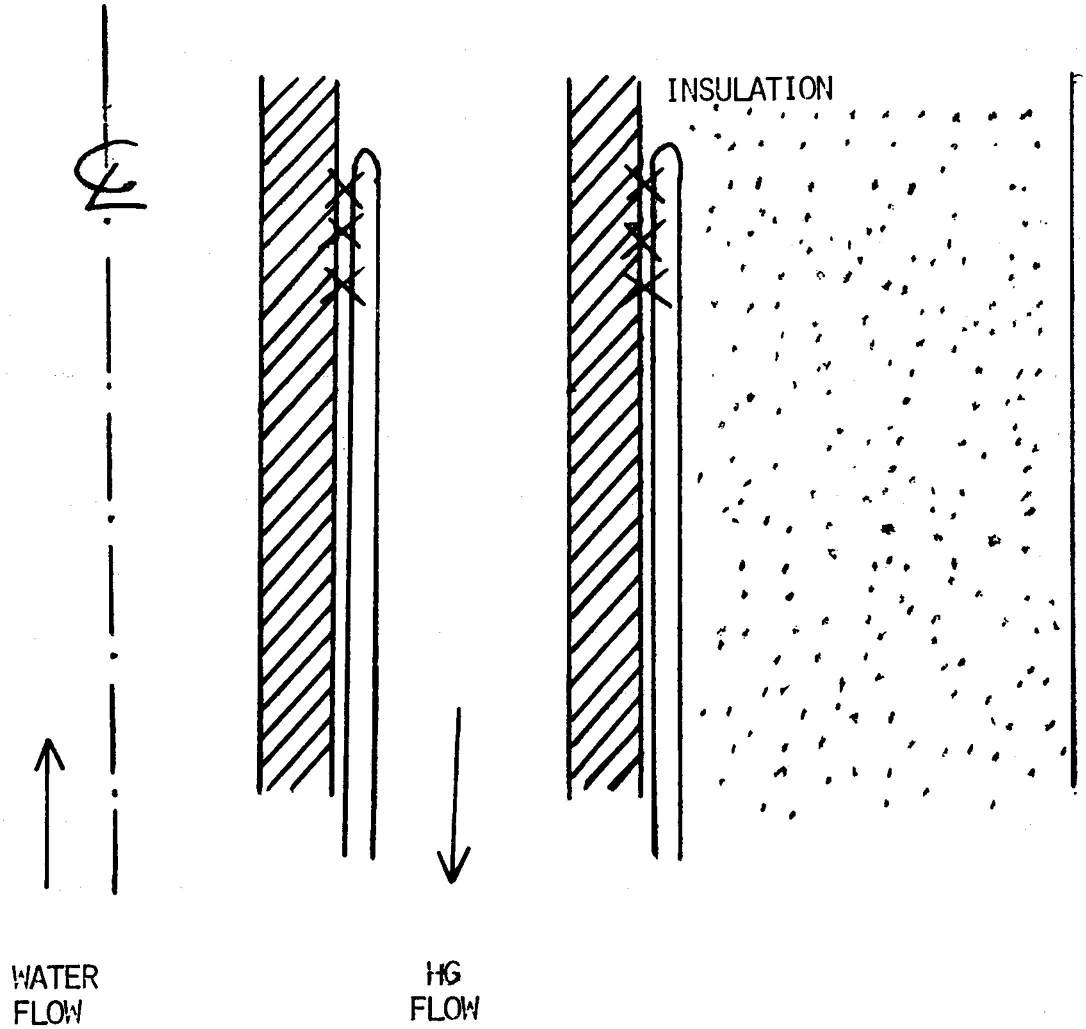

FIG. 3-1 SCHEMATIC OF THERMOCOUPLE ARRANGEMENT

the thermocouples in the outer pipe will read the temperature of the outer pipe wall. However, since the thermal conductivity of mercury (∿7 Btu/hr ft°F) is close to that of stainless steel (∿10 Btu/hr ft°F), the thermocouple on the inner wall is likely to be reading the temperature of the mercury a small distance from the inner wall rather than the wall temperature. Special test runs were required to elucidate this.

As expected, the experimentally determined temperatures at the inner thermocouple were substantially lower than those recorded by the outer thermocouple. In an ordinary fluid, such as water, the major temperature rise would occur in the film adjacent to the inner wall. The average fluid temperature could then be closely estimated by the temperature at the outer wall. However, in a liquid metal, there is a significant temperature gradient across the entire annulus tube. The temperature profile must therefore be calculated for reasonable estimates of T_{avg} to be obtained.

Calculation of the temperature profile is simplified by the fact that at the mercury flows of this experiment (approx. 5500 lbs/hr) the Peclet number is low (approx. 245). When the Peclet number is below a critical value (315 for annuli at Prandtl No. of .015[13]) turbulent mixing is negligible in comparison with radial conduction. The fluid may therefore be considered as if it were in rod-like flow and the temperature profile calculated by assuming all radial heat transport is by conduction. When only axial transport and radial conduction need to be considered, the basic differential equation for temperature distribution within the mercury may be written as

$$\frac{\partial^2 T}{\partial r^2} + \frac{1}{r}\frac{\partial T}{\partial r} = \frac{u_b}{\alpha'}\frac{\partial T}{\partial x} \qquad (3\text{-}5)$$

where r = radius

u_b = bulk velocity of mercury

x = axial distance

α' = thermal diffusivity = $\frac{k}{\rho c_p}$

k = thermal conductivity

ρ = density

c_p = specific heat

The above equation assumes that the hydrodynamic boundary layer is thin and that the velocity gradient in the mercury may be neglected (reasonable as Re ≈ 16,500).

A simple analytic solution to Equation (3-5) can be obtained when at some distance from the entrance heat addition per unit is a constant over a considerable distance. We then have $\partial T/\partial x$ = a constant and we have a total differential equation where the solution is

$$T = \frac{ar}{4} + C_1 \ln r + C_2 \qquad (3\text{-}6)$$

and

$$a = \partial T/_{\partial x} = \text{constant}$$

Unfortunately, in the present experiment $\partial T/\partial x$ is not a constant and no simple analytical solution is available.

The difficulty in obtaining a numerical solution can be minimized by observing the similarity between Equation (3-5) and the differential equation describing transient heat conduction in a hollow cylinder. For a cylinder in which there are no axial temperature gradients we have

$$\frac{\partial^2}{\partial r^2} + \frac{1}{r}\frac{\partial T}{\partial r} = \frac{1}{\alpha'}\frac{\partial T}{\partial \theta} \qquad (3\text{-}7)$$

where θ is time

If we rewrite Equation (3-3) as

$$\frac{\partial^2 T}{\partial r^2} + \frac{1}{r} \frac{\partial T}{\partial r} = \frac{1}{\alpha'} \frac{\partial T}{\partial (x \frac{1}{u_b})} \qquad (3\text{-}8)$$

A computer program capable of solving the transient conduction problem was developed at the University of Cincinnati for another project. In this program, the temperature gradient within the solid is determined as a function of time providing an initial temperature of the solid is specified and surface temperatures (at inner and outer surface) and thermal resistances at the boundaries are specified as a function of time. When applied to the current problem, the inlet temperature to the test section is equivalent to the initial temperature of the solid and the temperatures recorded by the thermocouples as a function of position are equivalent to surface temperatures as a function of time. Since an explicit solution procedure is used, short time steps must be specified. The program obtains temperatures at times (distances) between measurements by linear interpolation between the closest measured values.

The temperature measured by the outer thermocouples was at the outside of the outer pipe. The heat resistance at the outer boundary was therefore specified so that it presented a thermal resistance equal to that of the pipe wall. The inner thermocouples were in the mercury stream and hence a near zero thermal resistance was specified here. The computer program then determined the temperature distribution within the mercury stream for a given set of wall temperature measurements.

In order to determine whether the computer program was providing accurate results, a comparison between the numerical results and the analytic solution was conducted. The experimental geometry, mercury flow and mercury properties were specified but the change in temperature per unit length at each boundary surface was held constant. Under the conditions, the analytical solution of equation (3-5) should closely fit the temperature profile at the outlet of the test section. That this is indeed the case may be seen from Fig. 3-2 where the computer output is compared to the analytical solution obtained for this case. Close agreement is observed.

As a second check of the accuracy of the program, a subroutine which computed the heat loss by the mercury was added. The heat loss was determined in two ways. In the first method the radial heat flow at the boundaries was determined for each axial (time) increment from the temperature gradient at the boundaries. These losses were then summed to determine the total heat loss between thermocouple locations. In the second approach, the heat loss was determined using the radial temperature profiles suitably integrated to obtain T_{avg}. Comparison of the total heat loss between thermocouple elevations as determined by the two methods showed very close agreement (generally within 1%).

Once confidence had been established in the calculational procedure, the computer program was used to analyze the non-boiling data obtained at low wall temperatures and high water flow rates. Initially, it was assumed that the thermocouples at the inner pipe wall were recording the temperature of the inner tube wall. With this assumption, the radial temperature profiles were determined as a function of elevation for each of the runs. Heat transfer coefficients were then determined from the heat flow to the inner wall. The results of two typical runs are shown in Table 3-1. It will be

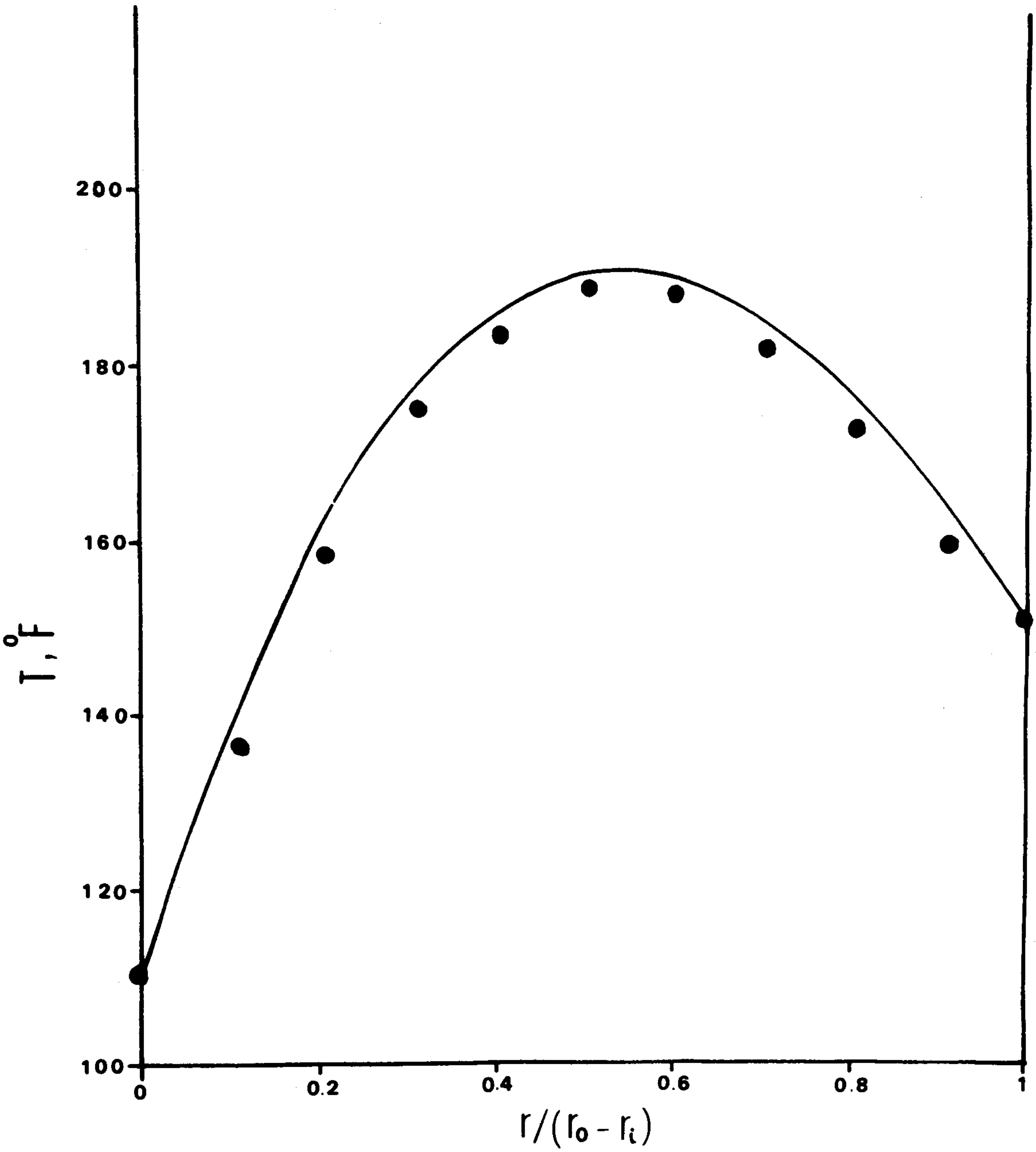

Fig. 3.2 Comparison of Analytic Solution With Numerical Results From Computer Program

observed that the calculated heat transfer coefficients close to the entrance of the test section were considerably lower than those obtained at the bottom of the test section. For the conditions of these tests, one would have expected that the heat transfer coefficients should have been very nearly uniform since the temperature and hence fluid properties changed very little (only about $10^{o}F$) across the test section and there was no boiling. Further, the maximum heat transfer coefficients calculated were below the h of 700 to 800 Btu/hr $ft^{2}{}^{o}F$ estimated from the Dittus-Boelter equation.

In all of these runs, the wall temperature was below the saturation temperature. Hence, the nonboiling assumption was clearly justified. Of course, Equation (3-1) could no longer be used for calculation of h and h was determined by dividing the heat flux by the difference between the wall and bulk temperatures.

In these runs, the bulk water temperatures at the several elevations were calculated by adding to the water inlet temperature the temperature increment obtained from a heat balance. The total heat transferred was obtained from the change in bulk mercury temperature. The maximum error in water flow rate measurement could have led to only about a $0.2^{o}F$ error in temperature difference and this could not explain the results obtained. Further, an inlet water temperature error would have raised or lowered the coefficients by nearly the same amount.

It was previously noted that the thermocouple affixed to the inner pipe wall was probably not reading the wall temperature but rather the temperature of the mercury a small distance from the wall. Sets of hand calculations were made in which it was assumed that the inner thermocouple read the mercury temperature at distances of 20 mils to 50 mils from the wall. The pipe wall temperatures were obtained by extrapolating the radial temperature profile to the inner wall boundary. The results of the corrections at 30 mils are also shown in Table 3-1. It is seen that the heat transfer coefficients have all increased since extrapolation of the temperature profiles leads to lower wall temperatures. However, the percentage change is most marked for the values at the top of the test section. There the change in the slope of the temperature profile between the wall and 30 mils from the wall is sharper than at the lower locations. This leads to an increased heat flux and hence higher coefficients. The values obtained are somewhat more uniform and closer to those expected. The results therefore indicate that assuming the couple is reading a temperature away from the wall is most appropriate.

Table 3-1

Effect of Thermocouple Location on Calculated Heat Transfer Coefficients

Run No.	Location	Heat transfer coefficients (BTU/hr ft^{o}F)	
		T.C. reads wall temp.	T.C. reads temp. 30 mils from wall
1101			
	1 (top)	392	682
	2	618	890
	3	681	695
	4 (bottom)	692	700
1102			
	1 (top)	339	750
	2	594	895
	3	645	691
	4 (bottom)	720	784

Examination of the results for calculations at other effective distances from the pipe wall showed the same trends as those illustrated in Table 3-1. However, the scatter of the results was such that one could only conclude that the couple was reading a temperature somewhere between 20 and 50 mils. A distance of 20-30 mils seems most in accord with the physical situation. A distance of 20 mils was selected for use in subsequent calculation as the assumption of greater distances from the pipe wall gave forced convection heat transfer coefficients above the expected range. The uncertainty in the location of this measured temperature was one of the items considered in the analysis of the data accuracy.

The foregoing calculations were all based on the assumption that there is no contact resistance between the mercury and the tube wall. It is believed that the thorough evacuation of the loop prior to filling assures that this is essentially correct. If the conclusion that the wall thermocouples actually measure temperature slightly away from the wall is correct, then any small remaining resistance would simply act to increase the effective distance from the wall at which the couples appear to be located.

An alternative calculational procedure was also examined. In this procedure, it was assumed that an equilibrium temperature profile (obtained from Equation (3-6) with C_1 and C_2 evaluated from temperatures at boundaries) existed at the lowest axial position. It was then assumed that the temperature profile at the next axial position could be represented by a cubic equation. The two measured temperatures were taken as boundary conditions. The third boundary condition came from the requirement that the average heat loss (as determined by average temperature slope at outer wall) agree with experimentally measured heat loss. The fourth boundary condition was obtained by requiring that the total heat transfer, as determined by average of temperature slopes at 3rd and 4th position, agree with the total heat transfer as determined by the difference in average temperatures between the 3rd and 4th level. With these boundary conditions, an iterative procedure allowed the temperature profile to be estimated at the 3rd position. This same procedure was then used to estimate the temperature profile at the upper elevations using the calculated temperature profile at the next lowest position as obtained above.

The results of the foregoing procedure were compared to the results obtained using the transient conduction program for several typical runs. Reasonable agreement between the two approaches was obtained at the lowest elevations (positions furthest from the inlet). However, it was concluded that the use of the transient condition program for calculation of temperature profiles was preferable since it was based on the actual physical phenomena and since it allowed the effective location of the inner thermocouple to be more easily varied.

3.2 Experimental Heat Transfer Coefficients

The calculation procedures of the previous section were used to establish temperature profiles and from there the average temperature was determined as a function of position. The total rate of heat transfer, q''_w, to the water at each thermocouple location is computed from the slope of temperature profile at the inner pipe walls (Equation 3-4). The total heat transfer so computed is compared with the total heat transfer determined from the change in mercury temperature making proper allowance for the heat loss to the surroundings. The wall temperature, T_{WL}, is then obtained after substituting the temperature drop through the wall based on the q''_w established.

The thermodynamic equilibrium quality, x_e, is determined by an overall heat balance. viz:

$$x_e = \frac{Q_T - Q_{loss} - Wc_{pW}\,(T_{sat} - T_{win})}{m_W H_{fg}} \qquad (3\text{-}7)$$

where Q_T = total heat transferred by Hg

Q_{loss} = heat transferred through pipe wall (based on Fig. 2.3)

T_{win} = inlet water temperature; W = Hg flow rate;

m_w = water flow rate; H_{fg} = heat vaporization.

The data thus obtained are plotted in Figure (3-3) - Fig. (3-20) as h vs. ΔT_{sat} and x_e vs. ΔT_{sat}.

If the plots at the various flow rates are examined, there is seen to be a significant variation between the heat transfer obtained from the several axial locations. The results at the lowest flows are seen to exhibit the greatest variation. This is due to the fact that the largest difference in quality exits between the several locations at lowest flow rate.

If a single plot for fixed mass flow and pressure is examined, it is observed that at low values of ΔT_{sat} (before transition boiling commences) the data points tend to be somewhat above McAdam's nucleate boiling curve. No definite order with respect to thermocouple locations can be seen. As ΔT_{sat} reaches its critical value, the rate of heat transfer drops below the nucleate boiling curve and decreases as ΔT_{sat} increases. Usually the heat transfer coefficients at the upper thermocouples are lower than those at the lower thermocouples. This variation would seem to be ascribable to the variation in quality with axial position. Because of the flow arrangement of the test section, the qualities increase with increasing distance from the entrance. As expected, the heat transfer coefficients are lower at higher qualities and higher ΔT_{sat}.

The overall heat transfer coefficients, in general, increase with increasing water flow rate. There are two factors that may contribute to this increase in h. The lower void fractions brought about at higher mass flow rates may be expected to increase the critical heat flux and observed h. In addition, at G's above about 50,000 lbs/hr ft^2, (see Ref. 9), increased mass velocity will increase the critical heat flux, and hence, increase transition boiling h's.

The operating pressure also appears to affect the observed heat transfer coefficients. If the h vs ΔT_{sat} plots for the flow rate of 2.8×10^4 lbm/hr ft^2 are examined at three pressure ranges studied, one concludes that somewhat higher heat transfer coefficients are seen at higher pressures. This trend is not unexpected since lower void fractions will be obtained for a given quality and the predictions of Ramu and Weisman(12) indicate improved heat transfer coefficients at lower voids.

In Fig. 3-21, the data of Ramu and Weisman(12) for a mass flow rate of 12,000 to 13,650 lbs/hr ft^2 are reproduced. If these data are compared to the data of Figs. 3-3 to 3-20, it is seen that the heat transfer coefficients of Ramu and Weisman drop much more sharply at high temperature differences than those of the present tests. It is believed that part of the reason lies in the fact that the previous study was not able to take into account the change in temperature profile within the mercury.

In the previous tests, mercury temperatures were based on a single thermocouple placed near the center of the tube in which the mercury was flowing. Under conditions of uniform heat removal per unit axial length, all temperature profiles are similar (see Fig. 3-22a). An estimation of the change in average mercury temperature based on the changing center temperature (T_c) only will be correct since the temperature changes at any given radial position is invariant ($\Delta T_w = \Delta T_c$). However, when there is a non-uniform rate of heat removal, the temperature profile varies. For the transition boiling tests in which considerably lower h's were seen at the upper position, the situation seen in Fig. 3-22 b would prevail (the temperature profile becomes steeper at higher rates of heat removal). The assumption that the change in average temperature equals the change in central temperature is no longer correct. The error will be greatest at the upper position where the temperature profile change is the greatest. Use of the center temperature alone for this calculation will tend to underestimate the heat release. The underestimate will be greatest at the upper position where the temperature differences between water and mercury sides are the greatest.

It should also be noted that the heat transfer obtained in an annulus with an unheated outer wall may actually be lower than that under similar flows and average quality in a heated round tube. Tong and Young[15] have suggested that the heat transfer is controlled by the higher local quality, x_ℓ, adjacent to the heated wall. They conclude

$$x_\ell = x_b \left(\frac{D_h}{D_e}\right)^{1/2} \qquad (3\text{-}8)$$

where x_b = bulk quality

D_h = equivalent diameter based on heated perimeter

D_e = equivalent diameter based on wetted perimeter

Use of a quality computed as in Equation (3-8) would reduce the discrepancy between predictions and Ramu's observations at high temperature differences.

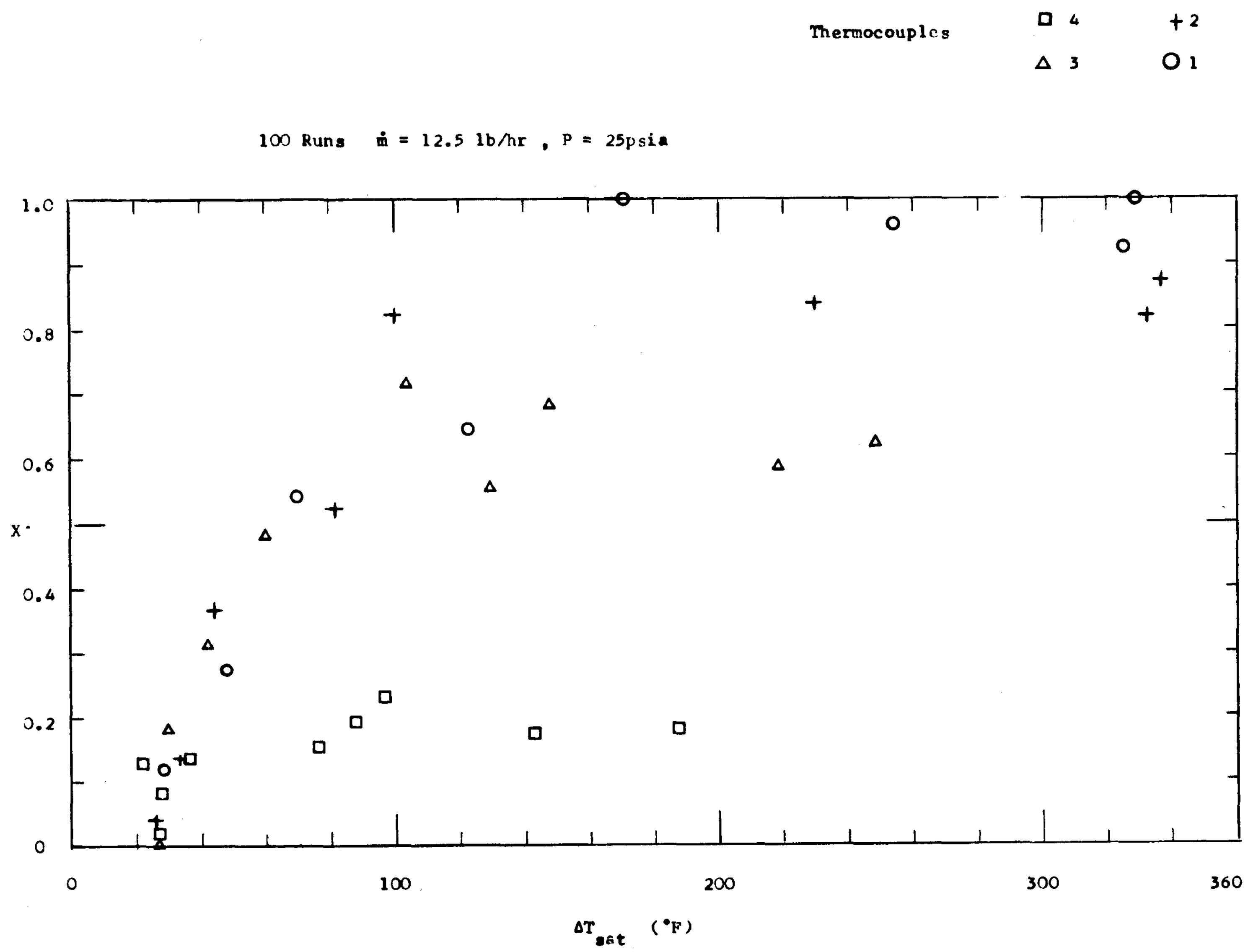

Fig. 3.3 Qualities Seen During 100 Series Runs

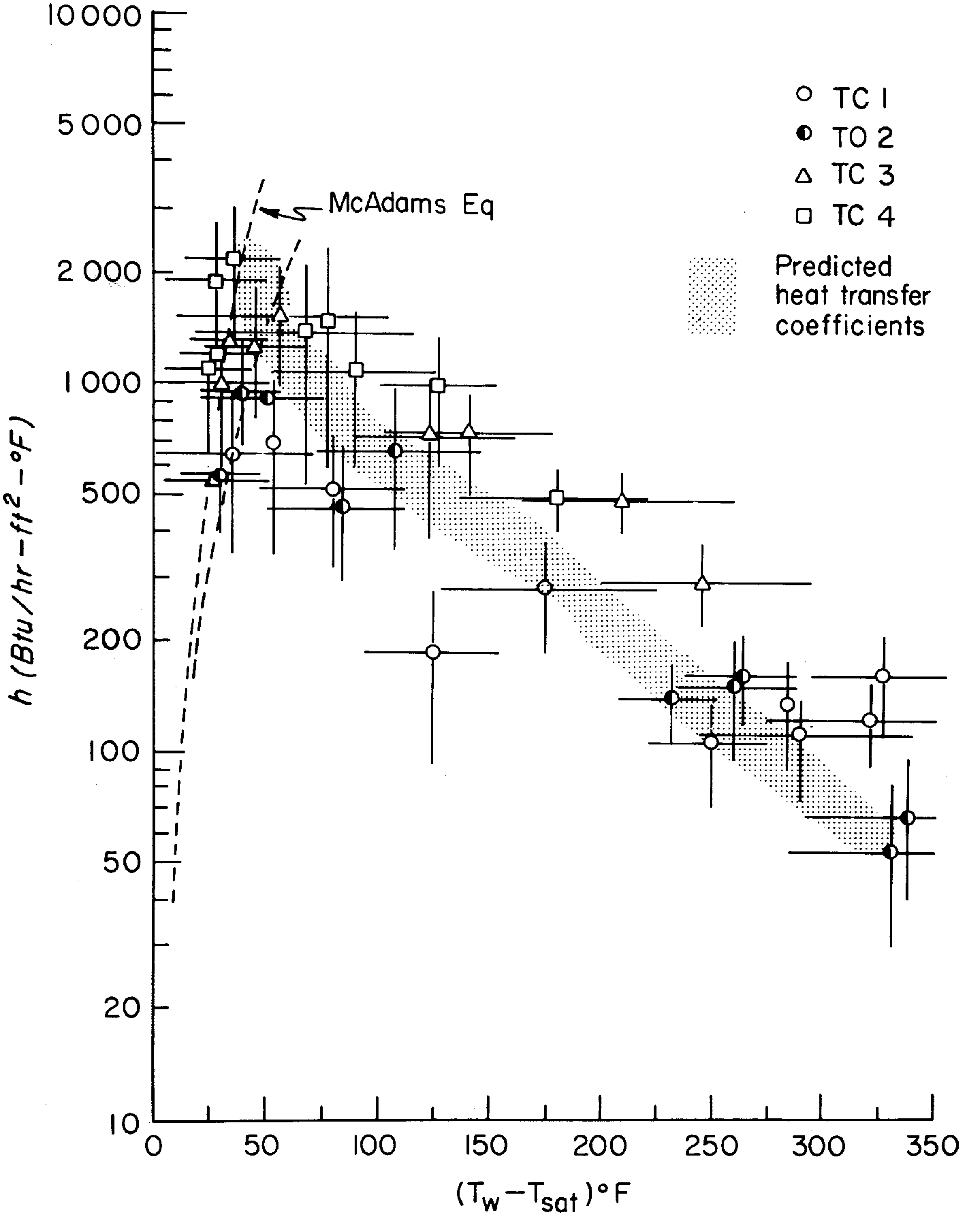

Fig. 3.4 Heat Transfer Coefficients From 100 Series Runs

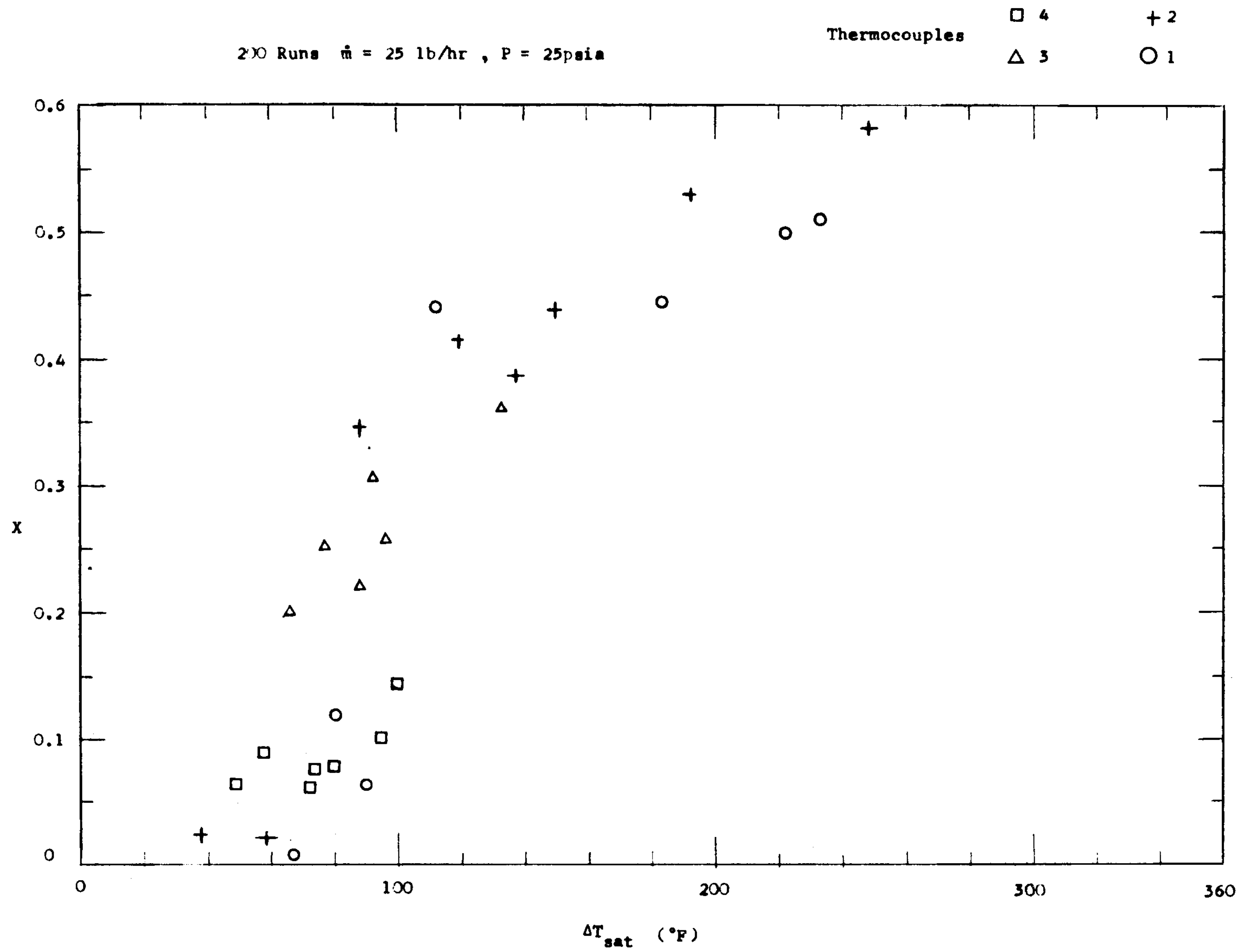

Fig. 3.5 Qualities Seen During 200 Series Runs

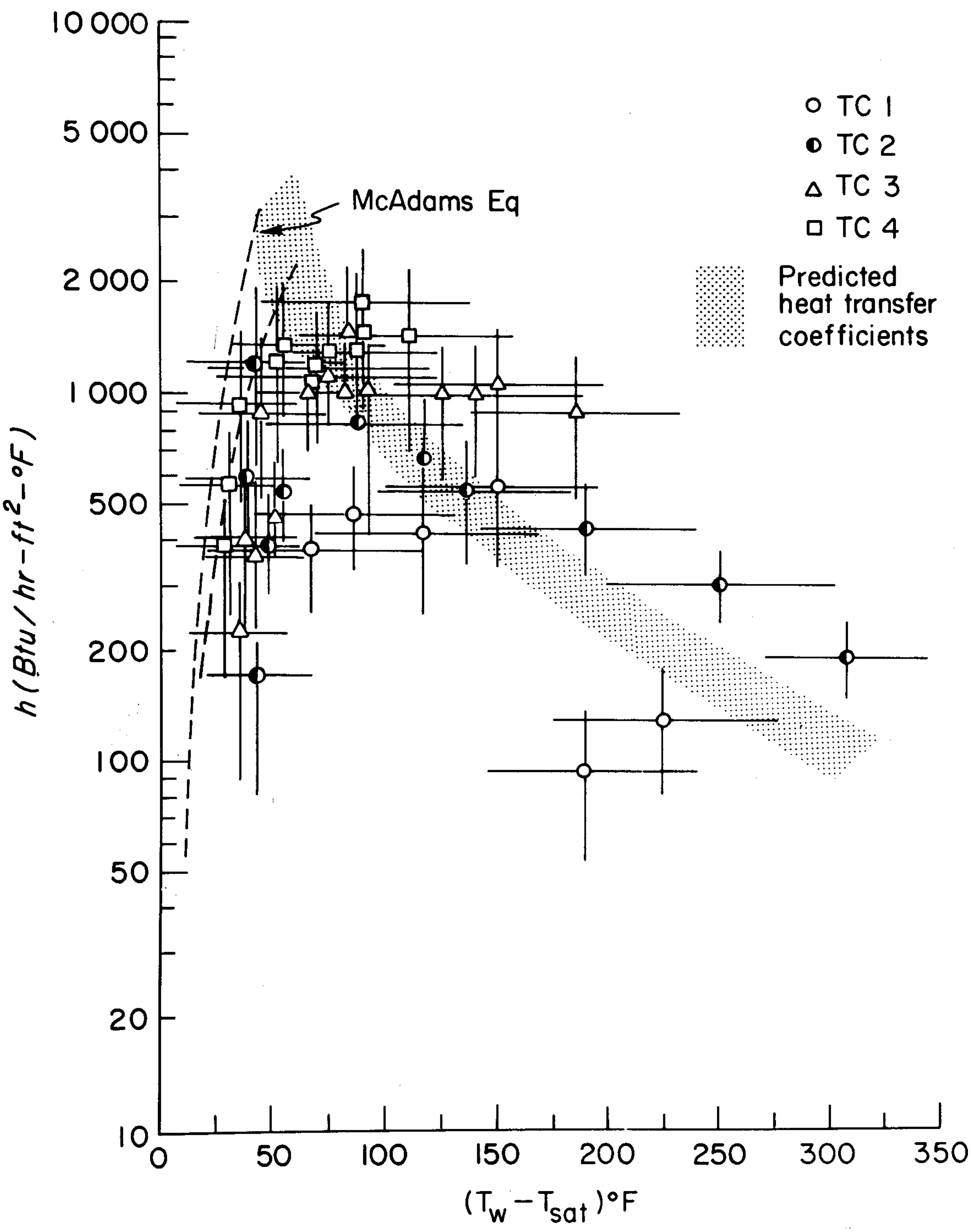

Fig. 3.6 Heat Transfer Coefficients From 200 Series Runs

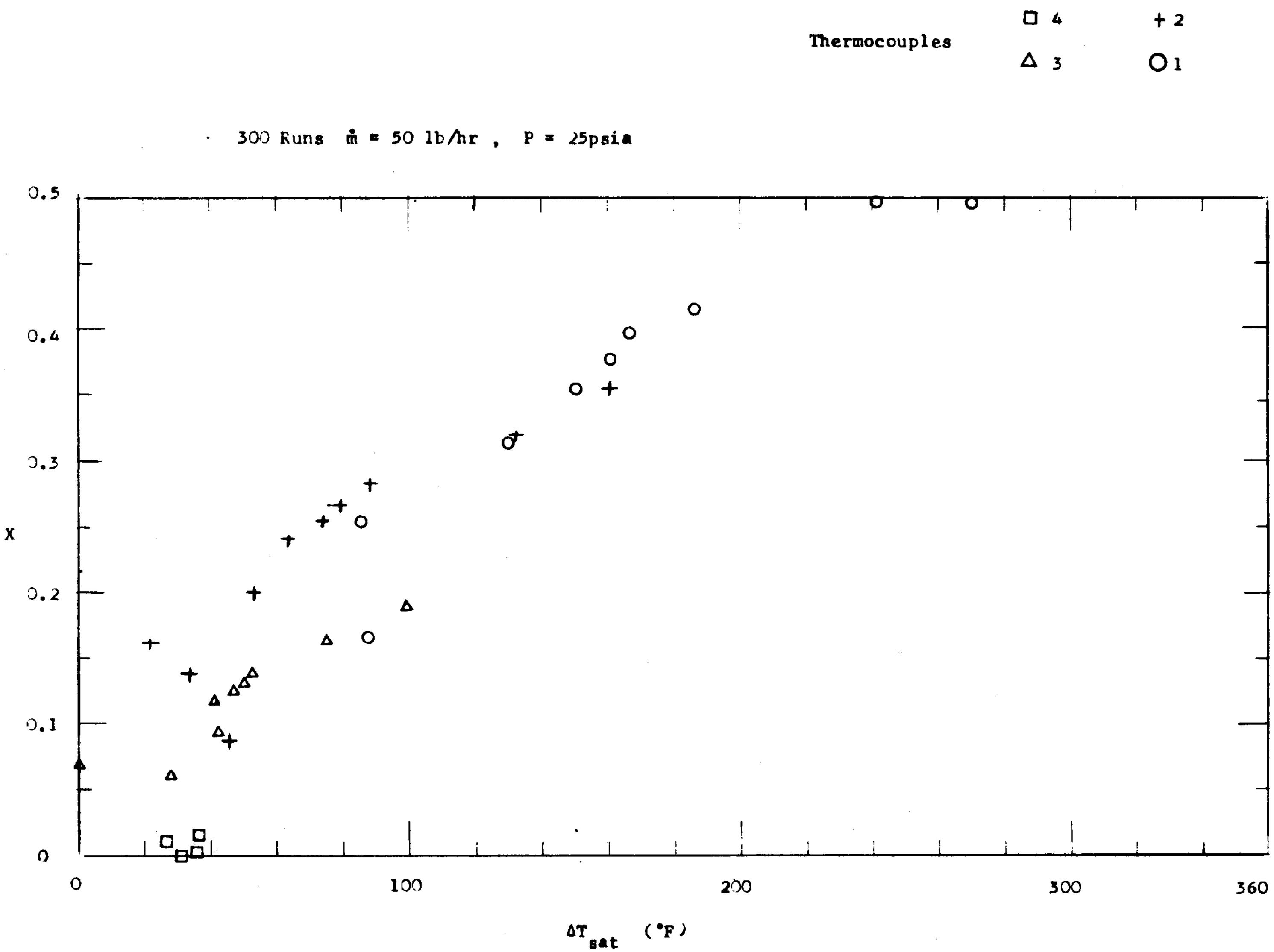

Fig. 3.7 Qualities Seen During 300 Series Runs

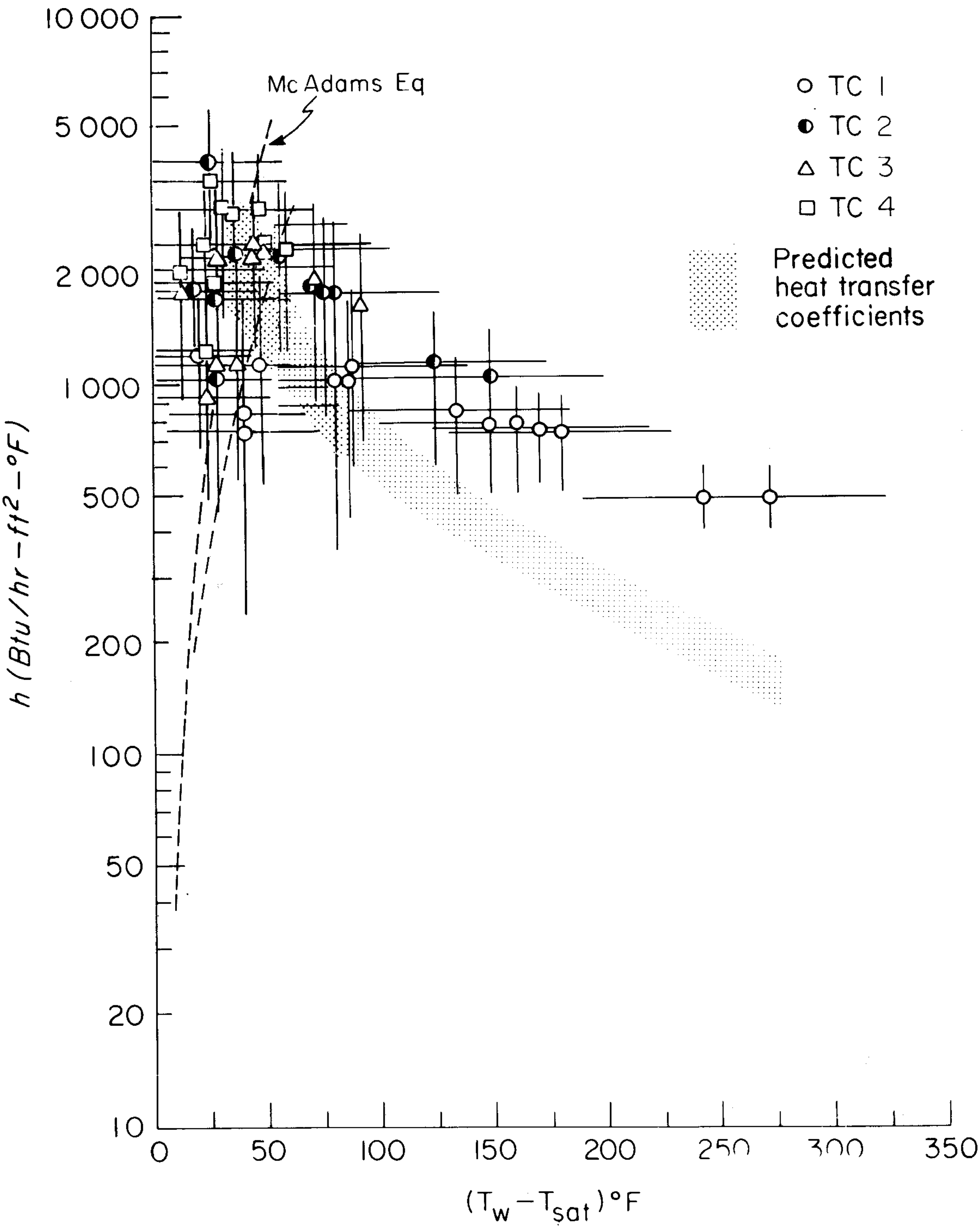

Fig. 3.8 Heat Transfer Coefficients From 300 Series Runs

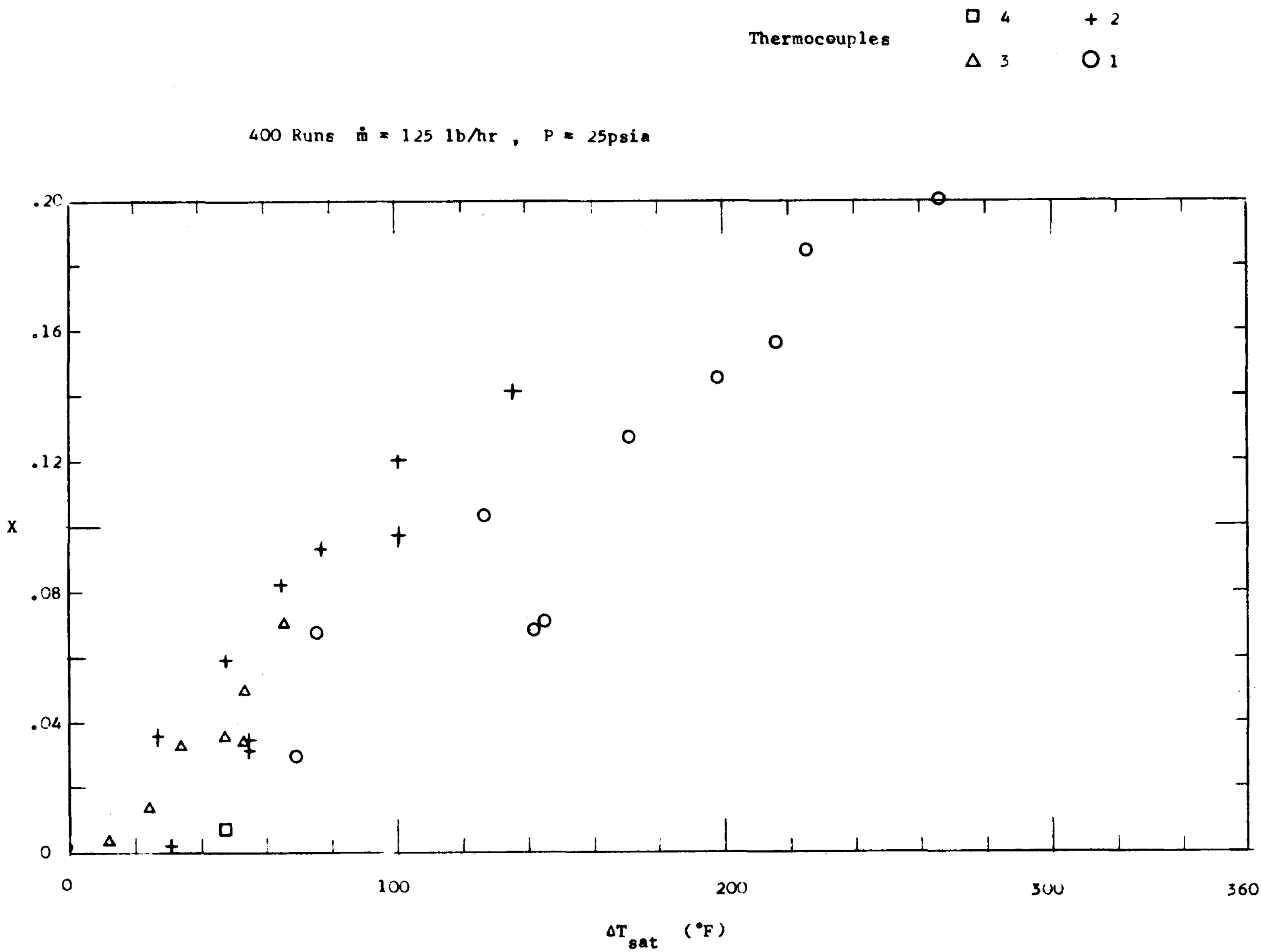

Fig. 3.9 Qualities Seen During 400 Series Runs

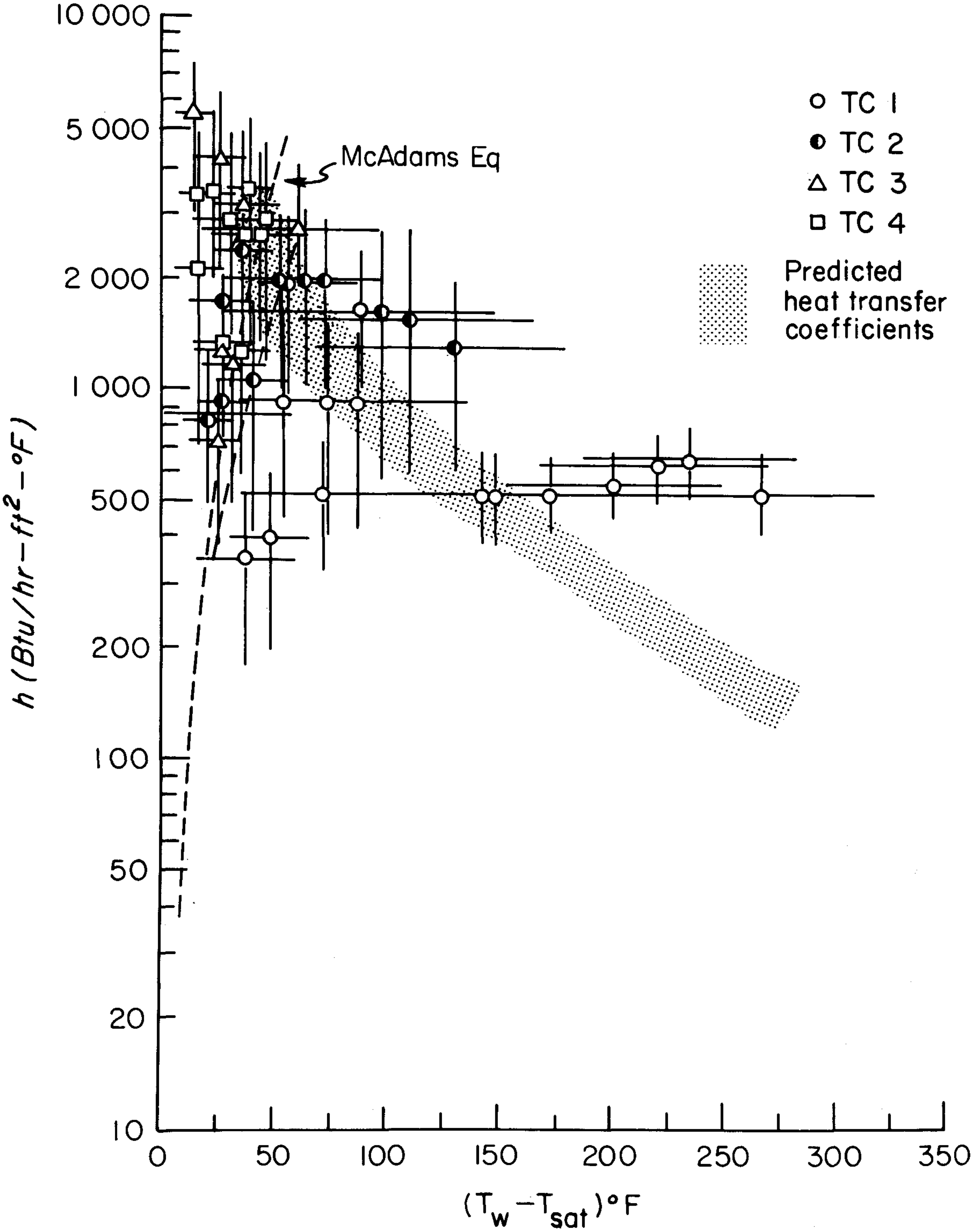

Fig. 3.10 Heat Transfer Coefficients From 400 Series Runs

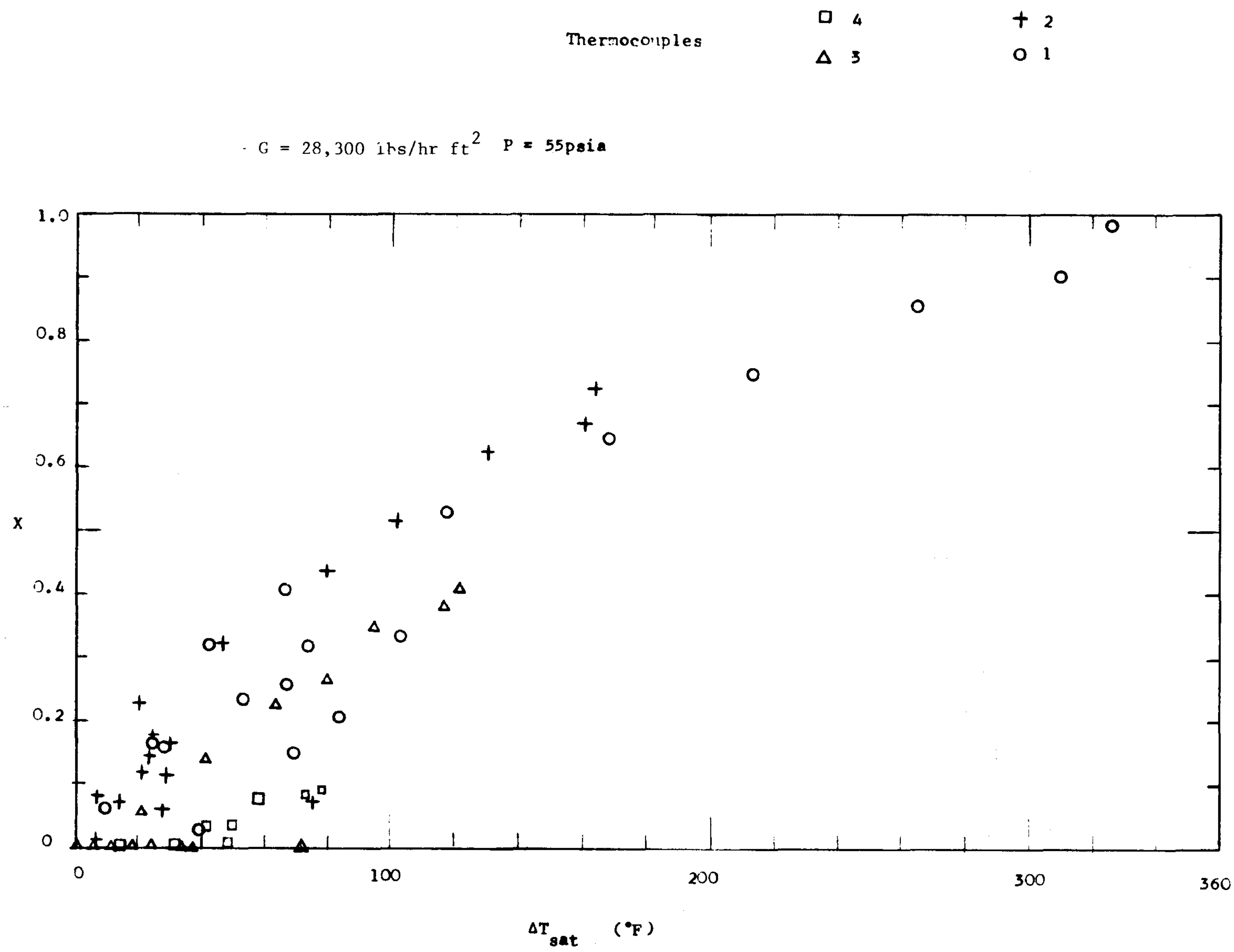

Fig. 3.11 Qualities Seen During 500 Series Runs

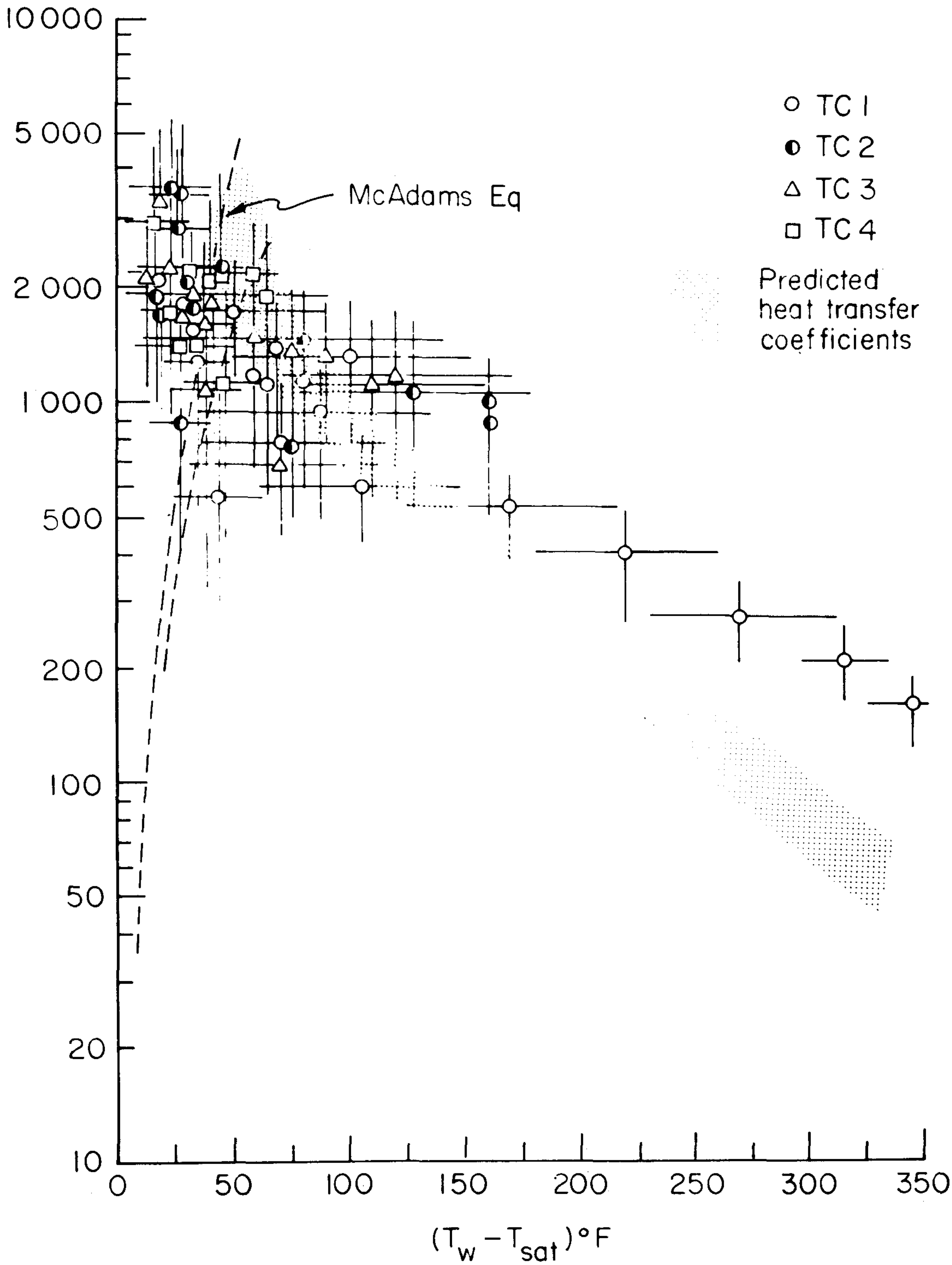

Fig. 3.12 Heat Transfer Coefficients From 500 Series Runs

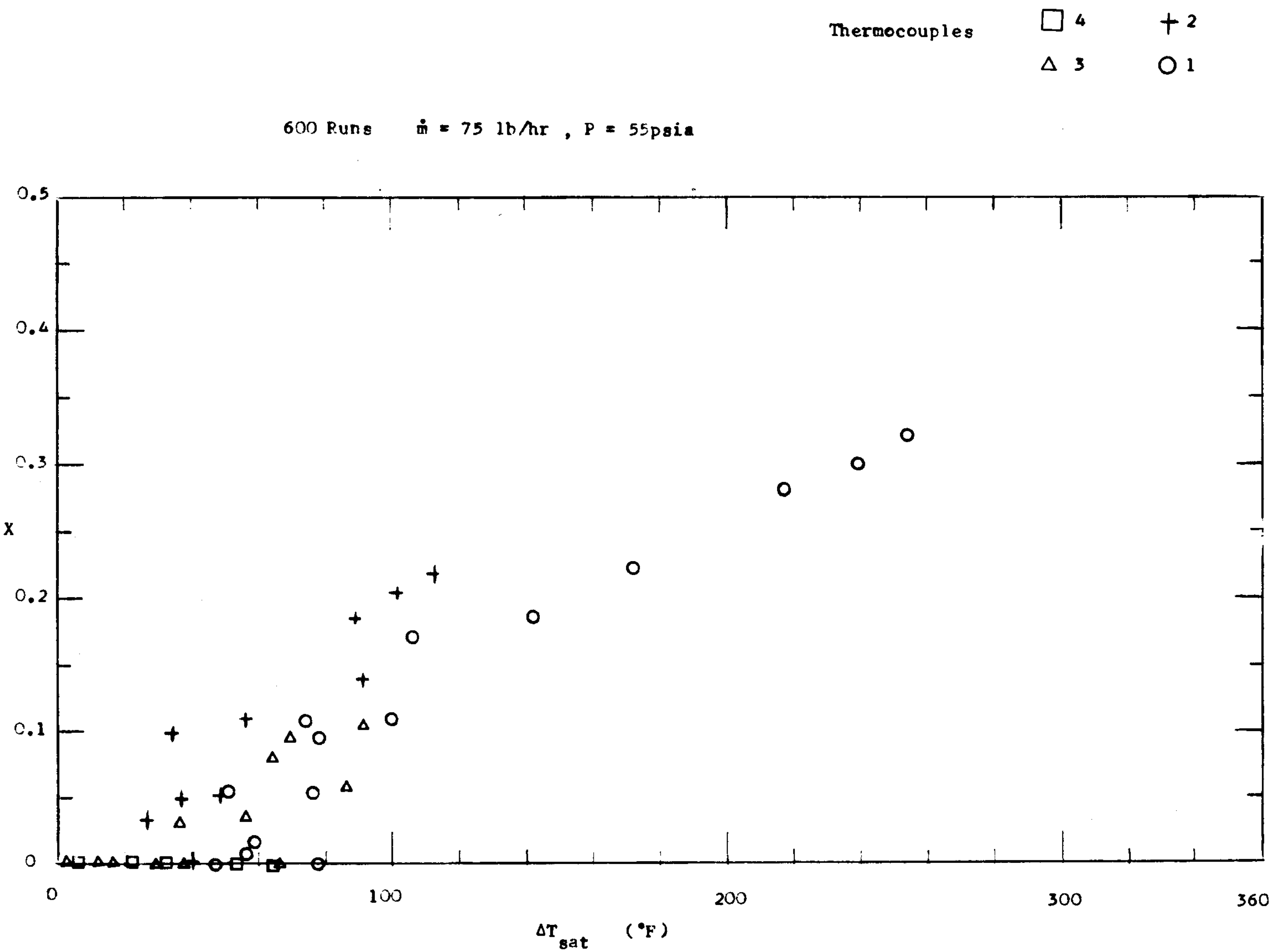

Fig. 3.13 Qualities Seen During 600 Series Runs

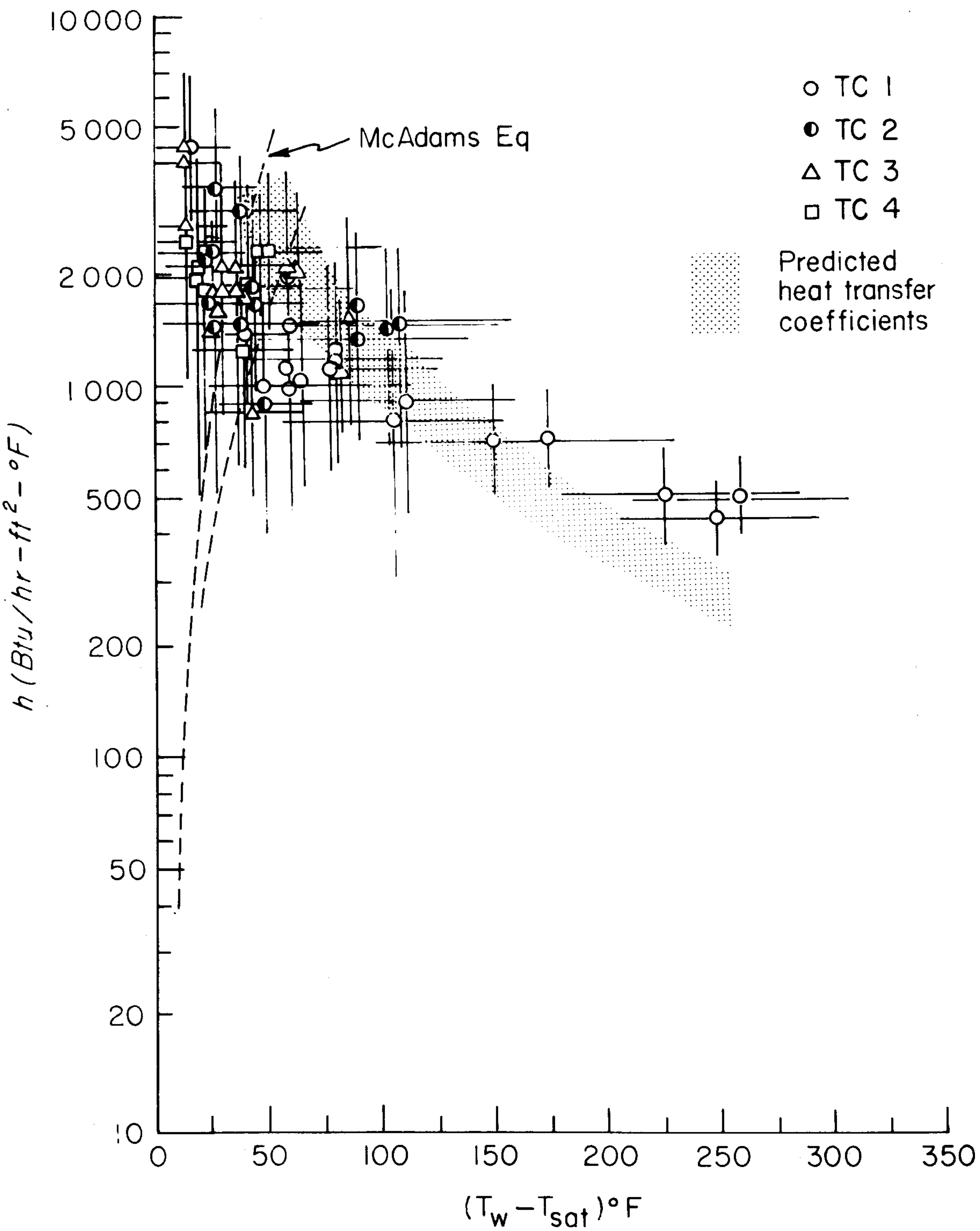

Fig. 3.14 Heat Transfer Coefficients From 600 Series Runs

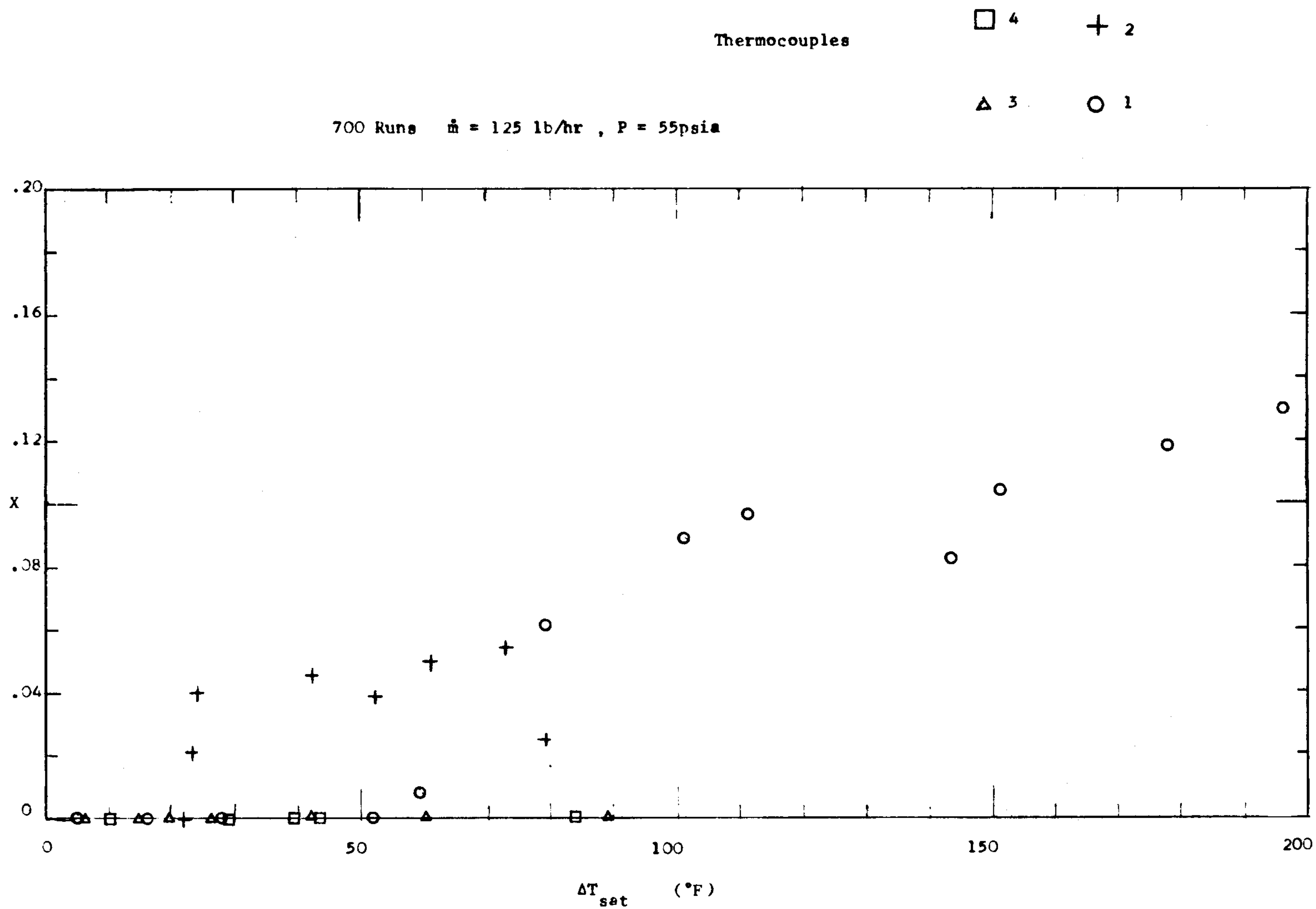

Fig. 3.15 Qualities Seen During 700 Series Runs

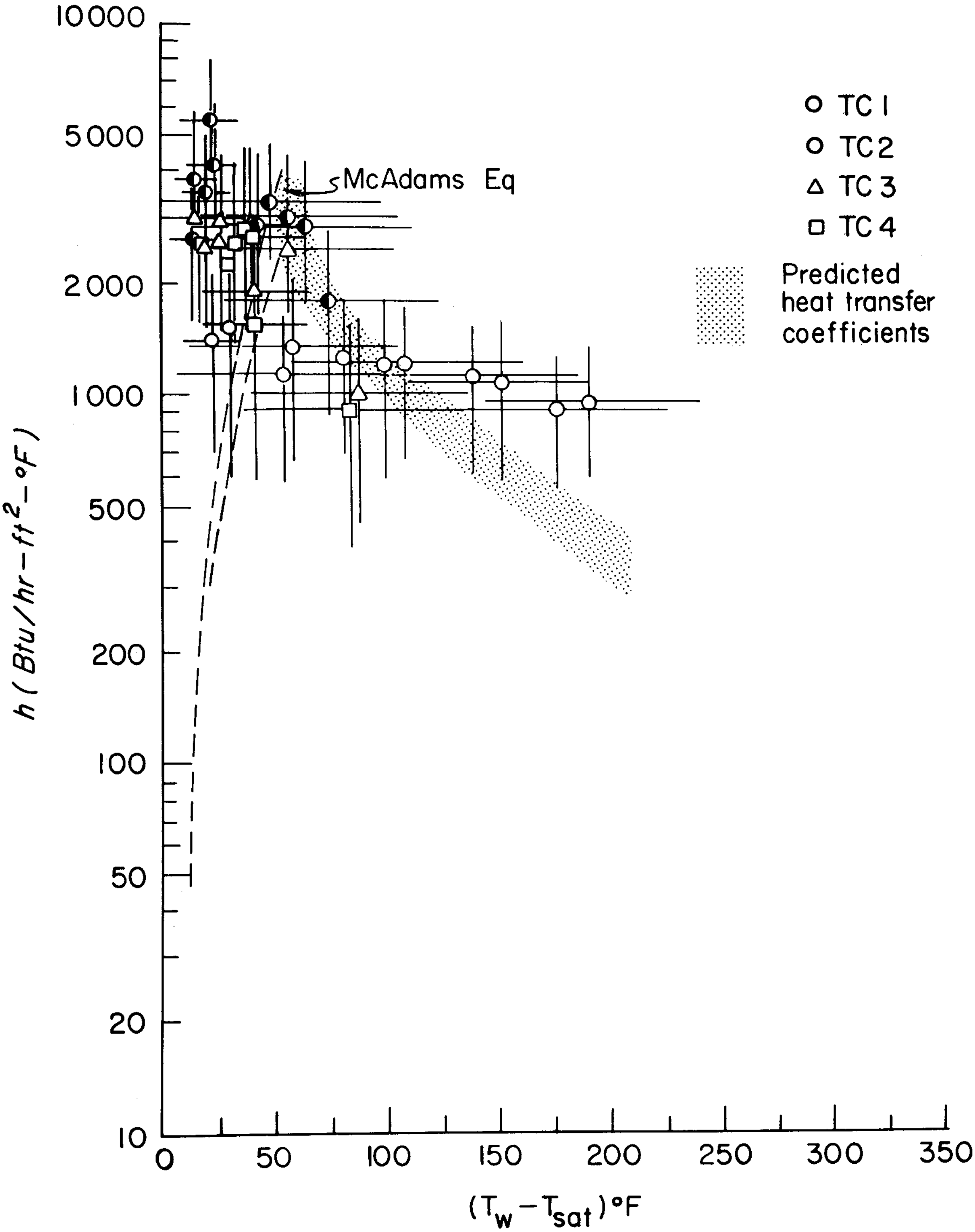

Fig. 3.16 Heat Transfer Coefficients From 700 Series Runs

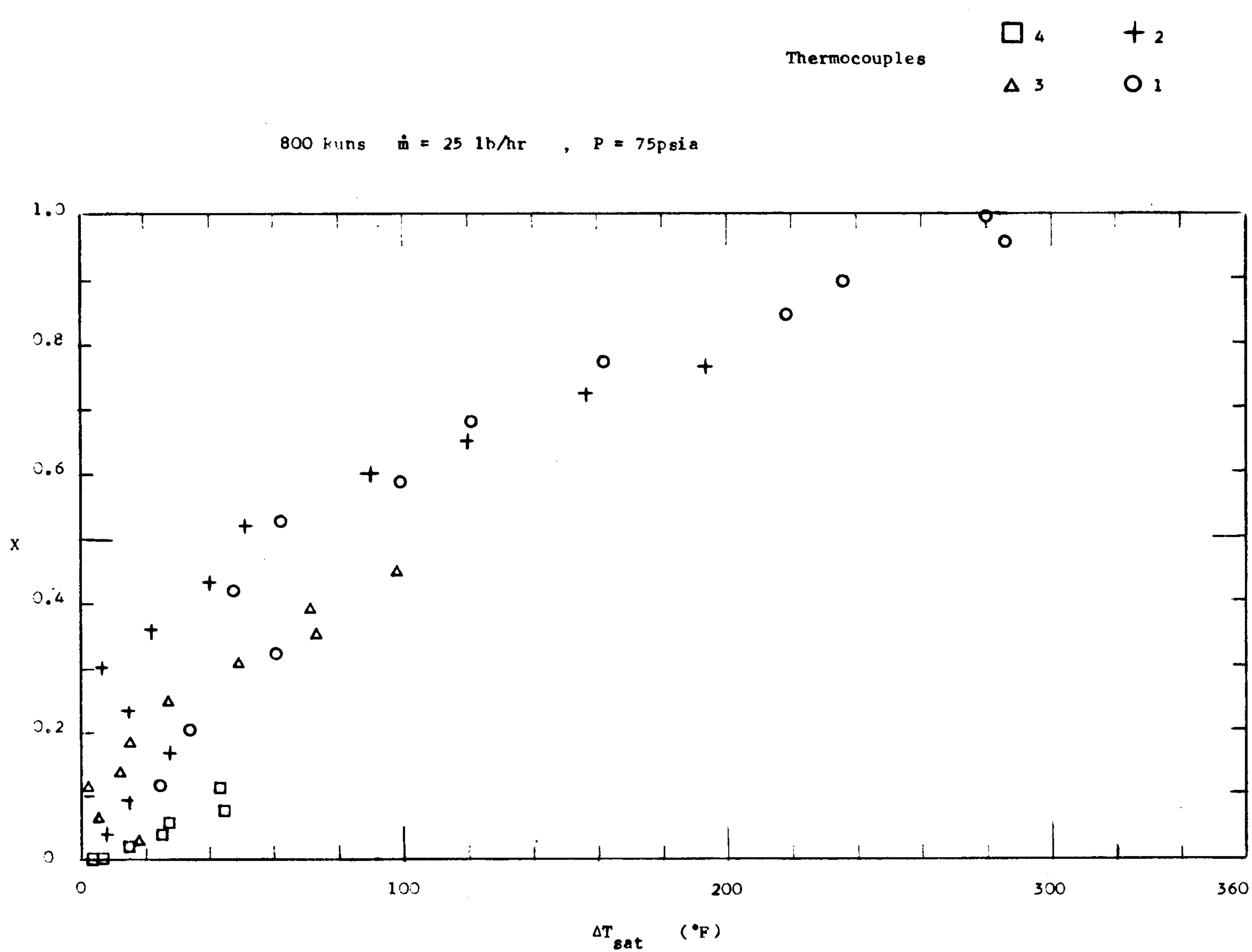

Fig. 3.17 Qualities Seen During 800 Series Runs

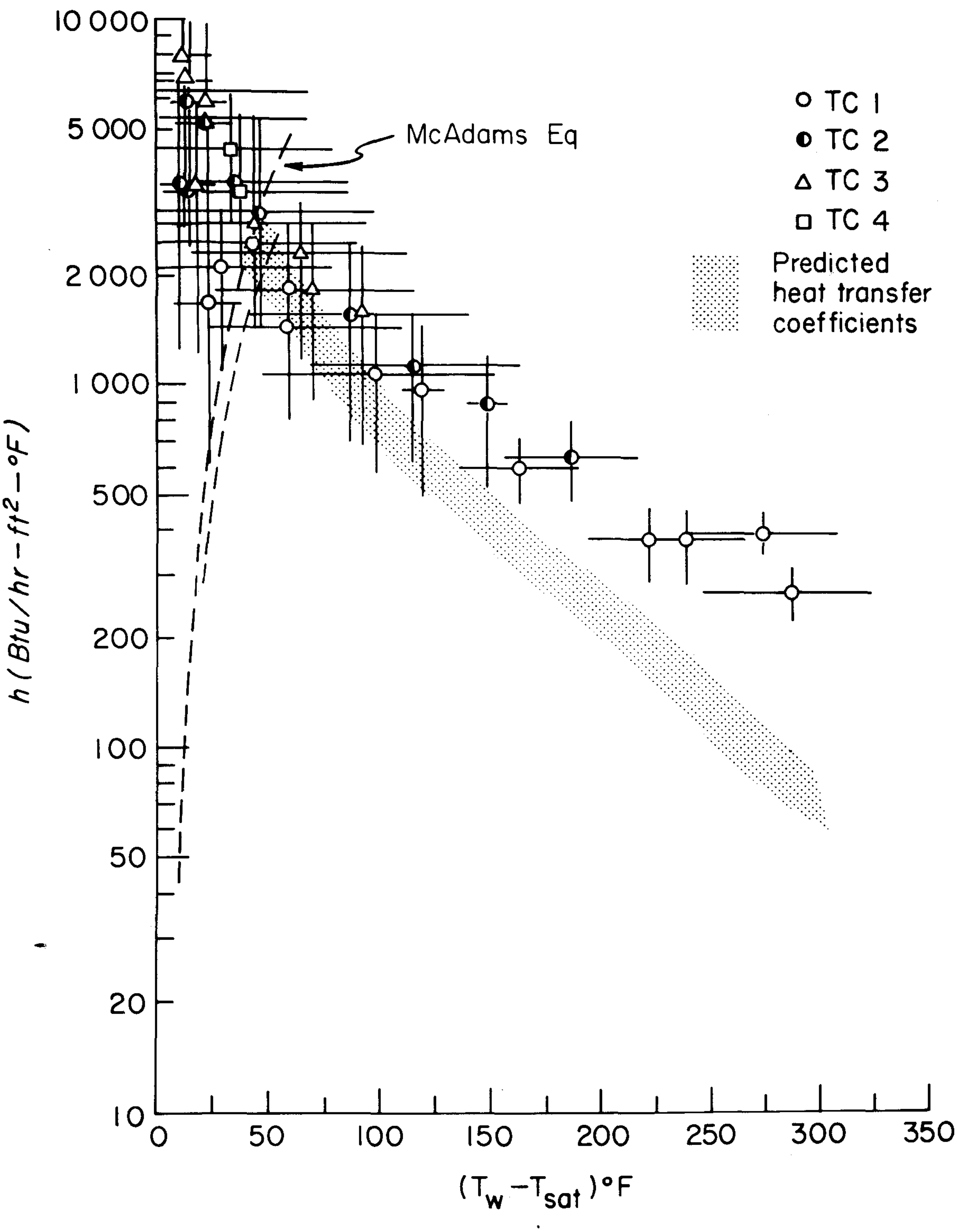

Fig. 3.18 Heat Transfer Coefficients From 800 Series Runs

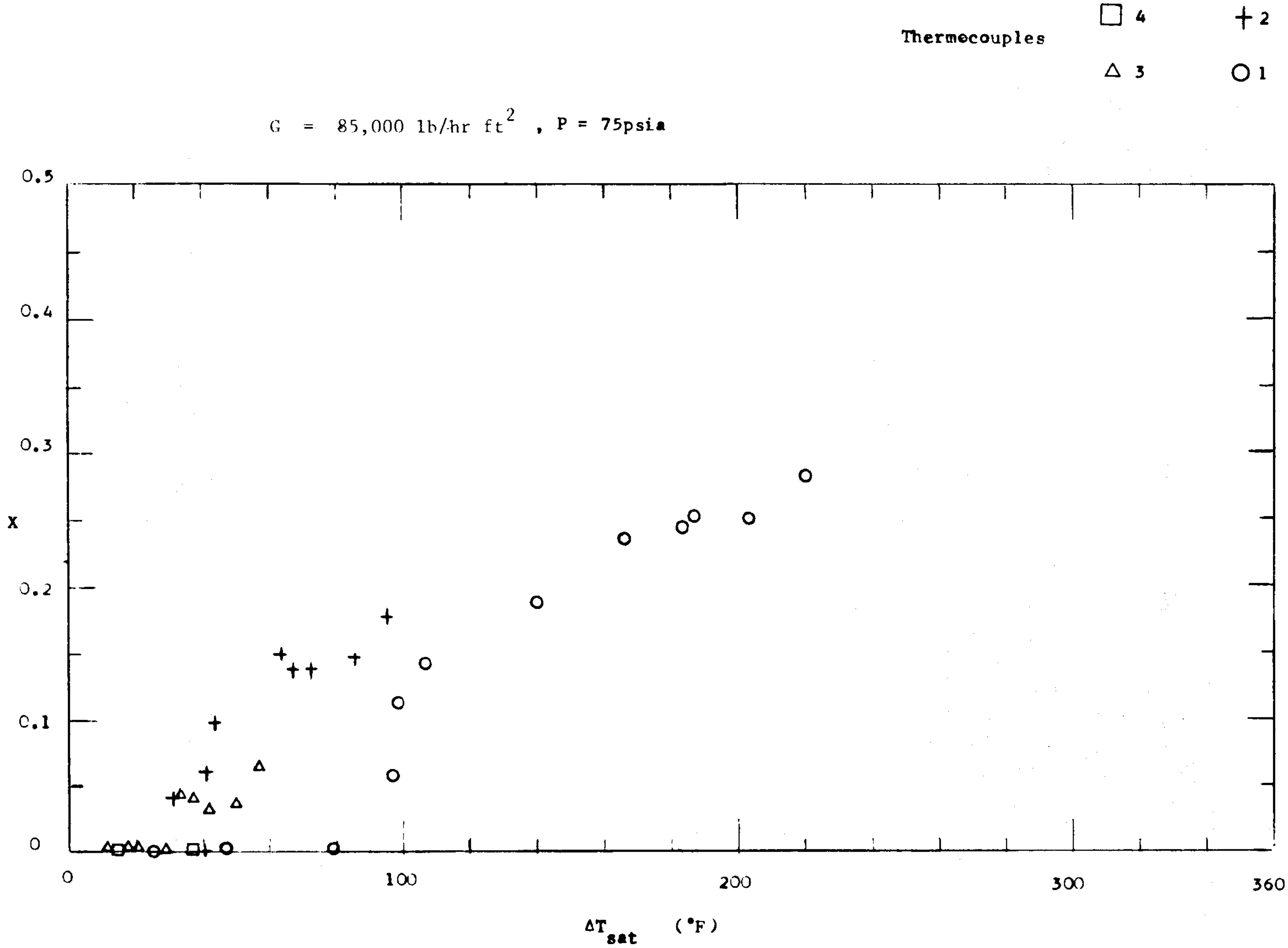

Fig. 3.19 Qualities Seen During 900 Series Runs

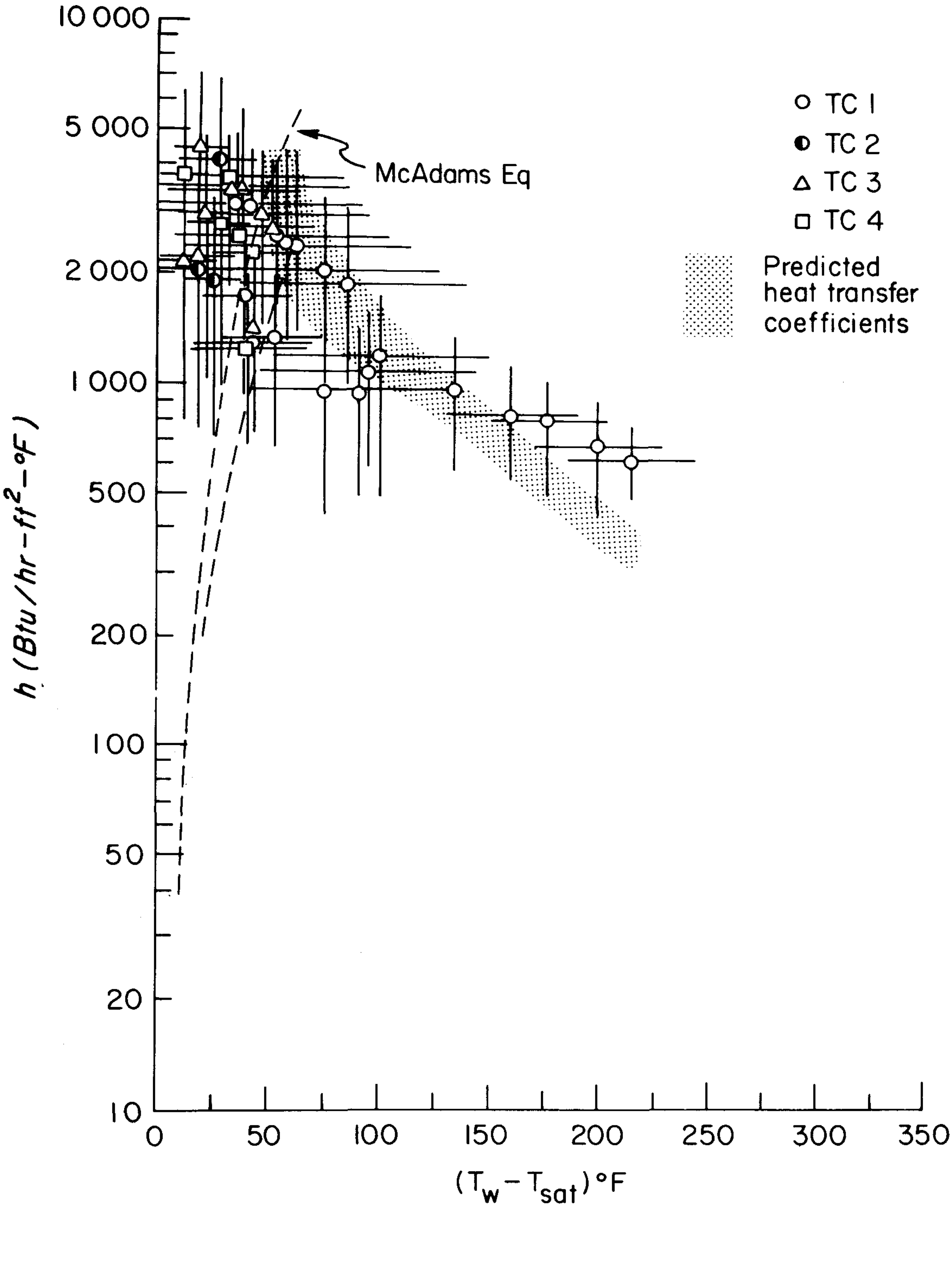

Fig. 3.20 Heat Transfer Coefficients From 900 Series Runs

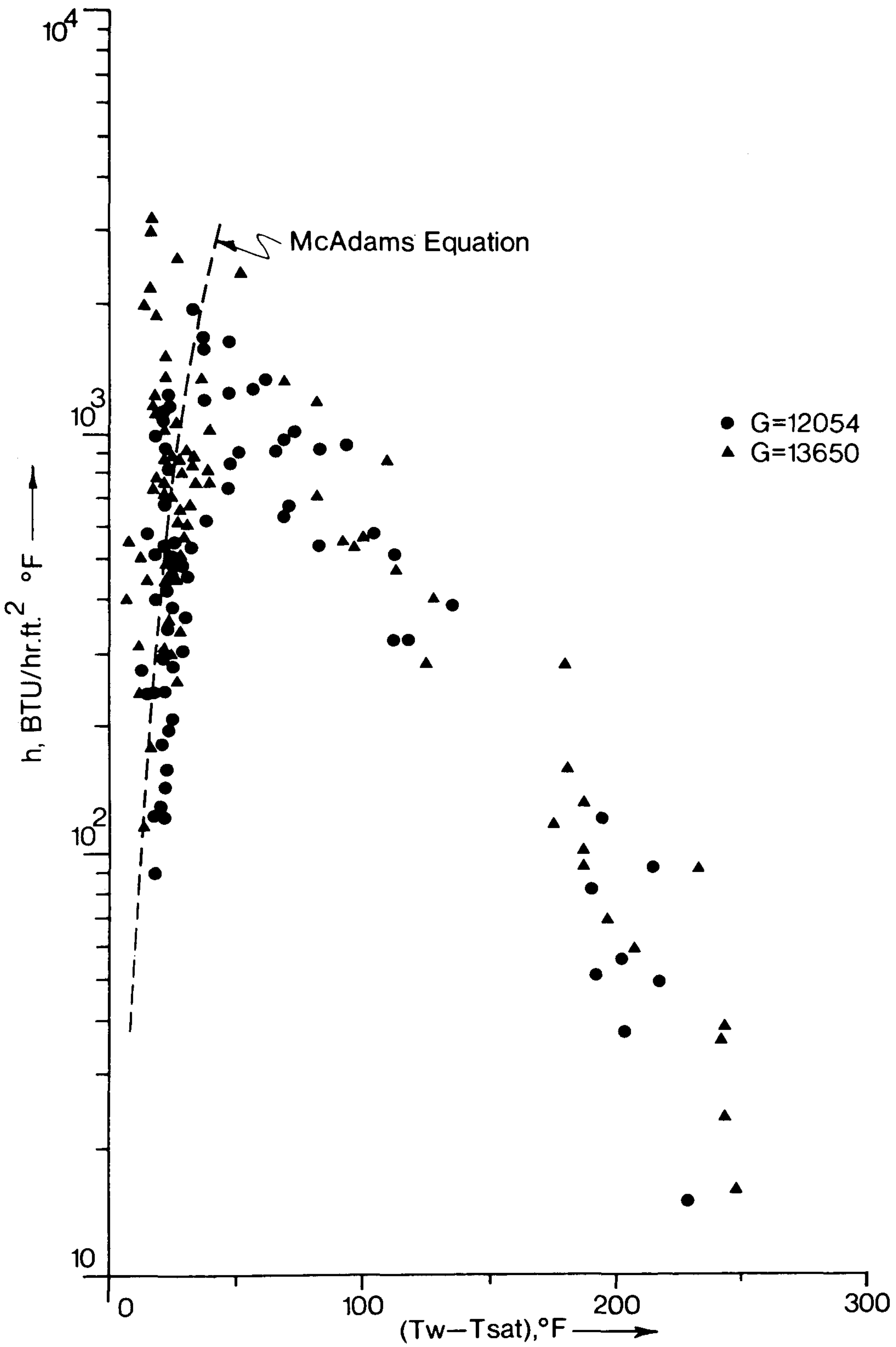

Fig. 3.21 Ramu's Data for Transition Boiling in an Annulus

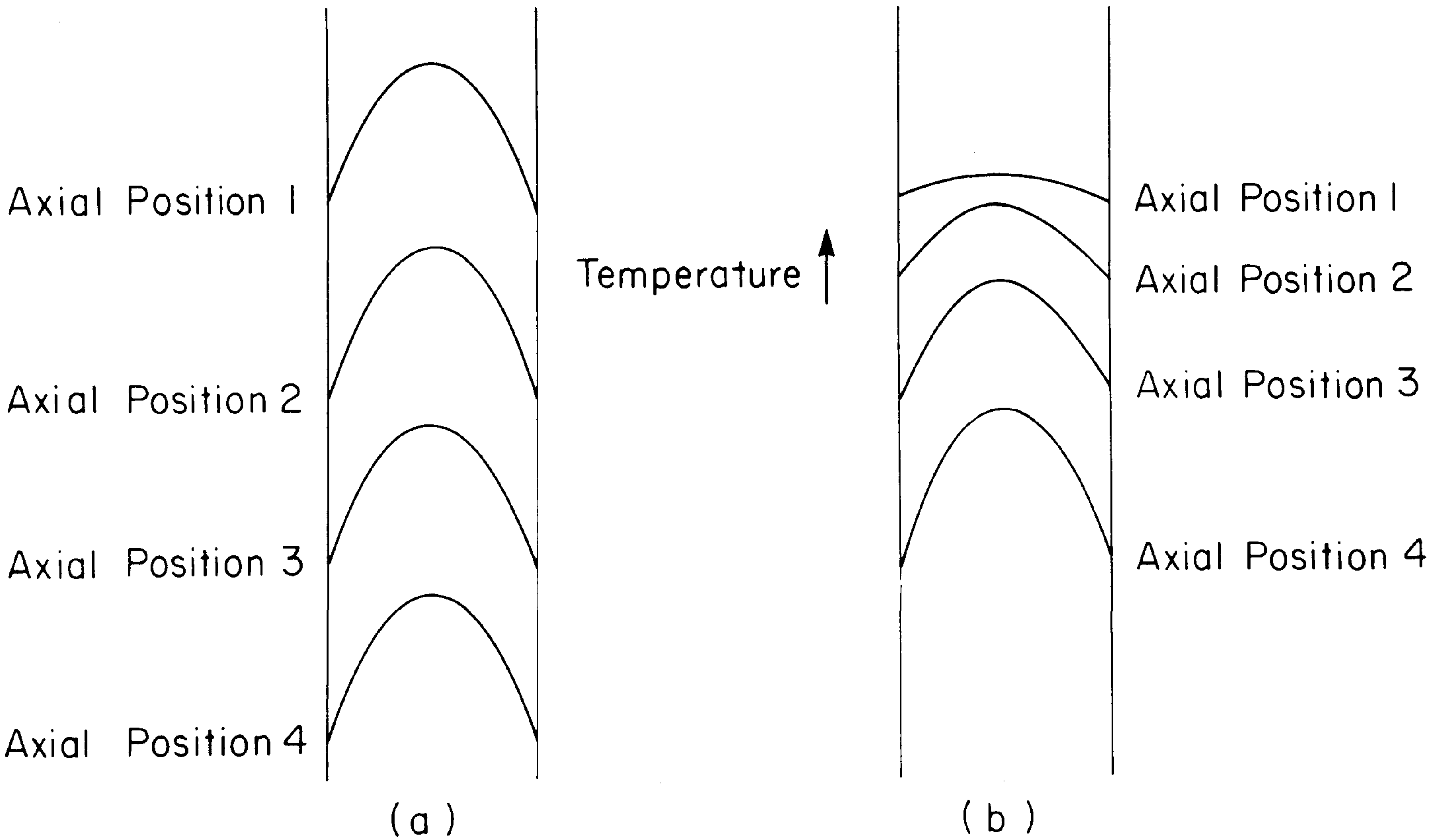

Fig. 3.22 Radial Temperature Profiles Under Conditions of Uniform and Nonuniform Heat Removal

3.3 Uncertainty Analysis

Experimental errors in all heat transfer investigations are significant and must be considered in assessing the data. This is particularly true in studies of transition boiling where fluctuations in the wall temperatures add to the difficulty of determining an appropriate average tmeperature difference.

In the present experiment, the uncertainties in the computed values of h can be divided into two groups: errors in determination of the temperature difference and errors in determination of the heat flux. The temperature difference uncertainties may be attributed to error in the actual wall temperature measurement (due primarily to wall temperature fluctuations), error in the determination of the saturation temperature and the errors arising from the uncertainty in the effective location of the thermocouple on the inner pipe wall. The maximum uncertainties assigned to the first two of these factors is shown in Table 3-2. The errors introduced by the latter factor was determined by examining computer runs in which the location of the inner thermocouple was assumed to vary by 20 mils from that selected previously (error was evaluated as a function of h and ΔT_{sat}).

Each of the foregoing maximum errors were assumed to be equivalent to the error which is exceeded only 5% of the time. Thus the temperature errors were considered to be 2σ errors. The variance for the temperature difference was then obtained by summing the individual σ^2 values.

Since the heat flux, q" is based upon

$$q'' = Q/_A = \frac{wc_p \Delta T_m}{\pi D(\Delta L)} \quad (3\text{-}9)$$

where w = mercury flow

c_p = specific heat Hg

ΔT_m = change in mean temp. of mercury over length ΔL

D = pipe diameter

the uncertainties arise from errors in determining the mercury flow, and the change in ΔT_m. The maximum errors (2σ values) assigned are also indicated in Table 3-2. The ΔT_M error is based on assuming a 9°F maximum error in the inner wall (water side with temp. fluctuations) temperature difference and a 3°F error in the outer temperature difference (steady readings, no fluctuation). Note that the temperature fluctuations on the inner wall cause error in the temperature difference which is nearly twice that of the error in a single temperature reading. The errors in inner and outer wall temperature differences were combined assuming that the temperature profile in the mercury is close to that of a parabola. For a parabolic profile, the average temperature difference equals 2/3 the outer wall temperature difference plus 1/3 the inner wall temperature difference. These weighting factors were used in calculating the σ for ΔT_m; viz.

$$\sigma^2_{\Delta T_m} = 2/3\ \sigma^2_{\Delta T_0} + 1/3\ \sigma^2_{\Delta T_i} \quad (3\text{-}10)$$

The variance in h, expressed in percent, was obtained as the sum of the percentage variances in q" and ΔT_{sat} ($h = q''/\Delta T_{sat}$). The percentage variance in q" was in turn computed as the sum of the percentage variances in ΔT_m and w. The computations were conducted for a matrix of h and ΔT_{sat}

Table 3-2

Estimated Maximum Errors in Observed Quantities

Affecting Calculation of h

Inner wall temperature Reading Error	5°F
Error due to uncertainty in effective location of couple	error obtained as function of h from study of computer output
Saturation Temperature	Equivalent of 1 psi
Mercury Flow Rate	4% of flow
Difference in Mercury Temperature	∿ 4°F

h	ΔT_{sat}					
Btu/hr ft^2°F	50°F	100°F	150°F	200°F	250°F	300°F
1000	29.5	26.4				
750	22.7	21.7	19.2	15.4		
500	25.2	17.5	16.0	13.8	11.9	
300		20.1	15.0	12.3	10.4	
200		25.3	17.8	14.2	11.4	
100			32.5	24.6	19.7	
50				48.5	38.8	32.3

Table 3-3: Estimated Standard Deviation (in %) for Experimental Heat Transfer Coefficients

values which covered the ranges investigated. From the tabulated results shown in Table 3-3, it can be seen that over the bulk of the range in which actual data fell, σ varied from about 10% to 20%. Somewhat higher uncertainties (up to 29.5%) are observed at the lowest temperature differences. Appreciably higher uncertainties (σ from 35 to 50% of measured h) are encountered at very high temperature differences where very low values of h (under 100 Btu/hr ft°F) are found. Error bars corresponding $\pm 2\sigma$ are shown in Figs. 3.4-3.21 where predicted and measured heat transfer coefficients are compared.

The degree to which data at a particular set of conditions could be reproduced was examined by conducting repeat runs after an interval of several months. Before taking the repeat data, the thermocouples measuring mercury inlet and outlet temperatures were replaced by metallic sheathed couples tack-welded to the pipe wall. These couples were found to be free of the bias previously noted. The results of these tests are shown in Fig. 3-23 along with the original data at the same flow rate at pressure ($G \simeq 28{,}300$ lbs/hr ft^2 and $\rho \simeq 25$ psia). It may be seen that the new data generally are within the scatter seen in the original run.

In addition to those experimental uncertainties which affected the estimation of h directly, there are additional uncertainties which affect the predicted values to which the observed values are compared. The most significant of these are water flow rate and water inlet temperature which influence the quality of the steam-water mixture. The quality in turn determines the α and hence predicted boiling heat transfer coefficient. The inlet water flow rates were measured using a rotameter. The maximum error in flow is about $\pm$ 15 cc/min and this was significant at the two lowest flow rate, 100 cc/min and 200 cc/min, but accounted for very small error at the higher flows (500 to 1000 cc/min). Inaccuracy on the inlet water temperature measurement was estimated to be about $\pm$ 5°F. This leads to only a small error in quality but this can lead to significant errors in α at low void fractions. Fortunately, however, when transition boiling was observed the quality was in general above 0.1. At such qualities the error in inlet water temperature does not lead to a significant change in the boiling portion of the heat transfer coefficient.

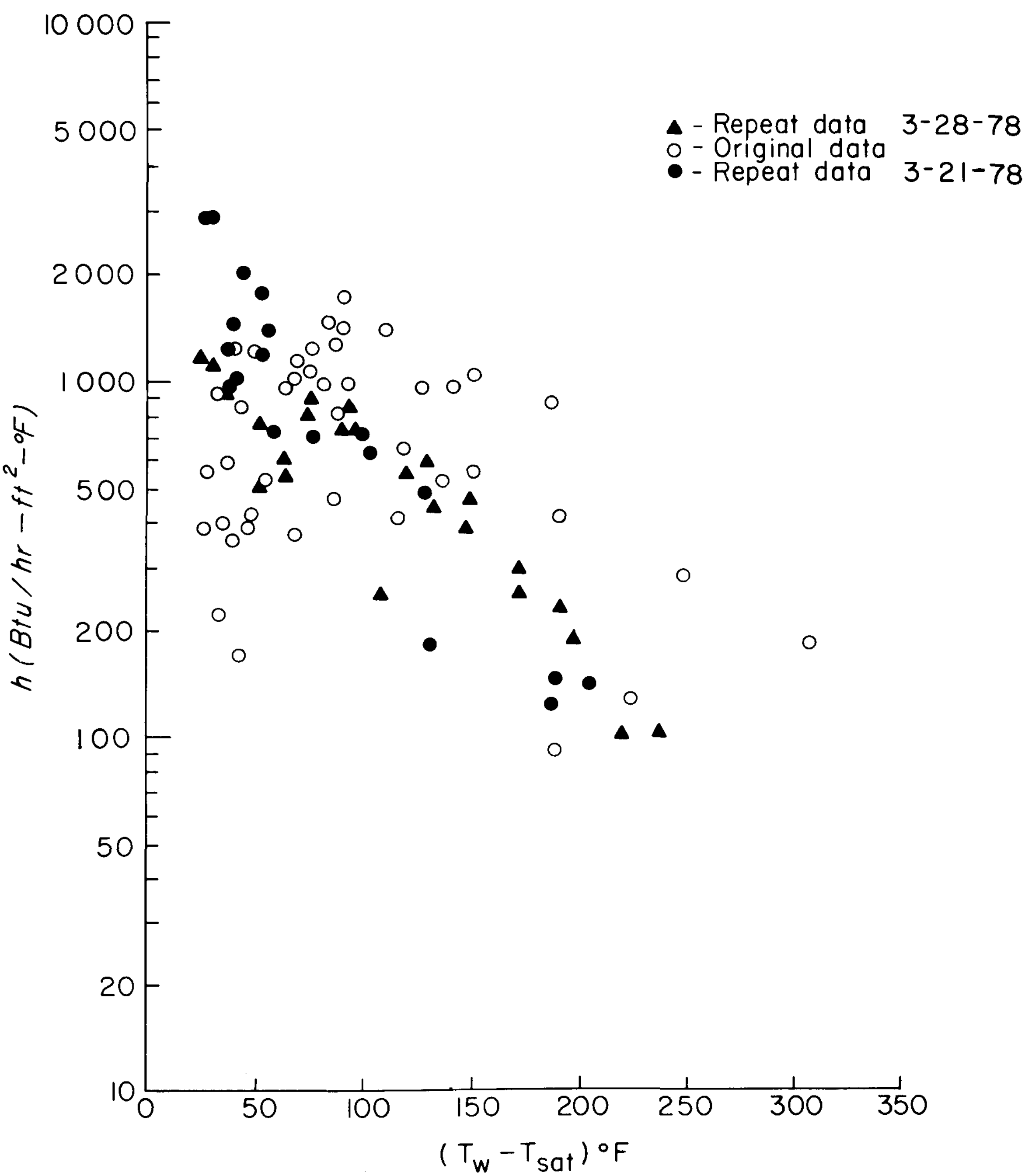

Fig. 3-23 Comparison of Transition Boiling Data at G=28,300 and P≈25 psia Taken at Various Time

3.4 Comparison of Experimental Data With Predictions

By following a line of reasoning similar to that used by Rohsenow[14] and Tong and Young[15], Ramu and Weisman[16] correlated the then available high pressure transition boiling data by defining an overall heat transfer coefficient, h, which is the sum of boiling and convective components:

$h = h_c + h_b$

h_c = convective heat transfer coefficient, Btu/hr ft^2°F

h_b = boiling heat transfer coefficient Btu/hr ft^2°F

For the sake of simplicity, the convective component was calculated by Quinn's forced convection correlation[17]. For round tubes, Quinn proposed

$$h_c = 0.023 \left(\frac{k_B}{D}\right) \left(\frac{\mu_B}{\mu_w}\right)^{0.14} Pr_B^{1/3} \left(\frac{GDx}{\mu_B}\right)^{0.8} \left[1 + \left(\frac{1-x}{x}\right) \frac{\rho_B}{\rho_1}\right]^{0.8} \qquad (3.11a)$$

and for annuli,

$$h_c = 0.023 \left(\frac{k_B}{D_e}\right) \left(\frac{\mu_B}{\mu_W}\right)^{0.14} Pr_B^{1/3} \left(\frac{GD_e x}{\mu_B}\right)^{0.8} \left[1 + \left(\frac{1-x}{x}\right) \frac{\rho_B}{\mu_1}\right]^{2/3} \qquad (3.11b)$$

where

D = tube diameter

D_e = equivalent diameter

G = total mass velocity

k_B = thermal conductivity of bulk vapor

Pr_B = Prandtl No. for vapor at bulk condition

x = quality

μ_B, μ_w = viscosity of vapor at bulk and wall conditions, respectively

ρ_B, ρ_w = density of vapor at bulk and wall conditions, respectively

μ_1 = liquid viscosity

ρ_1 = liquid density

It was assumed that the boiling component h_b could be expressed in terms of h_m the maximum h reached at the given quality and mass velocity. Examination of the available high pressure, high velocity data indicated that h_m occurred at approximately the same temperature difference, ΔT_m, at which the maximum heat transfer coefficient, h_{max}, occurred in pool boiling. However, at the high qualities and flows encountered nucleate boiling was suppressed and h_m was appreciably less than h_{max}. Hence, the critical h was written as

$$h_m = Sh_{max}, \tag{3.12}$$

where values of the suppresion factor, S, were obtained from the correlation of Chen [18].

Once the critical temperature difference is exceeded, the heat transfer coefficient decays rapidly. Ramu & Weisman were able to correlate the transition boiling component of the data of refs. [2,3,5,6], by the expression

$$h_b/h_m = 0.5 \{\exp [- 0.0078(\Delta T - \Delta T_m)] + \exp[-0.0693(\Delta T - \Delta T_m)]\} \tag{3.13}$$

The correlation also reasonably fitted a line derived for typical test conditions from the prediction of McDonough et al.[4] (original data no longer available).

Fig. 3-24 compares the predictions obtained from the sum of eqs. 3-11a and 3-13 with the data of refs. [2,3,5,6] as well as with a sampling of the more recent high pressure data of Bailey[1]. Also shown are the low-pressure subcooled transition boiling data of Ellion[9]. For these low-pressure highly subcooled data, the value of h_m was estimated from the actual boiling curve. Since eq. (3-11a) cannot be used for estimation of h_c when $x < 0$, h_c was taken as 50 Btu/hr ft^2°F based on the film boiling coefficients seen by Ellion at very high temperatures. Since h_c is very low, an error in its estimation is significant only at a very high value of ΔT. It may be seen that the data of Ellion are in good agreement with the proposed correlation while those of Bailey tend to lie somewhat below the predictions.

It can be seen that the maximum discrepancy between Bailey's data and the proposed correlation occurs at relatively low values of h (high wall temperature). Bailey's data were obtained under conditions designed to produce liquid droplets in a bulk vapor core. In this dispersed flow regime at high wall temperatures, significant deviations from thermo-dynamic equilibrium due to vapor superheat is expected. The actual quality, x_a, is likely to be significantly less than the equilibrium quality, x_e. The degree of thermo-dynamic equilibrium x_a/x_e would be expected to decrease as wall temperature increases. For conditions such as these, a convective heat transfer correlation which considers the non-equilibrium effect (e.g. correlation of Tong and Young[15]) should be used. For

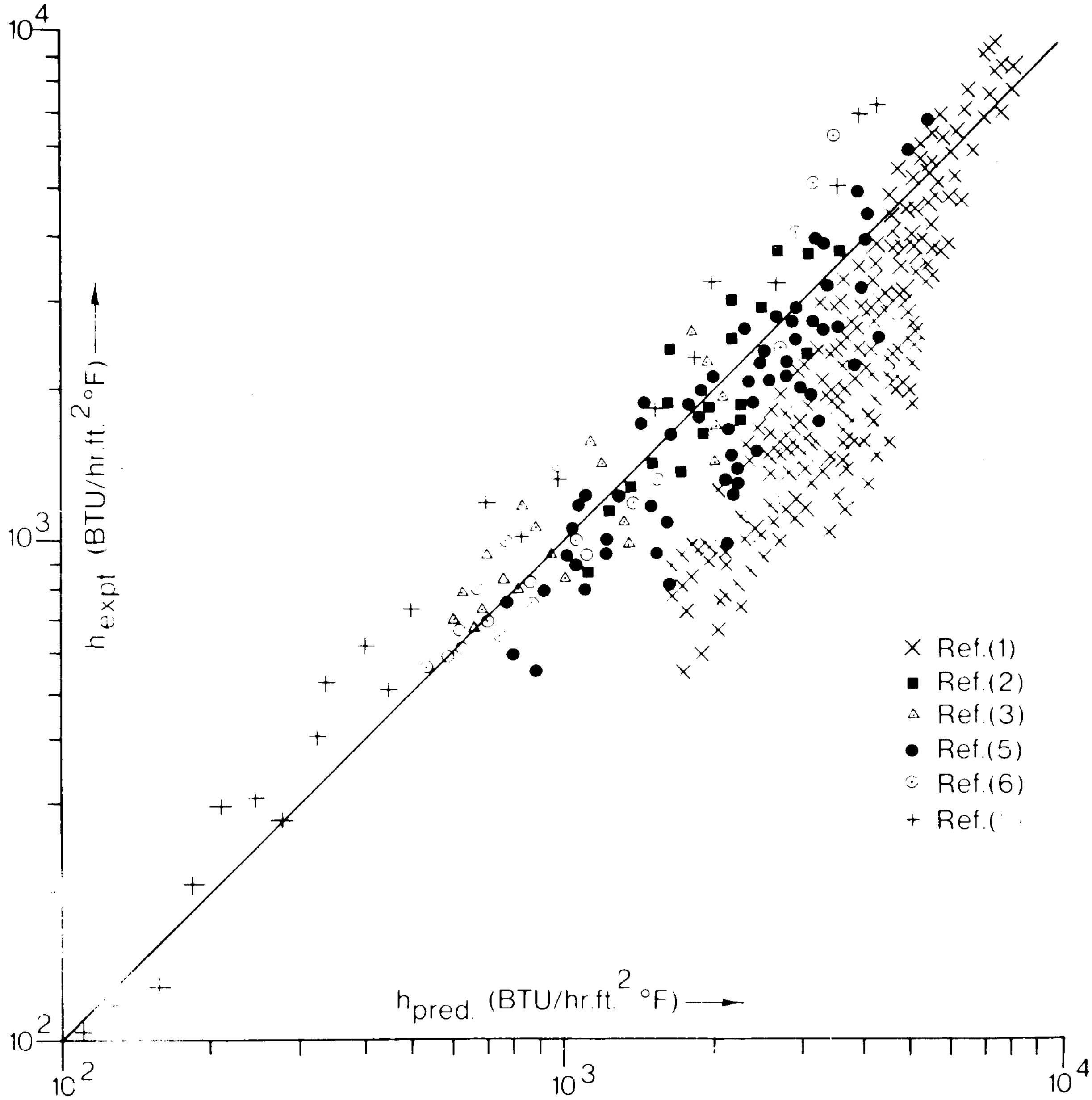

Fig. 3-24 Comparison of literature data with transition boiling heat transfer coefficient correlation

the low pressure, low flow situations encountered in reflooding, the convective component, h_c, is quite low and its estimation has little effect on the prediction of total heat transfer.

It should be noted that the data shown on Fig. 3-24 was all obtained at pressure above 600 psi. The extensive Bailey data was all obtained at pressures above 2400 psi. The only non-transient data at low pressures available at the beginning of this study were those of Ellion[9] and those previously obtained at Cincinnati with the present loop by Ramu and Weisman[12]. Since reflood is at low pressures, the tests described in this report thus help fill an important gap in our knowledge.

At the low mass velocities of the transition boiling tests of Ramu and Weisman[12], the Chen suppression factor was not far from unity. Nevertheless, the maximum value of h was far below the maximum pool boiling h. Ramu and Weisman therefore proposed an alternative procedure whereby at low flows the value of h_m be obtained from the critical heat flux.

To obtain the data for critical heat flux, they utilized Avedesian and Griffith's[19] study of critical heat flux for Freon-113 at low flow rates. These investigators concluded that at very low flows the critical heat flux was a function of void fraction only. Their data, illustrated in Figure 3-24, shows that for α below 0.4 the critical heat flux remains nearly constant and slightly below the pool boiling critical heat flux. When α increases beyond this level the CHF drop sharply. This relation was used to estimate h_m, the value of the critical heat flux in the presence of substantial voids to the pool boiling flux determined by Addoms[20].

The void fraction needed for use with Fig. 3-25 was obtained from the quality, x, of the steam water mixture. Under conditions of the present tests, as well as those of Ramu and Weisman, h_c is quite low and steam superheating values are very low. Experimental observations indicate that the maximum superheating observed was no more than 30°F at very high qualities. At low qualities essentially none is observed.

Hence, the actual qualities x_a, differs only slightly from the thermodynamics equilibrium quality, x_e. It was therefore assumed that $x_a \simeq x_e$. The void fraction, α, was then estimated by Hughmark[21] α vs x relationship. At void fraction above about 0.75, Hughmark's correlation tends to be somewhat unreliable. To estimate α at the highest void range, the Hughmark curve from 0 to 0.75 was extrapolated so that is went through the point $\alpha = 1$, $x = 1$ following a smooth curve.

Once q''_{cr}, is obtained h_m and ΔT_m were estimated using McAdams[22] nucleate boiling curve for low pressures. This nucleate boiling correlation yields

$$q''_{cr} = 0.074 \ (\Delta T_m)^{3.86} \tag{3-14}$$

These values were then used to calculate h_b in Equation (3.13.)

Exactly the same procedure as described above was used for each of the transition boiling data points obtained in the present investigation. The results of these calculations are shown as the shaded bands on the h graphs of Figs. 3-3 to 3-20. The band represents the variation in prediction over the quality range corresponding to the quality change observed between the lowest and highest axial position. It may be seen that

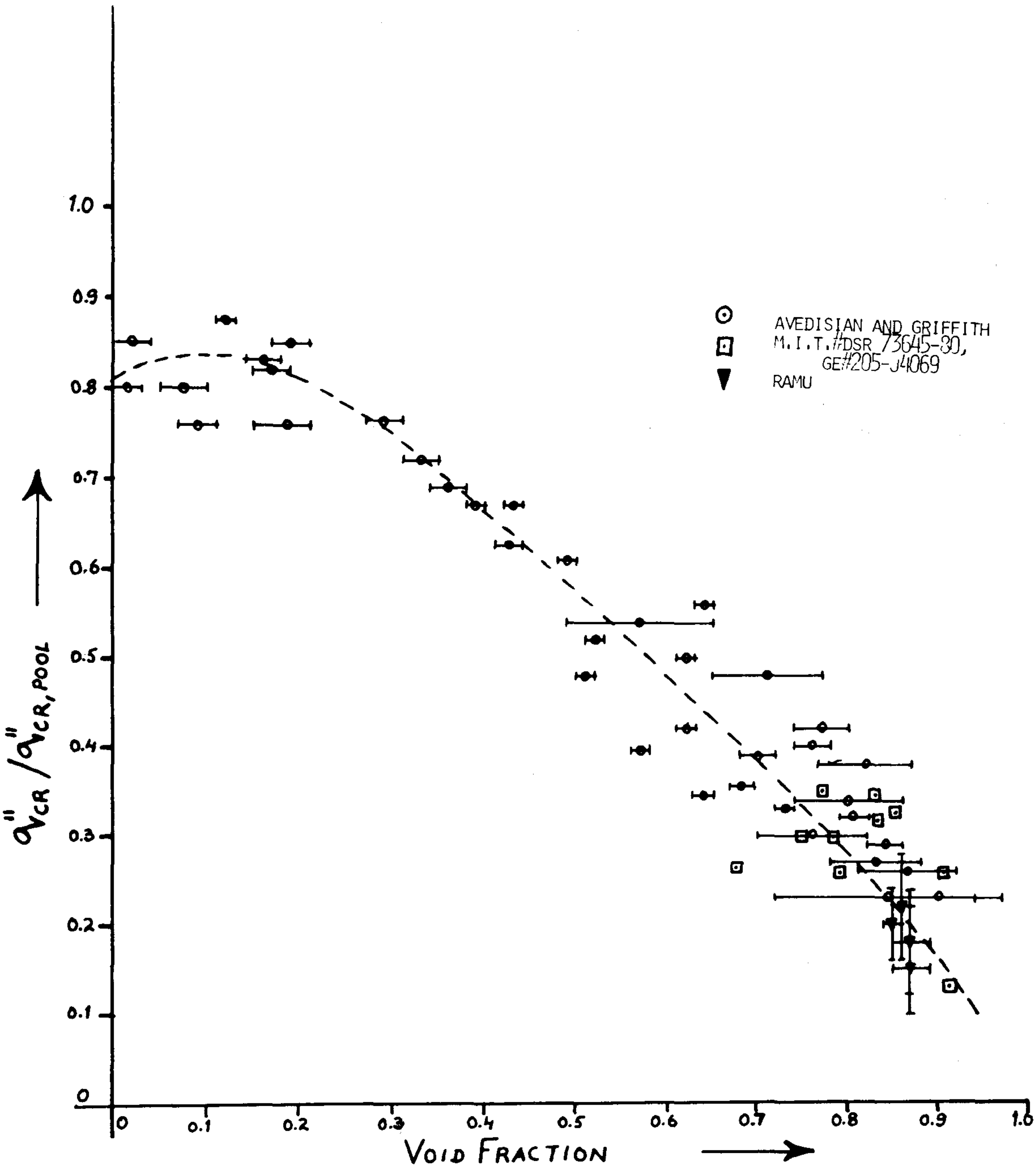

Fig. 3.25 Effect of Void Fraction on Critical Heat Flux at Low Flows

in general reasonable agreement is obtained between predictions and observations although there is significant scatter. At the lowest temperature difference in the transition region, observations tend to lie below the predictions. This may be explained in part by the fact that, at the flows and qualities of the present tests, the boiling suppression factor (Chen's[18] S factor) is significantly less than unity. Thus the nucleate boiling coefficients are, in most cases, substantially below the predictions of McAdams nucleate boiling curve. This is shown on the lower dotted curve plotted on the h vs ΔT graph. The boiling coefficients on the lower curves were obtained by multiplying McAdams equation by the suppression factor corresponding to the average test conditions.

At the highest temperature differences, the observed heat transfer coefficients tend to lie some above the predictions. The greatest discrepancy appears at the highest values of (ΔT_{sat}). This trend is general except for a few anomalous points at the lowest axial position shown in Fig. 3-6.

It is also interesting to note that the width of the prediction band is much narrower than the observed h variation at any given ΔT_{sat}. Hence, the experimental observations appear to indicate a greater change in h with axial position than indicated by the prediction. For most of the transition boiling runs the α values are above 0.85 and don't vary greatly over the range of axial positions observed. Hence h_b, which is the major component of h, is predicted to show only a small change.

In Fig. 3-26, predictions obtained from the sum of Equation (3-10a) and (3-13) are plotted versus the experimentally determined heat transfer coefficients. Again it is clear that the experimental points tend to lie below the predictions at high h values (low ΔT_{sat}) and of ΔT_{sat}. This latter trend is in marked contrast to date of Ramu and Weisman[12] which tended to lie below the predicted values at high ΔT_{sat}. It has been noted that the manner in which Ramu and Weisman's data were obtained and interpreted would tend to underestimate the actual values particularly at high ΔT_{sat}. The present observations would appear to be in somewhat better agreement with the FLECHT data[23] which tended to lie above the data of Ramu and Weisman[12].

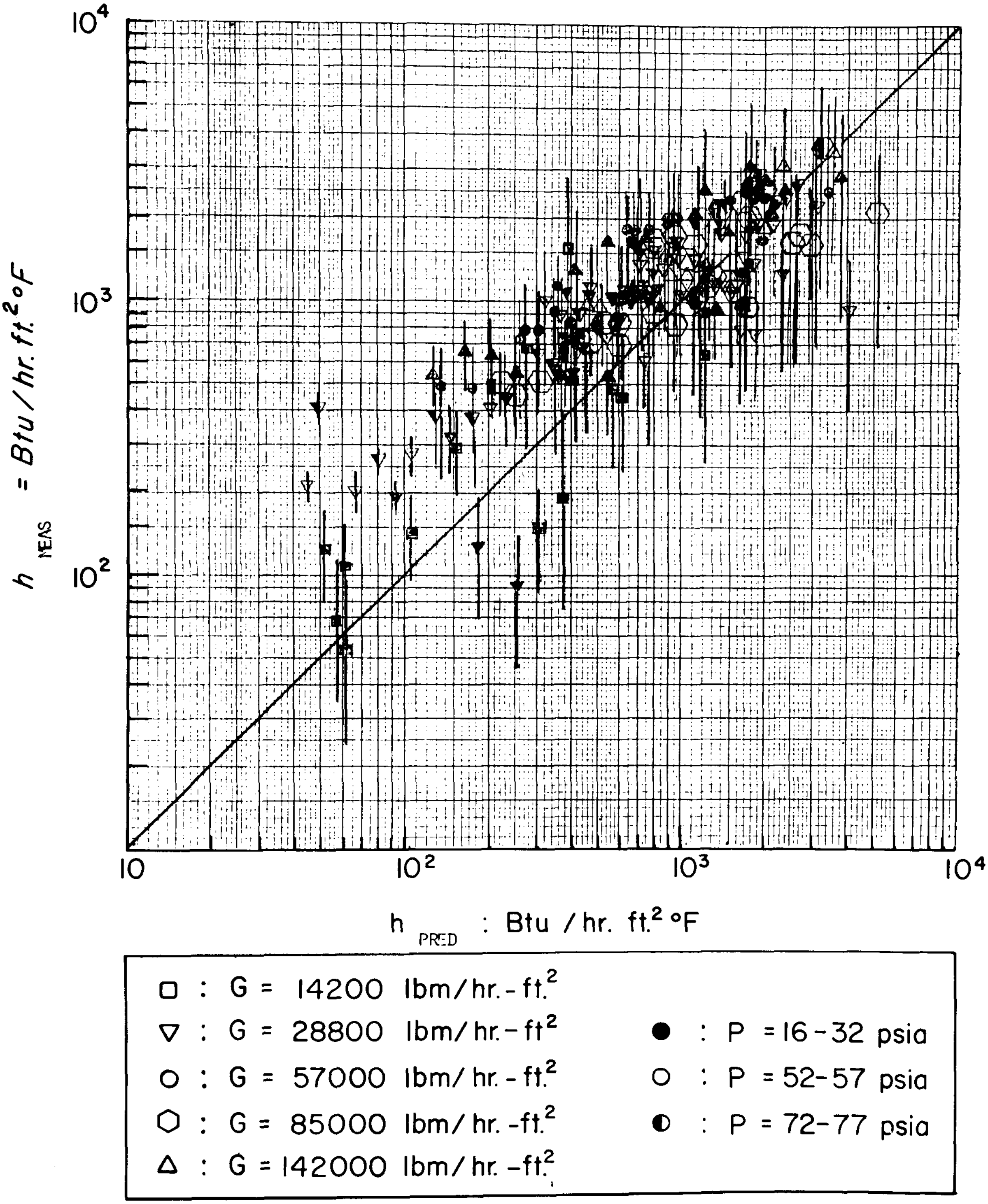

Fig. 3.26 Comparison of Experimental Heat Transfer Coefficients With Predictions

4.0 Conclusions

The tests described herein have provided steady state transition boiling data at flows and pressures similar to those seen during reflood. Where experiment conditions overlap, the transition boiling data obtained in the present experimental series indicate reasonable agreement with the steady state heat transfer coefficients obtained previously by Ramu and Weisman[12]. However, the decrease in heat transfer at high values of ΔT_{sat} was less precipitous than that seen previously.

The present study shows that the temperature profile in the mercury canchange significantly as the rate of heat removal changes. By not allowing for this change, the previous tests tended to underestimate the experimental heat transfer coefficients and this underestimation was greatest at the highest values of ΔT_{sat}. The discrepancies between the present and previous tests thus appear to be explainable.

The predictive method of Ramu and Weisman[12] appears to provide a reasonable estimate of transition boiling heat transfer conditions typical of reflood. The fact that the data tends to be somewhat above the predictions at the higher ΔT_{sat} is in agreement with previous comparisons of FLECHT data with the suggested correlation. It would be desirable to compare the data presented here with other transition boiling correlations such as that presented by Chen et al.[24]. Alternatively, it would be useful to develop improvements in the present correlation. The major difficulties with the present correlation are the difficulty in obtaining an accurate estimate of α and the considerable inaccuracy inherant in the estimation of the effect of α on h_m. Since h_m depends so strongly on the α, errors in estimation of α and its effect can lead to very substantial errors in predictions of transition boiling heat transfer coefficients (at high voids, a 10% error in α could lead to 50% change in the predicted value of h). Alternative means for determination of h_m at high voids and low pressures would be highly desirable.

The present tests were successful in extending the range of data to higher flows and other pressures than previously examined at steady state under reflood like conditions. It was not possible to obtain transition boiling at substantially lower qualities than examined in the previous tests. It would be highly desirable to use the present apparatus to examine transition boiling under transient conditions. Reversing the water flow direction would allow transition boiling data to be obtained at high ΔT_{sat} but low water quality. Transient boiling tests would allow a comparison of state-state and transient transition boiling heat transfer coefficients to be obtained in the same apparatus.

References

(1) N.A. Bailey, UKAE Report AEEW-R-807, Winfrith, England (1973).

(2) M. Cumo and G.C. Urbani, Trans. ANS 14 (1) (1971) 245.

(3) J.E. Hench, ASME Paper 64-WA/HT-44 (1964).

(4) J.B. McDonough, W. Milich and E.C. King, Chem. Eng. Progr. Symp.

(5) L. Nobel, European Atomic Energy Community, Report EUR-4561e Ispra, Italy (1970).

(6) E.E. Polomik, USAEC Report, GEAP-5563, General Electric Co., San Jose, Calif. (1967).

(7) A.W. Bennett, H.A. Kearsey and R.K.F. Keyes, UKAE Report, AERE-R-4352, Harwell, England (1964).

(8) J. Cermak, A.S. Kitzes, F.F. Cadek, R.H. Leyse and D.P. Dominicus, USAEC Report, WCAP-7435, Westinghouse Electric Corp. (1970).

(9) M.E. Ellion, PhD Thesis, Cal. Inst. of Tech. (1954).

(10) D.N. Plummer, P. Griffith & W.M. Rohsenow, "Post Critical Heat Transfer to Flowing Fluid in Vertical Tube Paper No. 76-CSME/CSChE-13, 16th Nat. Heat Transfer Conf., St. Louis (1976).

(11) W.C. Peterson, M.M. Aboul Fetouh and M.G. Zaalouk, Boiling curve measurements from a controlled forced convection process. Proc. Nucl. Eng. Society (1973).

(12) K. Ramu and J. Weisman, Nuc. Eng. & Design 40, 285 (1977).

(13) J. Weisman, ed. "Elements of Nuclear Reactor Design", p. 231 Elsevier Publishing Company (1977).

(14) W.M. Rohsenhaw "Heat Transfer - A Symposium, 1952" Eng. Research Institute, Univ. of Michigan, Ann Arbor (1952).

(15) L.S. Tong and J.P. Young, "A Phenomenological Transition and Film Boiling Correlation". Proceedings of 5th International Heat Transfer Conference, Vol. IV, 133.0, Tokyo (1974).

(16) K. Ramu and J. Weisman, A Method for the Correlation of Transition Boiling Heat Transfer Data, Proc. 5th International Heat Transfer Conference, Tokyo (1974).

(17) E.P. Quinn, ASME Paper 66 WA/HT-36 (1966).

(18) J.C. Chen, "A Correlation for Boiling Heat Transfer to Saturated Fluids In Convective Flow", ASME Paper 63-HT-34 (1963).

(19) C.F. Avedisian and P. Griffity, Report 80620-84, Eng. Projects Lab., Dept. of Mech. Eng., MIT (1974).

(20) J.N. Addoms, ScD Thesis, Dept. of Chem. Eng., MIT, Cambridge, Mass. (1948).

(21) G.A. Hughmark, Chem. Eng. Progr. 58 (4) (1962) 62.

(22) W.H. McAdams, W.E. Kennel, C.S. Minden, R. Carl, P.M. Pecornell, and J.E. Dew, "Heat Transfer at High Rate to Water With Surface Boiling", Inst. Chem. Eng. 41, 1945 (1949).

(23) L.E. Hochreiter, Westinghouse Electric Corp., Personal Communication (1974).

(24) J.C. Chen, R.K. Sundaram, F.T. Ozaynah, "A Phenomenological Correlation of Post CHF Heat Transfer", Lehigh University Report TS-774 (1977).

Appendix: Tabulation of Data

In this section, measures (corrected) and calculated data are both included. In each set of runs, there are 4 sets of q'', ΔT_{sat}, h and x_e corresponding to four thermocouple pairs in the test section. Symbols used in the table are listed below.

G	=	water flow rate in lbm/hr ft^2
T_{min}	=	temperature of mercury at inlet to test section, °F
T_{mout}	=	temperature of mercury at outlet to test section, °F
T_{win}	=	temperature of water at inlet to test section, °F
T_{wout}	=	temperature of water at outlet to test section, °F
P_w	=	pressure of water at inlet to test section, psig
T_{wlwo}	=	temperature of thermocouple at the outer wall of the inner tube of the test section
T_{wlmo}	=	temperature of thermocouple at the outer wall of the outer pipe of the test section
q''		wall heat flux in Btu/hr ft^2
ΔT_{sat}		wall temperature above saturation, °F
h		heat transfer coefficient, Btu/hr ft^2°F
x_e		equilibrium quality (values greater than 1.0 represent superheat conditions)

Note: All nonboiling heat transfer coefficients have been omitted from the tables that follow. All tabulated heat transfer coefficients are defined by Equation (3-1).

$G = 14{,}200$						
Run #101	$T_{min} = 297$	$T_{mout} = 285$	$T_{win} = 126$	$T_{wout} = 262$		$P_w = 10.$
POSITION	T_{wlwo}	T_{wlmo}	$q''/10^4$	ΔT_{sat}	h	X_e
1	281	296	2.21	33.9	652.6	0.121
2	273	294	1.64	28.3	581.7	0.05
3	269	292	1.42	24.9	572.4	0
4	258	285	2.04	10.0	2041	0
Run #102	$T_{min} = 350$	$T_{mout} = 304$	$T_{win} = 101$	$T_{wout} = 262$		$P_w = 14.$
POSITION	T_{wlwo}	T_{wlmo}	$q''/10^4$	ΔT_{sat}	h	X_e
1	323	345	3.80	59.	644	0.273
2	301	337	3.66	37.5	977	0.134
3	291	332	3.04	29	1051	0
4	281	319	2.77	24.5	1131	0
Run# 103	$T_{min} = 365$	$T_{mout} = 318$	$T_{win} = 204$	$T_{wout} = 245$		$P_w = 7.$
POSITION	T_{wlwo}	T_{wlmo}	$q''/10^4$	ΔT_{sat}	h	X_e
1	335	355	4.22	85.	497	0.542
2	203	349	4.69	49.5	948	0.371
3	285	342	4.38	32.	1370	0.185
4	278	331	3.58	29.5	1214	0.017
Run# 104	$T_{min} = 402$	$T_{mout} = 373$	$T_{win} = 235$	$T_{wout} = 267$		$P_w = 14.$
POSITION	T_{wlwo}	T_{wlmo}	$q''/10^4$	ΔT_{sat}	h	X_e
1	385	396	2.35	124	190	0.648
2	354	393	3.98	88.5	450	0.517
3	319	390	5.68	44	1291	0.311
4	301	368	5.15	26.5	1945	0.080
Run#105	$T_{min} = 482$	$T_{mout} = 418$	$T_{win} = 242$	$T_{wout} = 262$		$P_w = 13.$
POSITION	T_{wlwo}	T_{wlmo}	$q''/10^4$	ΔT_{sat}	h	X_e
1	448	474	5.03	176.	286	1.000
2	394	464	7.33	108	679	0.823
3	349	452	8.52	60	1420	0.488
4	322	438	8.00	34.5	2320	0.133

*Below saturation nonboiling data

**Anomalous data

G = 14,200						
Run #106	T_{min} = 517	T_{mout} = 469	T_{win} = 222	T_{wout} = 241		P_w = 5.
POSITION	T_{wlwo}	T_{wlmo}	$q''/10^4$	ΔT_{sat}	h	X_e
1	499	506	2.21	258	107.	0.96
2	477	503	2.63	231	141	0.84
3	402	483	7.42	124	741	0.56
4	351	474	10.04	72	1395	0.15
Run #107	T_{min} = 556	T_{mout} = 491	T_{win} = 220	T_{wout} = 241		P_w = 4.
POSITION	T_{wlwo}	T_{wlmo}	$q''/10^4$	ΔT_{sat}	h	X_e
1	535	550	2.64	294	114.1	1.26
2	509	542	3.06	260	153.	1.12
3	393	538	1.10	91	1506	0.716
4	372	519	7.99	89	1108	0.236
Run# 108	T_{min} = 569	T_{mout} = 517	T_{win} = 229	T_{wout} = 250		P_w = 9.
POSITION	T_{wlwo}	T_{wlmo}	$q''/10^4$	ΔT_{sat}	h	X_e
1	543	560	3.19	284	139	1.14
2	522	554	2.96	264	139	1.00
3	437	487	8.68	141	761	0.673
4	379	379	9.58	76.	1557	0.192
Run# 109	T_{min} = 609	T_{mout} = 562	T_{win} = 234	T_{wout} = 254		P_w = 10.
POSITION	T_{wlwo}	T_{wlmo}	$q''/10^4$	ΔT_{sat}	h	X_e
1	583	600	3.26	322	126.	0.920
2	581	594	1.43	331	539	0.827
3	523	593	5.79	245	293	0.619
4	436	569	10.32	127	1008	0.177
Run# 110	T_{min} = 626	T_{mout} = 564	T_{win} = 232	T_{wout} = 252		P_w = 9.
POSITION	T_{wlwo}	T_{wlmo}	$q''/10^4$	ΔT_{sat}	h	X_e
1	592	607	4.36	326	166	1.00
2	588	600	1.86	337	68.5	0.878
3	502	592	8.27	210	489.	0.582
4	467	562	7.33	180	505	0.186

*Below saturation nonboiling data

**Anomalous data

$G = 28{,}800$						
Run #201	T_{min} = 281	T_{mout} = 262	T_{win} = 139	T_{wout} = 248		P_w = 8.0
POSITION	T_{wlwo}	T_{wlmo}	$q''/10^4$	ΔT_{sat}	h	X_e
1	287	281	**	**	**	**
2	276	276	0.71	41.5	172	0
3	270	273	0.76	34	225	0
4	263	271	0.99	25.5	390	0
Run #202	T_{min} = 313	T_{mout} = 294	T_{win} = 151	T_{wout} = 257		P_w = 11.
POSITION	T_{wlwo}	T_{wlmo}	$q''/10^4$	ΔT_{sat}	h	X_e
1	311	311	0.20	**	**	0
2	293	307	1.78	45.5	392	0
3	287	304	1.46	40	367	0
4	282	302	1.44	35.5	406	0
Run# 203	T_{min} = 351	T_{mout} = 312	T_{win} = 150	T_{wout} = 256		P_w = 12.
POSITION	T_{wlwo}	T_{wlmo}	$q''/10^4$	ΔT_{sat}	h	X_e
1	342	345	1.00	91	136.	0.063
2	317	337	2.86	60.5	474	0.02
3	308	332	2.35	54	437	0
4	302	309	1.98	50.5	393.7	0
Run# 204	T_{min} = 405	T_{mout} = 359	T_{win} = 216	T_{wout} = 269		P_w = 15.
POSITION	T_{wlwo}	T_{wlmo}	$q''/10^4$	ΔT_{sat}	h	X_e
1	393	425	3.89	117	411	0.483
2	304	397	**	**	**	0.350
3	290	379	5.64	**	**	0.202
4	280	364	?	?	**	0.063
Run#205	T_{min} = 441	T_{mout} = 392	T_{win} = 222	T_{wout} = 251		P_w = 7.0
POSITION	T_{wlwo}	T_{wlmo}	$q''/10^4$	ΔT_{sat}	h	X_e
1	430	441	1.39	188	92	0.450
2	361	431	6.04	88	854	0.350
3	333	411	5.42	64	1060	0.202
4	313	381	6.20	49.5	1254	0.063

*Below saturation nonboiling data

**Anomalous data

G = 28,800						
Run #206	T_{min}=469	T_{mout}= 386	T_{win}= 229	T_{wout}= 250		P_w=6.
POSITION	T_{wlwo}	T_{wlmo}	$q''/10^4$	ΔT_{sat}	h	X_e
1	471	471	**	240	**	0.512
2	391	458	6.50	117	688	0.420
3	349	438	6.59	74	1108	0.251
4	325	415	7.36	57.5	1280	0.087
Run #207	T_{min}= 502	T_{mout}= 425	T_{win}= 229	T_{wout}= 245		P_w= 6.0
POSITION	T_{wlwo}	T_{wlmo}	$q''/10^4$	ΔT_{sat}	h	X_e
1	517	502	**	**	**	**
2	425	491	6.87	149	571	0.44
3	373	470	7.49	92	1011	0.26
4	345	441	6.67	69	1198	0.073
Run# 208	T_{min}= 497	T_{mout}= 419	T_{win}= 235	T_{wout}= 256		P_w= 9.0
POSITION	T_{wlwo}	T_{wlmo}	$q''/0^4$	ΔT_{sat}	h	X_e
1	478	485	2.34	225	129	0.500
2	414	474	6.05	136	554	0.390
3	369	455	6.85	83	1028	0.223
4	345	429	5.84	67	1080	0.058
Run# 209	T_{min}= 553	T_{mout}= 483	T_{win}= 235	T_{wout}= 256		P_w= 9.0
POSITION	T_{wlwo}	T_{wlmo}	$q''/10^4$	ΔT_{sat}	h	X_e
1	566	554	**	**	**	**
2	477	532	6.90	194	442	0.530
3	390	519	10.17	84	1504	0.306
4	366	490	7.80	75	1293	0.076
Run# 210	T_{min}= 595.6	T_{mout}= 520.8	T_{win}= 233.5	T_{wout}= 255.6		P_w= 10.0
POSITION	T_{wlwo}	T_{wlmo}	$q''/10^4$	ΔT_{sat}	h	X_e
1	562	587	**	**	**	**
2	530	578	6.27	249	313	0.583
3	435	565	10.59	124	1056	0.361
4	391	532	9.51	86	1364	0.100

*Below saturation nonboiling data

**Anomalous data

G = 28,800

Run # 211 — T_{min} = 624, T_{mout} = 553, T_{win} = 235, T_{wout} = 256, P_w = 10.

POSITION	T_{wlwo}	T_{wlmo}	$q''/10^4$	ΔT_{sat}	h	X_e
1	651	616	**	**	**	**
2	579	608	4.81	308	194	0.633
3	458	601	11.96	139	1070	0.440
4	404	567	10.92	90	1053	0.142

Run # 212 — T_{min} = 661, T_{mout} = 547, T_{win} = 200, T_{wout} = 253, P_w = 9.0

POSITION	T_{wlwo}	T_{wlmo}	$q''/10^4$	ΔT_{sat}	h	X_e
1	677	646	**	**	**	**
2	669	635		**	**	**
3	585	631	14.59	151	1195	0.423
4	414	607	12.97	89	1807	0.075

Run# 213 — T_{min} = 680, T_{mout} = 624, T_{win} = 208, T_{wout} = 249, P_w = 9.

POSITION	T_{wlwo}	T_{wlmo}	$q''/10^4$	ΔT_{sat}	h	X_e
1	683	651	**	**	**	**
2	678	643	**	**	**	**
3	511	639	13.45	185	901	0.420
4	433	614	12.89	109	1467.	0.082

Run# 214 — T_{min} = 372, T_{mout} = 328, T_{win} = 89, T_{wout} = 250, P_w = 9.0

POSITION	T_{wlwo}	T_{wlmo}	$q''/10^4$	ΔT_{sat}	h	X_e
1	344	357	3.23	85	472	0.117
2	303	344	5.27	39.5	1335	0.230
3	295	334	3.48	41	875	0
4	286	328	3.18	33.5	950	0

Run# 215 — T_{min} = 310, T_{mout} = 283, T_{win} = 105, T_{wout} = 248, P_w = 8.

POSITION	T_{wlwo}	T_{wlmo}	$q''/10^4$	ΔT_{sat}	h	X_e
1	294	287	2.07	53	391	0
2	279	293	2.16	36.5	594	0
3	275	288	1.46	35	419	0
4	268	285	1.60	28.5	563	0

*Below saturation nonboiling data

**Anomalous data

G = 57,000						
Run #301	T_{min} = 294	T_{mout} = 251	T_{win} = 81	T_{wout} = 173		P_w = 1.0
POSITION	T_{wlwo}	T_{wlmo}	$q''/10^4$	ΔT_{sat}	h	X_e
1	280	302	3.08	40	772	0
2	264	295	2.76	25.5	1083	0
3	259	293	2.19	23	953	0
4	245	282	2.81	13.5	2085	0
Run #302	T_{min} = 281	T_{mout} = 270	T_{win} = 103	T_{wout} = 229		P_w = 8.0
POSITION	T_{wlwo}	T_{wlmo}	$q''/10^4$	ΔT_{sat}	h	X_e
1	263	278	2.42	20	1212	0
2	249	275	1.83	*	*	0
3	247	274	1.27	*	*	0
4	238	272	*	*	*	0
Run# 303	T_{min} = 316	T_{mout} = 291	T_{win} = 125	T_{wout} = 252		P_w = 9
POSITION	T_{wlwo}	T_{wlmo}	$q''/10^4$	ΔT_{sat}	h	X_e
1	291	313	3.41	40	853	0
2	270	306	3.42	18.5	1852	0
3	263	302	2.58	14	1847	0
4	256	298	2.05	*	*	0
Run# 304	T_{min} = 354	T_{mout} = 312	T_{win} = 135	T_{wout} = 259		P_w = 12
POSITION	T_{wlwo}	T_{wlmo}	$q''/10^4$	ΔT_{sat}	h	X_e
1	315	342	5.44	47	1158	0.011
2	290	337	4.50	25.5	1765	0
3	285	327	3.19	27	1184	0
4	279	327	2.82	22.5	1257	0
Run# 305	T_{min} = 441	T_{mout} = 329	T_{win} = 176	T_{wout} = 253		P_w = 12
POSITION	T_{wlwo}	T_{wlmo}	$q''/10^4$	ΔT_{sat}	h	X_e
1	379	433	7.28	87	1038	0.147
2	333	420	8.07	49.5	1632	0.086
3	314	401	6.71	37	1816	0.011
4	302	379	5.74	29.5	1946	0

*Below saturation nonboiling data

**Anomalous data

G = 57,000

Run #306 T_{min} = 429 T_{mout} = 345 T_{win} = 195 T_{wout} = 249 P_w = 9.0

POSITION	T_{wlwo}	T_{wlmo}	$q''/10^4$	ΔT_{sat}	h	X_e
1	367	412	7.16	83	1079	0.22
2	316	403	8.39	36.5	2300	0.14
3	299	384	6.48	29	2236	0.062
4	288	365	5.51	22.5	2450	0

Run #307 T_{min} = 434 T_{mout} = 247 T_{win} = 202 T_{wout} = 251 P_w = 9

POSITION	T_{wlwo}	T_{wlmo}	$q''/10^4$	ΔT_{sat}	h	X_e
1	371	435	7.62	83	1134	0.253
2	310	424	9.92	24	4134	0.164
3	283	394	*	*	*	0.071
4	266	366	*	*	*	0

Run# 308 T_{min} = 508 T_{mout} = 382 T_{win} = 204 T_{wout} = 251 P_w = 9.0

POSITION	T_{wlwo}	T_{wlmo}	$q''/10^4$	ΔT_{sat}	h	X_e
1	432	500	9.21	135	849	0.314
2	357	485	11.93	59.5	2006	0.203
3	330	455	9.64	43	2242	0.093
4	310	425	8.58	28.5	3014	0

Run# 309 T_{min} = 528 T_{mout} = 398 T_{win} = 210 T_{wout} = 252 P_w = 10

POSITION	T_{wlwo}	T_{wlmo}	$q''/10^4$	ΔT_{sat}	h	X_e
1	450	513	9.48	149	791	0.360
2	366	501	12.68	60.5	2097	0.240
3	336	468	10.21	42	2433	0.120
4	313	436	9.39	25.5	3686	0.012

Run# 310 T_{min} = 553 T_{mout} = 409 T_{win} = 213 T_{wout} = 252 P_w = 10

POSITION	T_{wlwo}	T_{wlmo}	$q''/10^4$	ΔT_{sat}	h	X_e
1	468	539	10.31	162	791	0.380
2	383	520	10.72	71	1880	0.252
3	346	487	11.31	47	2408	0.124
4	323	354	9.71	31.5	3085	0.01

*Below saturation nonboiling data

**Anomalous data

G = 57,000						
Run #311	T_{min} = 567	T_{mout} = 419	T_{win} = 215	T_{wout} = 253		P_w = 10.
POSITION	T_{wlwo}	T_{wlmo}	$q''/10^4$	ΔT_{sat}	h	X_e
1	480	553	10.71	171	777	0.40
2	392	533	11.16	77	1800	0.270
3	351	500	12.18	49	2486	0.130
4	328	464	10.08	34.5	2932	0.010
Run #312	T_{min} = 582	T_{mout} = 429	T_{win} = 218	T_{wout} = 253		P_w = 11.
POSITION	T_{wlwo}	T_{wlmo}	$q''/10^4$	ΔT_{sat}	h	X_e
1	494	565	10.87	182	741	0.414
2	400	546	11.67	80	1824	0.280
3	358	512	12.40	51	2433	0.140
4	333	476	10.87	35.5	3064	0.013
Run# 313	T_{min} = 673	T_{mout} = 495	T_{win} = 225	T_{wout} = 259		P_w = 13.0
POSITION	T_{wlwo}	T_{wlmo}	$q''/10^4$	ΔT_{sat}	h	X_e
1	589	656	10.81	274	490	0.500
2	481	633	12.96	149	1081	0.350
3	421	597	12.20	93	1636	0.190
4	381	557	13.53	62.5	2165	0.031
Run# 314	T_{min} = 630	T_{mout} = 475	T_{win} = 225	T_{wout} = 264		P_w = 14.0
POSITION	T_{wlwo}	T_{wlmo}	$q''/10^4$	ΔT_{sat}	h	X_e
1	554	615	9.63	244	489	0.500
2	453	593	11.95	125	1185	0.320
3	396	558	11.28	71.6	1960	0.170
4	362	326	11.54	46	2509	0.024
Run#	T_{min} =	T_{mout} =	T_{win} =	T_{wout} =		P_w =
POSITION	T_{wlwo}	T_{wlmo}	q''	ΔT_{sat}	h	X_e
1						
2						
3						
4						

*Below saturation nonboiling data

**Anomalous data

G = 142,000						
Run #401	T_{min} = 218	T_{mout} = 198	T_{win} = 103	T_{wout} = 145		P_w = 1,0
POSITION	T_{wlwo}	T_{wlmo}	$q''/10^4$	ΔT_{sat}	h	X_e
1	222	227	*	*	*	0
2	211	226	*	*	*	0
3	204	224	*	*	*	0
4	193	218	*	*	*	0
Run #402	T_{min} = 270	T_{mout} = 238	T_{win} = 125	T_{wout} = 167		P_w = 1.0
POSITION	T_{wlwo}	T_{wlmo}	$q''/10^4$	ΔT_{sat}	h	X_e
1	267	276	1.28	37	348	0
2	254	272	1.68	20.5	823	0
3	247	269	1.19	10	1192	0
4	233	256	*	*	*	0
Run#403	T_{min} = 290	T_{mout} = 267	T_{win} = 153	T_{wout} = 204		P_w = 4.
POSITION	T_{wlwo}	T_{wlmo}	$q''/10^4$	ΔT_{sat}	h	X_e
1	281	294	1.87	48	390	0
2	263	288	2.37	25.5	933	0
3	259	285	1.83	25	733	0
4	249	284	2.21	12	1844	0
Run#404	T_{min} = 354	T_{mout} = 305	T_{win} = 164	T_{wout} = 226		P_w = 9.
POSITION	T_{wlwo}	T_{wlmo}	$q''/10^4$	ΔT_{sat}	h	X_e
1	329	355	3.09	71	543	0
2	299	349	4.42	41.5	1067	0
3	287	340	3.76	32	1178	0
4	279	334	3.40	25.5	1334	0
Run# 405	T_{min} = 357	T_{mout} = 323	T_{win} = 188	T_{wout} = 242		P_w = 11.
POSITION	T_{wlwo}	T_{wlmo}	$q''/10^4$	ΔT_{sat}	h	X_e
1	323	358	5.08	59	862	0
2	293	350	4.86	27.5	1769	0
3	384	340	3.66	27	1357	0
4	276	330	3.49	16.5	2120	0

*Below saturation nonboiling data

**Anomalous data

G = 142,000

Run #406 — T_{min} = 402, T_{mout} = 345, T_{win} = 192, T_{wout} = 246, P_w = 12.0

POSITION	T_{wlwo}	T_{wlmo}	$q''/10^4$	ΔT_{sat}	h	X_e
1	354	401	5.56	73	943	0.028
2	310	390	7.03	31.5	2232	0.002
3	294	372	5.60	21	2668	0
4	284	354	4.90	15.5	3167	0

Run #407 — T_{min} = 466, T_{mout} = 373, T_{win} = 192, T_{wout} = 242, P_w = 10.0

POSITION	T_{wlwo}	T_{wlmo}	$q''/10^4$	ΔT_{sat}	h	X_e
1	424	474	6.16	144	530	0.070
2	345	355	10.51	50.5	2083	0.032
3	319	425	8.68	35	2482	0
4	309	386	4.53	34.9	1298	0

Run #408 — T_{min} = 478, T_{mout} = 382, T_{win} = 194, T_{wout} = 244, P_w = 10

POSITION	T_{wlwo}	T_{wlmo}	$q''/10^4$	ΔT_{sat}	h	X_e
1	427	474	6.11	147	515	0.071
2	349	460	10.52	55.5	1896	0.034
3	325	430	8.34	43	1940	0
4	308	405	7.33	30.5	2404	0

Run #409 — T_{min} = 532, T_{mout} = 421, T_{win} = 224, T_{wout} = 257, P_w = 15.

POSITION	T_{wlwo}	T_{wlmo}	$q''/10^4$	ΔT_{sat}	h	X_e
1	473	533	7.51	174	535	0.130
2	381	511	10.26	62	2066	0.082
3	342	471	11.20	35	3200	0.033
4	326	442	8.56	29.5	2902	0

Run #410 — T_{min} = 576, T_{mout} = 442, T_{win} = 216, T_{wout} = 249, P_w = 13

POSITION	T_{wlwo}	T_{wlmo}	$q''/10^4$	ΔT_{sat}	h	X_e
1	505	577	9.14	200	567	0.145
2	399	547	12.14	72	2076	0.093
3	358	503	12.62	47	2687	0.036
4	338	470	10.71	38.5	2616	0

*Below saturation nonboiling data

**Anomalous data

G = 142,000						
Run #411	T_{min}= 669	T_{mout}= 497	T_{win}= 222	T_{wout}= 249		P_w= 9.0
POSITION	T_{wlwo}	T_{wlmo}	$q''/10^4$	ΔT_{sat}	h	X_e
1	578	642	11.51	267	535	0.203
2	460	611	13.85	130	1323	0.142
3	387	560	16.75	63	2631	0.071
4	354	516	13.52	45.5	2972	0.007
Run #412	T_{min}= 656	T_{mout}= 473	T_{win}= 203	T_{wout}= 225		P_w= 9.0
POSITION	T_{wlwo}	T_{wlmo}	$q''/10^4$	ΔT_{sat}	h	X_e
1	554	631	12.81	235	677	0.185
2	440	597	14.60	109	1600	0.12
3	373	548	16.16	51	3170	0.05
4	344	508	12.94	37.5	3452	0
Run# 413	T_{min}= 624	T_{mout}= 457	T_{win}=204	T_{wout}=249		P_w= 12.
POSITION	T_{wlwo}	T_{wlmo}	$q''/10^4$	ΔT_{sat}	h	X_e
1	535	605	11.15	219	630	0.160
2	427	571	12.91	96	1660	0.10
3	371	528	14.49	52	2787	0.034
4	347	500	11.46	42.5	2697	0
Run#414	T_{min}= 510	T_{mout}= 409	T_{win}= 207	T_{wout}= 249		P_w= 12.
POSITION	T_{wlwo}	T_{wlmo}	$q''/10^4$	ΔT_{sat}	h	X_e
1	438	493	11.91	87	1691	0.103
2	358	473	10.76	59.5	1810	0.06
3	321	440	10.32	25	4131	0.013
4	308	423	7.88	23.2	3400	0
Run# 415	T_{min}= 418	T_{mout}= 345	T_{win}= 200	T_{wout}= 233		P_w= 6.
POSITION	T_{wlwo}	T_{wlmo}	$q''/10^4$	ΔT_{sat}	h	X_e
1	360	400	6.68	86	963	0.07
2	307	390	8.04	34.5	2333	0.04
3	280	367	7.25	13.1	5541	0.004
4	273	348	5.32	15.5	3433	0

*Below saturation nonboiling data

**Anomalous data

$G = 28,300$						
Run #501	$T_{min} = 466$	$T_{mout} = 394$	$T_{win} = 208$	$T_{wout} = 301$		$P_w = 40$
POSITION	T_{wlwo}	T_{wlmo}	$q''/10^4$	ΔT_{sat}	h	X_e
1	402	451	7.50	66	1405	0.410
2	353	442	8.38	22.2	3777	0.234
3	339	424	6.12	18	3400	0.080
4	331	408	5.18	16.8	3089	0
Run #502	$T_{min} = 441$	$T_{mout} = 377$	$T_{win} = 183$	$T_{wout} = 301$		$P_w = 40$
POSITION	T_{wlwo}	T_{wlmo}	$q''/10^4$	ΔT_{sat}	h	X_e
1	381	419	6.90	49	1751	0.322
2	350	411	6.15	29.2	2109	0.180
3	340	401	5.13	23	2233	0.057
4	332	387	5.01	8.7	5766	0
Run#503	$T_{min} = 429$	$T_{mout} = 370$	$T_{win} = 183$	$T_{wout} = 301$		$P_w = 40$
POSITION	T_{wlwo}	T_{wlmo}	$q''/10^4$	ΔT_{sat}	h	X_e
1	381	419	5.59	57	1197	0.237
2	349	411	5.70	31.2	1827	0.115
3	337	401	4.65	26	1789	0.003
4	332	387	3.75	25.8	1456	0
Run# 504	$T_{min} = 382$	$T_{mout} = 342$	$T_{win} = 200$	$T_{wout} = 301$		$P_w = 40.$
POSITION	T_{wlwo}	T_{wlmo}	$q''/10^4$	ΔT_{sat}	h	X_e
1	345	370	5.20	32.4	1605	0.16
2	324	367	3.20	16.2	1978	0.071
3	317	360	3.02	14	2160	0
4	311	354	2.77	10.1	2748	0
Run# 505	$T_{min} = 345$	$T_{mout} = 322$	$T_{win} = 195$	$T_{wout} = 301$		$P_w = 40$
POSITION	T_{wlwo}	T_{wlmo}	$q''/10^4$	ΔT_{sat}	h	X_e
1	320	340	3.48	16.4	2126	0.064
2	308	335	2.51	9.3	2708	0.007
3	304	335	2.18	8.8	2483	0
4	300	330	1.73	*	*	0

*Below saturation nonboiling data

**Anomalous data

G = 28,300						
Run #506	T_{min} = 351	T_{mout} = 312	T_{win} = 188	T_{wout} = 306	P_w = 40	
POSITION	T_{wlwo}	T_{wlmo}	$q''/10^4$	ΔT_{sat}	h	X_e
1	341	377	5.27	28.4	1857	0.180
2	317	373	4.46	7.6	5877	0.085
3	307	369	*	*	*	0
4	301	355	*	*	*	0
Run #507	T_{min} = 446	T_{mout} = 384	T_{win} = 200	T_{wout} = 306	P_w = 40	
POSITION	T_{wlwo}	T_{wlmo}	$q''/10^4$	ΔT_{sat}	h	X_e
1	434	478	5.43	112	603	0.333
2	364	470	9.31	26.2	3556	0.165
3	422	457	6.39	33	1937	0.085
4	317	432	*	*	*	0
Run#508	T_{min} = 357	T_{mout} = 313	T_{win} = 134	T_{wout} = 306	P_w = 40	
POSITION	T_{wlwo}	T_{wlmo}	$q''/10^4$	ΔT_{sat}	h	X_e
1	340	354	2.41	41.4	583	0.027
2	325	347	2.39	26.2	915	0
3	311	343	2.73	10.8	2533	0
4	293	335	*	*	*	0
Run#509	T_{min} = 421	T_{mout} = 357	T_{win} = 143	T_{wout} = 306	P_w = 40	
POSITION	T_{wlwo}	T_{wlmo}	$q''/10^4$	ΔT_{sat}	h	X_e
1	384	413	4.39	68	797	0.15
2	359	406	4.48	48.2	930	0.054
3	345	399	4.07	37	1100	0
4	331	380	4.07	22.8	1786	0
Run#510	T_{min} = 477	T_{mout} = 402	T_{win} = 114	T_{wout} = 306	P_w = 40	
POSITION	T_{wlwo}	T_{wlmo}	$q''/10^4$	ΔT_{sat}	h	X_e
1	419	470	6.90	87	983	0.210
2	394	462	4.75	74	790	0.073
3	383	451	3.90	69	698	0
4	362	422	5.36	45.8	1172	0

*Below saturation nonboiling data

**Anomalous data

G = 28,300						
Run #511	T_{min} = 373	T_{mout} = 338	T_{win} = 151	T_{wout} = 306		P_w = 40
POSITION	T_{wlwo}	T_{wlmo}	$q''/10^4$	ΔT_{sat}	h	X_e
1	342	362	4.35	33.4	1303	
2	324	358	3.30	19.2	1722	
3	313	353	3.11	10.5	2966	
4	306	337	2.70	5.6	4825	
Run #512	T_{min} = 441	T_{mout} = 386	T_{win} = 146	T_{wout} = 310		P_w = 40
POSITION	T_{wlwo}	T_{wlmo}	$q''/10^4$	ΔT_{sat}	h	X_e
1	390	429	6.00	64	1164	0.26
2	347	417	7.03	23.2	3031	0.12
3	338	404	4.95	25	1981	0
4	326	393	4.58	14.8	3100	0
Run #513	T_{min} = 473	T_{mout} = 408	T_{win} = 182	T_{wout} = 312		P_w = 40
POSITION	T_{wlwo}	T_{wlmo}	$q''/10^4$	ΔT_{sat}	h	X_e
1	412	460	7.22	78	1145	0.32
2	360	448	7.66	26.2	2927	0.144
3	352	430	5.77	35	1651	0
4	345	413	10.77	32.8	1455	0
Run #514	T_{min} = 517	T_{mout} = 434	T_{win} = 262	T_{wout} = 313		P_w = 41
POSITION	T_{wlwo}	T_{wlmo}	$q''/10^4$	ΔT_{sat}	h	X_e
1	457	500	7.27	122	739	0.52
2	387	490	10.21	44.2	2312	0.33
3	370	466	7.60	40	1902	0.14
4	354	445	6.57	29.8	2206	0
Run #515	T_{min} = 562	T_{mout} = 443	T_{win} = 241	T_{wout} = 313		P_w = 41
POSITION	T_{wlwo}	T_{wlmo}	$q''/10^4$	ΔT_{sat}	h	X_e
1	503	543	7.36	167	545	0.64
2	425	530	9.09	76	1481	0.44
3	400	507	7.26	60	1484	0.30
4	372	476	8.53	38.8	2200	0.03

*Below saturation nonboiling data

**Anomalous data

G = 28,300						
Run #516	T_{min} = 608	T_{mout} = 489	T_{win} = 278	T_{wout} = 313		P_w = 40
POSITION	T_{wlwo}	T_{wlmo}	$q''/10^4$	ΔT_{sat}	h	X_e
1	551	592	7.22	218	411	0.75
2	455	575	10.58	98	1343	0.52
3	421	547	8.61	76	1407	0.29
4	388	522	10.23	45.8	2235	0.08
Run #517	T_{min} = 645	T_{mout} = 517	T_{win} = 281	T_{wout} = 313		P_w = 41
POSITION	T_{wlwo}	T_{wlmo}	$q''/10^4$	ΔT_{sat}	h	X_e
1	597	629	6.14	270	282	0.86
2	487	610	11.24	126	1101	0.63
3	444	582	9.76	90	1339	0.35
4	404	552	9.47	52	2261	0.08
Run #518	T_{min} = 677	T_{mout} = 549	T_{win} = 281	T_{wout} = 313		P_w = 41
POSITION	T_{wlwo}	T_{wlmo}	$q''/10^4$	ΔT_{sat}	h	X_e
1	636	659	5.27	314	208	0.90
2	522	648	11.50	158	901	0.70
3	470	622	10.55	111	1175	0.40
4	424	568	10.45	65	1978	0.09
Run #519	T_{min} = 705	T_{mout} = 562	T_{win} = 281	T_{wout} = 313		P_w = 41.0
POSITION	T_{wlwo}	T_{wlmo}	$q''/10^4$	ΔT_{sat}	h	X_e
1	659	683	5.80	334	215	0.98
2	531	671	12.93	158	1015	0.72
3	480	641	11.19	117	1184	0.41
4	433	606	11.07	70	1945	0.10
Run #	T_{min} =	T_{mout} =	T_{win} =	T_{wout} =		P_w =
POSITION	T_{wlwo}	T_{wlmo}	$q''/10^4$	ΔT_{sat}	h	X_e
1						
2						
3						
4						

*Below saturation nonboiling data

**Anomalous data

G = 85,000						
Run #601	T_{min} = 497	T_{mout} = 402	T_{win} = 195.5	T_{wout} = 301		P_w = 40.
POSITION	T_{wlwo}	T_{wlmo}	$q''/10^4$	ΔT_{sat}	h	X_e
1	349	487	7.06	106	823	0.109
2	386	472	6.98	52	1667	0.0525
3	365	452	6.95	40	1738	0
4	284	428	*	*	*	0
Run #602	T_{min} = 485.2	T_{mout} = 409	T_{win} = 236	T_{wout} = 307		P_w = 45.
POSITION	T_{wlwo}	T_{wlmo}	$q''/10^4$	ΔT_{sat}	h	X_e
1	418	473	8.04	79	1265	0.109
2	373	458	8.10	42.2	1920	0.0506
3	357	442	6.39	35	1828	0
4	352	422	4.86	38.8	1255	0
Run #603	T_{min} = 445	T_{mout} = 382	T_{win} = 200.4	T_{wout} = 301		P_w = 40
POSITION	T_{wlwo}	T_{wlmo}	$q''/10^4$	ΔT_{sat}	h	X_e
1	384	432	7.01	50	1738	0.0599
2	340	421	7.27	12.2	5963	0.0023
3	329	407	5.51	12	4595	0
4	319	392	4.74	5.8	8176	0
Run #604	T_{min} = 433.6	T_{mout} = 179.5	T_{win} = 301	T_{wout} =		P_w = 40
POSITION	T_{wlwo}	T_{wlmo}	$q''/10^4$	ΔT_{sat}	h	X_e
1	387	423	5.47	64	1055	0.0009
2	355	412	5.74	38.2	1504	0
3	341	402	4.67	29	1613	0
4	331	387	4.07	21.8	1870	0
Run # 605	T_{min} = 398	T_{mout} = 338	T_{win} = 192	T_{wout} = 297		P_w = 40
POSITION	T_{wlwo}	T_{wlmo}	$q''/10^4$	ΔT_{sat}	h	X_e
1	363	387	4.94	51.4	962	0
2	333	380	4.74	21.2	2240	0
3	323	373	3.57	16	2233	0
4	316	362	3.06	11.8	2595	0

*Below saturation nonboiling data

**Anomalous data

G = 85,000

Run #606 — T_{min} = 357, T_{mout} = 326, T_{win} = 200, T_{wout} = 281, P_w = 40

POSITION	T_{wlwo}	T_{wlmo}	$q''/10^4$	ΔT_{sat}	h	X_e
1	330	350	3.71	24.4	1524	0
2	309	347	2.84	*	*	0
3	304	343	2.11	*	*	0
4	297	338	*	*	*	0

Run #607 — T_{min} = 366, T_{mout} = 311, T_{win} = 192, T_{wout} = 264, P_w = 40

POSITION	T_{wlwo}	T_{wlmo}	$q''/10^4$	ΔT_{sat}	h	X_e
1	344	389	4.64	46.4	1004	0
2	325	385	2.57	41.2	770	0
3	357	377	3.17	18	2151	0
4	297	372	*	*	*	0

Run #608 — T_{min} = 372, T_{mout} = 342, T_{win} = 194, T_{wout} = 274, P_w = 40

POSITION	T_{wlwo}	T_{wlmo}	$q''/10^4$	ΔT_{sat}	h	X_e
1	340	391	7.09	15.4	4608	0.01
2	320	383	3.98	*	*	0
3	312	375	3.24	*	*	0
4	300	368	*	*	*	0

Run #609 — T_{min} = 421, T_{mout} = 375, T_{win} = 200, T_{wout} = 399, P_w = 40

POSITION	T_{wlwo}	T_{wlmo}	$q''/10^4$	ΔT_{sat}	h	X_e
1	379	405	6.04	61.21	984	0.02
2	342	395	5.71	24.2	2363	0
3	332	384	4.26	23	1855	0
4	322	377	3.76	14.8	2546	0

Run #610 — T_{min} = 382, T_{mout} = 339, T_{win} = 167, T_{wout} = 369, P_w = 40

POSITION	T_{wlwo}	T_{wlmo}	$q''/10^4$	ΔT_{sat}	h	X_e
1	353	378	4.15	46.4	896	0
2	331	370	3.72	25.2	1480	0
3	321	364	3.14	16	1968	0
4	308	354	**	*	*	0

*Below saturation nonboiling data

**Anomalous data

G = 85,000						
Run #611	T_{min} = 393	T_{mout} = 357	T_{win} = 188	T_{wout} = 306		P_w =40
POSITION	T_{wlwo}	T_{wlmo}	$q''/10^4$	ΔT_{sat}	h	X_e
1	354	383	5.52	39.4	1402	0
2	333	378	4.13	24.2	1710	0
3	320	372	3.62	13.	2788	0
4	315	362	2.84	11.8	2415	0
Run #612	T_{min} = 470	T_{mout} = 386	T_{win} = 192	T_{wout} = 306		P_w =40.0
POSITION	T_{wlwo}	T_{wlmo}	$q''/10^4$	ΔT_{sat}	h	X_e
1	410	463	7.23	76	1180	0.05
2	369	444	7.51	43.2	1740	0.001
3	350	428	6.34	30	2116	0
4	338	410	5.42	22.8	2380	0
Run#613	T_{min} = 430	T_{mout} = 377	T_{win} = 176	T_{wout} =301		P_w =40
POSITION	T_{wlwo}	T_{wlmo}	$q''/10^4$	ΔT_{sat}	h	X_e
1	382	417	5.62	58	1195	0.01
2	342	406	6.30	20.2	3120	0
3	327	393	4.90	12.0	4089	0
4	323	384	3.70	14.8	2505	0
Run#614	T_{min} = 485	T_{mout} = 408	T_{win} = 216	T_{wout} = 306		P_w =40
POSITION	T_{wlwo}	T_{wlmo}	$q''/10^4$	ΔT_{sat}	h	X_e
1	418	466	7.99	79	1252	0.10
2	362	451	9.24	26.2	3528	0.030
3	352	429	5.78	31.	1865	0
4	342	419	5.34	26.8	1995	0
Run#615	T_{min} = 524	T_{mout} = 434	T_{win} = 253	T_{wout} = 309		P_w =40.
POSITION	T_{wlwo}	T_{wlmo}	$q''/10^4$	ΔT_{sat}	h	X_e
1	454	486	8.45	112	932	0.17
2	381	467	10.95	36.2	3025	0.10
3	363	463	7.62	35	2178	0.03
4	350	446	6.30	27.5	2293	0

*Below saturation nonboiling data

**Anomalous data

G = 85,000						
Run # 616	T_{min} = 560	T_{mout} = 441	T_{win} = 249	T_{wout} = 310		P_w = 40
POSITION	T_{wlwo}	T_{wlmo}	$q''/10^4$	ΔT_{sat}	h	X_e
1	490	536	8.57	148	719	0.20
2	410	514	9.65	58	2052	0.11
3	389	496	7.06	54	1625	0.04
4	369	467	7.84	40.8	1922	0
Run # 617	T_{min} = 610	T_{mout} = 473	T_{win} = 257	T_{wout} = 310		P_w = 40.
POSITION	T_{wlwo}	T_{wlmo}	$q''/10^4$	ΔT_{sat}	h	X_e
1	528	590	10.3	175	729	0.22
2	447	560	10.48	90	1443	0.14
3	423	531	7.86	83	1178	0.06
4	396	506	7.33	59	1534	0
Run# 618	T_{min} = 650	T_{mout} = 501	T_{win} = 257	T_{wout} = 313		P_w = 40
POSITION	T_{wlwo}	T_{wlmo}	$q''/10^4$	ΔT_{sat}	h	X_e
1	574	627	9.60	226	527	0.30
2	462	600	12.75	90	1750	0.20
3	418	567	10.59	39	2203	0.10
4	392	533	10.92	45.8	2385	0
Run# 619	T_{min} = 668	T_{mout} = 537	T_{win} = 262	T_{wout} = 310		P_w = 40
POSITION	T_{wlwo}	T_{wlmo}	$q''/10^4$	ΔT_{sat}	h	X_e
1	596	644	9.29	250	461	0.30
2	477	618	13.18	103	1588	0.20
3	427	589	11.27	64	2178	0.10
4	400	540	11.54	49.8	2318	0.0
Run# 620	T_{min} = 699	T_{mout} = 544	T_{win} = 257	T_{wout} = 310		P_w = 40
POSITION	T_{wlwo}	T_{wlmo}	$q''/10^4$	ΔT_{sat}	h	X_e
1	616	673	10.77	261	512	0.32
2	490	657	14.32	108	1637	0.22
3	450	607	11.25	87	1594	0.10
4	415	560	10.16	59	2123	0.0

*Below saturation nonboiling data

**Anomalous data

G = 141,700						
Run #701	T_{min} = 329	T_{mout} = 303	T_{win} = 192	T_{wout} = 242		P_w = 40
POSITION	T_{wlwo}	T_{wlmo}	$q''/10^4$	ΔT_{sat}	h	X_e
1	309	320	2.22	*	3792	0
2	295	317	*	*	*	0
3	284	313	*	*	*	0
4	272	311	*	*	*	0
Run #702	T_{min} = 350	T_{mout} = 319	T_{win} = 195	T_{wout} = 257		P_w = 40
POSITION	T_{wlwo}	T_{wlmo}	$q''/10^4$	ΔT_{sat}	h	X_e
1	326	341	3.32	23.4	1420	0
2	308	334	*	*	*	0
3	298	330	*	*	*	0
4	284	325	*	*	*	0
Run #703	T_{min} = 370	T_{mout} = 335	T_{win} = 200	T_{wout} = 269		P_w = 40
POSITION	T_{wlwo}	T_{wlmo}	$q''/10^4$	ΔT_{sat}	h	X_e
1	338	357	4.48	29.4	1524	0
2	318	350	3.37	12.2	2768	0
3	308	343	*	*	*	0
4	296	333	*	*	*	0
Run #704	T_{min} = 418	T_{mout} = 366	T_{win} = 204	T_{wout} = 290		P_w = 40.
POSITION	T_{wlwo}	T_{wlmo}	$q''/10^4$	ΔT_{sat}	h	X_e
1	374	403	6.28	55.4	1134	0
2	335	392	5.85	15.2	3854	0
3	325	381	4.50	15.	3000	0
4	317	374	3.60	9.8	3680	0
Run #705	T_{min} = 441	T_{mout} = 382	T_{win} = 220	T_{wout} = 306		P_w = 40.
POSITION	T_{wlwo}	T_{wlmo}	$q''/10^4$	ΔT_{sat}	h	X_e
1	386	422	6.43	57	1396	0.01
2	344	408	6.75	19.2	3518	0
3	333	396	4.90	19	2582	0
4	325	386	4.21	15.8	2668	0

*Below saturation nonboiling data

**Anomalous data

G = 141,700						
Run #711	T_{min} = 628	T_{mout} = 477	T_{win} = 213	T_{wout} = 306		P_w = 40
POSITION	T_{wlwo}	T_{wlmo}	$q''/10^4$	ΔT_{sat}	h	X_e
1	521	593	3.36	149	1115	0.10
2	421	561	16.10	49.2	3273	0.04
3	391	528	11.88	40	2972	0
4	375	517	9.53	36.8	2590	0
Run #712	T_{min} = 693	T_{mout} = 508	T_{win} = 204	T_{wout} = 310		P_w = 40
POSITION	T_{wlwo}	T_{wlmo}	$q''/10^4$	ΔT_{sat}	h	X_e
1	573	661	15.21	189	996	0.13
2	453	623	15.33	64	2966	0.05
3	420	579	11.37	56	2507	0
4	393	545	11.95	41.8	2861	0
Run#	T_{min} =	T_{mout} =	T_{win} =	T_{wout} =		P_w =
POSITION	T_{wlwo}	T_{wlmo}	$q''/10^4$	ΔT_{sat}	h	X_e
1						
2						
3						
4						
Run#	T_{min} =	T_{mout} =	T_{win} =	T_{wout} =		P_w =
POSITION	T_{wlwo}	T_{wlmo}	$q''/10^4$	ΔT_{sat}	h	X_e
1						
2						
3						
4						
Run#	T_{min} =	T_{mout} =	T_{win} =	T_{wout} =		P_w =
POSITION	T_{wlwo}	T_{wlmo}	$q''/10^4$	ΔT_{sat}	h	X_e
1						
2						
3						
4						

*Below saturation nonboiling data

**Anomalous data

G = 141,700						
Run #706	T_{min} = 493	T_{mout} = 409	T_{win} = 241	T_{wout} = 306		P_w = 39
POSITION	T_{wlwo}	T_{wlmo}	$q''/10^4$	ΔT_{sat}	h	X_e
1	421	468	8.52	80	1323	0.06
2	361	450	9.65	23.2	4161	0.02
3	348	430	6.89	26	2653	0
4	332	420	5.70	20.8	2741	0
Run #707	T_{min} = 533	T_{mout} = 434	T_{win} = 245	T_{wout} = 307		P_w = 40
POSITION	T_{wlwo}	T_{wlmo}	$q''/10^4$	ΔT_{sat}	h	X_e
1	450	523	10.07	98	1275	0.10
2	374	486	12.14	22.2	5469	0.04
3	360	461	8.37	28	2990	0
4	351	448	6.68	28.9	2312	0
Run# 708	T_{min} = 556	T_{mout} = 437	T_{win} = 250	T_{wout} = 306		P_w = 40
POSITION	T_{wlwo}	T_{wlmo}	$q''/10^4$	ΔT_{sat}	h	X_e
1	466	527	10.98	108	1257	0.10
2	393	503	12.31	41.2	2990	0.05
3	376	476	8.53	43	1986	0
4	366	457	6.75	42.8	1578	0
Run#709	T_{min} = 613	T_{mout} = 462	T_{win} = 225	T_{wout} = 310		P_w = 40
POSITION	T_{wlwo}	T_{wlmo}	$q''/10^4$	ΔT_{sat}	h	X_e
1	508	588	12.94	138	1162	0.10
2	434	551	10.91	74	1828	0.02
3	422	515	7.18	86	1032	0
4	408	493	5.89	90	802	0
Run#710	T_{min} = 656	T_{mout} = 486	T_{win} = 213	T_{wout} = 306		P_w = 40
POSITION	T_{wlwo}	T_{wlmo}	$q''/10^4$	ΔT_{sat}	h	X_e
1	549	629	3.42	175	949	0.12
2	437	593	17.40	57.2	3043	0.05
3	402	554	3.55	13	2736	0
4	383	525	10.67	37.8	2825	0

*Below saturation nonboiling data

**Anomalous data

$G = 28,300$						
Run #801	$T_{min} = 386$	$T_{mout} = 342$	$T_{win} = 164$	$T_{wout} = 313$		$P_w = 60$
POSITION	T_{wlwo}	T_{wlmo}	$q''/10^4$	ΔT_{sat}	h	X_e
1	355	393	4.31	25.9	4232	0.12
2	336	377	4.31	10.2	4232	0.04
3	322	373	*	?	**	0
4	305	363	*	?	**	0
Run #802	$T_{min} = 421$	$T_{mout} = 366$	$T_{win} = 171$	$T_{wout} = 318$		$P_w = 60$
POSITION	T_{wlwo}	T_{wlmo}	$q''/10^4$	ΔT_{sat}	h	X_e
1	374	415	6.92	31.9	2170	0.20
2	349	406	5.00	15.1	3314	0.10
3	335	399	*	**	**	0
4	322	386	*	?	**	0
Run #803	$T_{min} = 469$	$T_{mout} = 389$	$T_{win} = 181$	$T_{wout} = 321$		$P_w = 60$
POSITION	T_{wlwo}	T_{wlmo}	$q''/10^4$	ΔT_{sat}	h	X_e
1	411	460	6.96	58	1485	0.32
2	372	447	5.71	27.1	2107	0.17
3	356	433	5.64	17.2	3281	0.02
4	342	416	*	**	**	0
Run #804	$T_{min} = 481$	$T_{mout} = 414$	$T_{win} = 188$	$T_{wout} = 322$		$P_w = 60$
POSITION	T_{wlwo}	T_{wlmo}	$q''/10^4$	ΔT_{sat}	h	X_e
1	408	472	8.75	43	2486	0.42
2	366	459	7.94	14.1	5634	0.23
3	549	444	*	**	**	0.10
4	332	426	*	?	**	0
Run #805	$T_{min} = 505$	$T_{mout} = 418$	$T_{win} = 225$	$T_{wout} = 292$		$P_w = 60$
POSITION	T_{wlwo}	T_{wlmo}	$q''/10^4$	ΔT_{sat}	h	X_e
1	427	493	9.33	59	1958	0.53
2	368	476	*	**	**	0.31
3	351	456	*	?	?	0.11
4	341	434	*	?	**	0

*Below saturation nonboiling data

**Anomalous data

G = 28,300						
Run #806	T_{min} = 537	T_{mout} = 430	T_{win} = 220	T_{wout} = 326		P_w = 60
POSITION	T_{wlwo}	T_{wlmo}	$q''/10^4$	ΔT_{sat}	h	X_e
1	464	522	8.87	99	1108	0,60
2	391	505	11.97	23,1	5186	0,40
3	367	482	8.26	11,2	7376	0,14
4	357	457	*	*	*	0
Run #807	T_{min} = 566	T_{mout} = 461	T_{win} = 220	T_{wout} = 326		P_w = 60
POSITION	T_{wlwo}	T_{wlmo}	$q''/10^4$	ΔT_{sat}	h	X_e
1	488	554	9.61	119	1004	0.70
2	411	535	9.93	37	3332	0.43
3	377	510	9.92	12.6	7877	0.20
4	360	484	*	*	*	0
Run #808	T_{min} = 588	T_{mout} = 485	T_{win} = 262	T_{wout} = 329		P_w = 60
POSITION	T_{wlwo}	T_{wlmo}	$q''/10^4$	ΔT_{sat}	h	X_e
1	525	572	8.03	165	604	0.80
2	427	560	10.95	46	2923	0.52
3	392	532	10.69	24.6	4346	0.30
4	372	506	9.15	13.5	6785	0.020
Run #809	T_{min} = 629	T_{mout} = 508	T_{win} = 278	T_{wout} = 329		P_w = 60
POSITION	T_{wlwo}	T_{wlmo}	$q''/10^4$	ΔT_{sat}	h	X_e
1	575	615	6.87	224	381	0.84
2	469	597	11.32	86	1683	0.60
3	420	573	10.16	45	2792	0.31
4	390	543	10.46	2.15	4866	0.04
Run #810	T_{min} = 656	T_{mout} = 534	T_{win} = 278	T_{wout} = 329		P_w = 60
POSITION	T_{wlwo}	T_{wlmo}	$q''/10^4$	ΔT_{sat}	h	X_e
1	597	639	7.55	241	388	0.90
2	498	629	11.09	117	1173	0.70
3	447	608	10.42	69	1853	0.40
4	400	572	12.75	21.5	5933	0.06

*Below saturation nonboiling data

**Anomalous data

$G = 28,300$

Run #811	$T_{min} = 683$	$T_{mout} = 560$	$T_{win} = 278$	$T_{wout} = 329$		$P_w = 60$
POSITION	T_{wlwo}	T_{wlmo}	$q''/10^4$	ΔT_{sat}	h	X_e
1	634	666	6.30	286	273	0.95
2	530	657	11.11	150	921	0.72
3	455	638	12.29	65	2324	0.40
4	419	597	13.13	39.5	3325	0.10

Run #812	$T_{min} = 706$	$T_{mout} = 581$	$T_{win} = 290$	$T_{wout} = 326$		$P_w = 60$
POSITION	T_{wlwo}	T_{wlmo}	$q''/10^4$	ΔT_{sat}	h	X_e
1	638	685	8.86	274	401	1.0
2	560	672	9.91	184	656	0.80
3	481	653	12.13	93	1619	0.45
4	424	620	15.12	35.5	4260	0.11

Run#	$T_{min} =$	$T_{mout} =$	$T_{win} =$	$T_{wout} =$		$P_w =$
POSITION	T_{wlwo}	T_{wlmo}	$q''/10^4$	ΔT_{sat}	h	X_e
1						
2						
3						
4						

Run#	$T_{min} =$	$T_{mout} =$	$T_{win} =$	$T_{wout} =$		$P_w =$
POSITION	T_{wlwo}	T_{wlmo}	$q''/10^4$	ΔT_{sat}	h	X_e
1						
2						
3						
4						

Run#	$T_{min} =$	$T_{mout} =$	$T_{win} =$	$T_{wout} =$		$P_w =$
POSITION	T_{wlwo}	T_{wlmo}	$q''/10^4$	ΔT_{sat}	h	X_e
1						
2						
3						
4						

*Below saturation nonboiling data

**Anomalous data

$G = 85,000$						
Run #901	T_{min} = 389	T_{mout} = 338	T_{win} = 154	T_{wout} = 254		P_w = 60.0
POSITION	T_{wlwo}	T_{wlmo}	$q''/10^4$	ΔT_{sat}	h	X_e
1	355	373	4.64	22.9	2030	0
2	340	371	3.28	15.8	2088	0
3	333	368	2.40	11.6	2075	0
4	314	366	*	?	**	0
Run #902	T_{min} = 421	T_{mout} = 382	T_{win} = 164	T_{wout} = 285		P_w = 60
POSITION	T_{wlwo}	T_{wlmo}	$q''/10^4$	ΔT_{sat}	h	X_e
1	381	411	4.70	42	1360	0
2	356	406	4.62	23.8	1945	0
3	345	399	3.78	16.6	2280	0
4	311	390	*	?	**	0
Run #903	T_{min} = 469	T_{mout} = 393	T_{win} = 176	T_{wout} = 289		P_w = 60
POSITION	T_{wlwo}	T_{wlmo}	$q''/10^4$	ΔT_{sat}	h	X_e
1	420	464	5.92	42	1360	0
2	381	449	6.57	37.8	1740	0
3	360	434	5.97	20.6	2900	0
4	348	414	4.79	12.5	3835	0
Run #904	T_{min} = 505	T_{mout} = 414	T_{win} = 216	T_{wout} = 329		P_w = 60
POSITION	T_{wlwo}	T_{wlmo}	$q''/10^4$	ΔT_{sat}	h	X_e
1	445	493	7.24	90	990	0.10
2	403	478	6.19	53	1428	0
3	385	460	5.06	43	1456	0
4	325	435	5.15	40.4	1273	0
Run #905	T_{min} = 528	T_{mout} = 434	T_{win} = 216	T_{wout} = 329		P_w = 60
POSITION	T_{wlwo}	T_{wlmo}	$q''/10^4$	ΔT_{sat}	h	X_e
1	457	515	8.61	94	1137	0.11
2	390	497	10.38	24.8	4187	0.04
3	370	471	8.24	18.8	4386	0
4	353	446	*	**	**	0

*Below saturation nonboiling data

**Anomalous data

G = 85,000

Run #906	T_{min} = 556	T_{mout} = 450	T_{win} = 221	T_{wout} = 329		P_w = 60.
POSITION	T_{wlwo}	T_{wlmo}	$q''/10^4$	ΔT_{sat}	h	X_e
1	473	537	10.21	100	1269	0.14
2	405	522	11.39	35.8	3182	0.10
3	383	494	8.94	27.6	3240	0
4	372	471	6.95	25.5	2728	0

Run #907	T_{min} = 601	T_{mout} = 466	T_{win} = 225	T_{wout} = 329		P_w = 60
POSITION	T_{wlwo}	T_{wlmo}	$q''/10^4$	ΔT_{sat}	h	X_e
1	512	386	10.98	134	1014	0.20
2	425	563	11.27	43	3316	0.10
3	395	527	11.09	28.6	3880	0
4	382	495	8.35	27.5	3110	0

Run#908	T_{min} = 629	T_{mout} = 485	T_{win} = 249	T_{wout} = 329		P_w = 60
POSITION	T_{wlwo}	T_{wlmo}	$q''/10^4$	ΔT_{sat}	h	X_e
1	539	612	11.27	159	876	0.23
2	445	590	12.00	57	2588	0.14
3	408	583	12.11	34.6	500	0.04
4	395	574	9.21	3.65	2525	0

Run#909	T_{min} = 645	T_{mout} = 496	T_{win} = 245	T_{wout} = 329.		P_w = 60
POSITION	T_{wlwo}	T_{wlmo}	$q''/10^4$	ΔT_{sat}	h	X_e
1	559	625	10.3	193	534	0.30
2	448	600	13.7	67	2030	0.20
3	408	599	9.68	34.6	2800	0.04
4	391	522	5.32	21.5	2478	0

Run#910	T_{min} = 686	T_{mout} = 505	T_{win} = 232	T_{wout} = 329		P_w = 60
POSITION	T_{wlwo}	T_{wlmo}	$q''/10^4$	ΔT_{sat}	h	X_e
1	561	637	12.02	173	842	0.24
2	457	612	13.05	63	2575	0.14
3	417	572	13.18	38.6	3415	0.03
4	397	533	10.49	31.5	3332	0

*Below saturation nonboiling data

**Anomalous data

G = 85,000

Run #911	T_{min} = 668	T_{mout} = 512	T_{win} = 237	T_{wout} = 295		P_w = 60
POSITION	T_{wlwo}	T_{wlmo}	$q''/10^4$	ΔT_{sat}	h	X_e
1	578	648	11.54	197	727	0.24
2	470	622	13.15	75	2162	0.14
3	427	584	10.97	45	2977	0.04
4	410	545	8.57	44	2395	0

Run #912	T_{min} = 684	T_{mout} = 524	T_{win} = 253	T_{wout} = 329		P_w = 60
POSITION	T_{wlwo}	T_{wlmo}	$q''/10^4$	ΔT_{sat}	h	X_e
1	595	662	11.44	215	660	0.30
2	482	635	13.52	85	1973	0.20
3	436	597	11.38	52	2714	0.06
4	406	556	12.22	33.5	3650	0

Run#	T_{min} =	T_{mout} =	T_{win} =	T_{wout} =		P_w =
POSITION	T_{wlwo}	T_{wlmo}	$q''/10^4$	ΔT_{sat}	h	X_e
1						
2						
3						
4						

Run#	T_{min} =	T_{mout} =	T_{win} =	T_{wout} =		P_w =
POSITION	T_{wlwo}	T_{wlmo}	$q''/10^4$	ΔT_{sat}	h	X_e
1						
2						
3						
4						

Run#	T_{min} =	T_{mout} =	T_{win} =	T_{wout} =		P_w =
POSITION	T_{wlwo}	T_{wlmo}	$q''/10^4$	ΔT_{sat}	h	X_e
1						
2						
3						
4						

*Below saturation nonboiling data

**Anomalous data

G = 28,800

Run #1001 T_{min} = 350.0 T_{mout} = 321.3 T_{win} = 105.3 T_{wout} = 219.7 P_w = 10.

POSITION	T_{w1wo}	T_{w1mo}	$q''/10^4$	ΔT_{sat}	h	X_e
1	324.0	343.3	2.93	69.2	528	0.0930
2	298.0	337.0	3.17	40.7	968	0.0201
3	285.0	329.7	2.80	30.1	1159	0
4	278.3	317.3	2.36	26.3	1118	0

Run #1002 T_{min} = 391.7 T_{mout} = 313.3 T_{win} = 97.7 T_{wout} = 221.7 P_w = 15.

POSITION	T_{w1wo}	T_{w1mo}	$q''/10^4$	ΔT_{sat}	h	X_e
1	372.3	382.0	2.20	111.2	247	0.0821
2	340.0	365.7	3.34	70.7	588	0.0115
3	320.3	356.0	3.23	51.4	783	0
4	317.0	340.0	2.12	55.5	475	0

Run# 1003 T_{min} = 476.7 T_{mout} = 388.7 T_{win} = 189.3 T_{wout} = 214.3 P_w = 10

POSITION	T_{w1wo}	T_{w1mo}	$q''/10^4$	ΔT_{sat}	h	X_e
1	441.0	467.0	4.27	178.0	299	0.3606
2	402.3	451.0	4.74	135.1	437	0.2522
3	366.7	439.7	5.43	94.5	715	0.1237
4	347.3	418.5	4.83	78.9	762	0

Run#1004 T_{min} = 486.5 T_{mout} = 414.7 T_{win} = 202 T_{wout} = 227.7 P_w = 11.

POSITION	T_{w1wo}	T_{w1mo}	$q''/10^4$	ΔT_{sat}	h	X_e
1	460.7	476.7	3.11	202.5	191	0.3813
2	418.5	467.0	4.61	149.6	383	0.2845
3	376.5	454.0	5.85	98.8	737	0.1519
4	353.7	431.3	5.34	79.0	841	0.0143

Run#1005 T_{min} = 493 T_{mout} = 487.7 T_{win} = 196.3 T_{wout} = 225.7 P_w = 12

POSITION	T_{w1wo}	T_{w1mo}	$q''/10^4$	ΔT_{sat}	h	X_e
1	478.0	487.7	1.18	225.9	100.2	0.3259
2	442.3	478.0	3.62	177.9	253.3	0.2553
3	400.3	468.3	5.33	124.1	534.1	0.1402
4	371.3	449.0	5.43	94.1	718.8	0.6387

*Below saturation nonboiling data

**Anomalous data

G = 28,800						
Run # 2001	T_{min} = 341.7	T_{mout} = 305.0	T_{win} = 107.7	T_{wout} = 230		P_w = 10
POSITION	T_{wlwo}	T_{wlmo}	$q''/10^4$	ΔT_{sat}	h	X_e
1	320.0	339.0	2.45	68.3	447	0.1374
2	281.0	326.0	3.93	18.5	2648	0.0568
3	264.0	316.5	3.44	4.50	9506	0
4	258.0	307.8	2.68	3.59	9310	0
Run # 2002	T_{min} = 386.7	T_{mout} = 344.	T_{win} = 116	T_{wout} = 214.3		P_w = 11
POSITION	T_{wlwo}	T_{wlmo}	$q''/10^4$	ΔT_{sat}	h	X_e
1	348.0	380.2	4.45	80.7	687	0.16355
2	325.3	367.2	3.53	62.9	698	0.07242
3	302.5	354.2	3.85	37.8	1267	0
4	296.0	338.2	2.90	37.6	962	0
Run# 2003	T_{min} = 404.7	T_{mout} = 400	T_{win} = 189.7	T_{wout} = 220.		P_w = 12
POSITION	T_{wlwo}	T_{wlmo}	$q''/10^4$	ΔT_{sat}	h	X_e
1	388.0	404.7	2.04	134.3	189.6	0.2965
2	333.0	400.7	5.15	57.8	1110.	0.2006
3	311.0	391.7	4.60	39.0	1467	0.0823
4	307.3	378.7	3.47	42.8	1008	0
Run# 2004	T_{min} = 456.7	T_{mout} = 395.0	T_{win} = 201.3	T_{wout} = 217.3		P_w = 11
POSITION	T_{wlwo}	T_{wlmo}	$q''/10^4$	ΔT_{sat}	h	X_e
1	440.5	453.3	1.91	190.0	125	0.4037
2	382.3	447.0	5.44	107.8	628	0.3043
3	340.3	421.0	5.28	49.5	1329	0.01715
4						
Run# 2005	T_{min} = 468.7	T_{mout} = 412.0	T_{win} = 202.3	T_{wout} = 217		P_w = 12
POSITION	T_{wlwo}	T_{wlmo}	$q''/10^4$	ΔT_{sat}	h	X_e
1	449.3	460.7	2.29	194.2	146	0.4694
2	384.7	449.3	6.02	104.1	719	0.3560
3	333.3	436.3	7.22	43.8	2052	0.1906
4	310.0	413.7	6.25	26.4	2943	0.02525

*Below saturation nonboiling data

**Anomalous data

G = 28,800						
Run #2006	T_{min} = 482.3	T_{mout} = 430.0	T_{win} = 202	T_{wout} = 216.3		P_w = 12.
POSITION	T_{wlwo}	T_{wlmo}	$q''/10^4$	ΔT_{sat}	h	X_e
1	462.7	472.7	2.31	207.5	138.4	0.4765
2	407.7	462.7	5.34	131.8	504	0.3748
3	346.3	450.0	7.63	54.2	1750.	0.20879
4	317.0	430.3	6.83	29.7	2864.	0.03118
Run #	T_{min} =	T_{mout} =	T_{win} =	T_{wout} =		P_w =
POSITION	T_{wlwo}	T_{wlmo}	$q''/10^4$	ΔT_{sat}	h	X_e
1						
2						
3						
4						
Run#	T_{min} =	T_{mout} =	T_{win} =	T_{wout} =		P_w =
POSITION	T_{wlwo}	T_{wlmo}	$q''/10^4$	ΔT_{sat}	h	X_e
1						
2						
3						
4						
Run#	T_{min} =	T_{mout} =	T_{win} =	T_{wout} =		P_w =
POSITION	T_{wlwo}	T_{wlmo}	$q''/10^4$	ΔT_{sat}	h	X_e
1						
2						
3						
4						
Run#	T_{min} =	T_{mout} =	T_{win} =	T_{wout} =		P_w =
POSITION	T_{wlwo}	T_{wlmo}	$q''/10^4$	ΔT_{sat}	h	X_e
1						
2						
3						
4						

*Below saturation nonboiling data

**Anomalous data

G = 28,800						
Run # 1006	T_{min} = 518.7	T_{mout} = 445.3	T_{win} = 204.	T_{wout} = 221.3		P_w = 15
POSITION	T_{wlwo}	T_{wlmo}	$q''/10^4$	ΔT_{sat}	h	X_e
1	502.3	509.0	2.02	242.5	103.7	0.3686
2	466.7	499.3	3.66	195.8	232.9	0.2951
3	415.0	489.3	6.09	127.6	594.5	0.1669
4	382.7	466.7	6.08	94.8	797.8	0.01557
Run #	T_{min} =	T_{mout} =	T_{win} =	T_{wout} =		P_w =
POSITION	T_{wlwo}	T_{wlmo}	$q''/10^4$	ΔT_{sat}	h	X_e
1						
2						
3						
4						
Run#	T_{min} =	T_{mout} =	T_{win} =	T_{wout} =		P_w =
POSITION	T_{wlwo}	T_{wlmo}	$q''/10^4$	ΔT_{sat}	h	X_e
1						
2						
3						
4						
Run#	T_{min} =	T_{mout} =	T_{win} =	T_{wout} =		P_w =
POSITION	T_{wlwo}	T_{wlmo}	$q''/10^4$	ΔT_{sat}	h	X_e
1						
2						
3						
4						
Run#	T_{min} =	T_{mout} =	T_{win} =	T_{wout} =		P_w =
POSITION	T_{wlwo}	T_{wlmo}	$q''/10^4$	ΔT_{sat}	h	X_e
1						
2						
3						
4						

*Below saturation nonboiling data

**Anomalous data